jamk.fi

Development of a demonstration device for vibrations

Jonathan Gengenbach

Bachelor's thesis
May 2015

Degree Programme in Mechanical and Production Engineering

JYVÄSKYLÄN AMMATTIKORKEAKOULU
JAMK UNIVERSITY OF APPLIED SCIENCES

JYVÄSKYLÄN AMMATTIKORKEAKOULU
JAMK UNIVERSITY OF APPLIED SCIENCES

Description

Author(s)	Type of publication	Date
Gengenbach, Jonathan	Bachelor's	22.05.2015
		Language of publication: English
	Number of pages: 110	Permission for web publication: Granted

Title of publication
Development of a demonstration device for vibrations

Degree programme
Degree Programme in Mechanical and Production Engineering

Tutor(s)
Kurki, Matti

Assigned by
Matilainen, Jorma, JAMK University of Applied Sciences

Abstract

Unbalanced rotors vibrate while turning. This effect can be described on a simplified model, the Laval-Rotor. The Laval-Rotor consists of a pin-supported massless shaft and a centric attached disk. The Laval-Rotor can be transferred into a plane damped mass-spring system with a certain undamped natural frequency. Due to the imbalance of the rotor, its centre of mass is not on the shaft axis. The distance between both is called eccentricity. Through turning, the imbalance excites the rotor to oscillate. Depending on the damping of the system, the deflexion of the rotor varies differently. The Laval-Rotor's transfer function shows a maximum deflexion at a revolution speed similar to the systems natural frequency. Since high shaft deflexions bring the risk of a prematurely collapse and further hazards, this revolution speed is called the shaft's critical speed. The Laval-Rotor has due to the assumed simplifications just a single degree of freedom. In general, each degree of freedom has an own natural frequency and so an own critical speed. Therefore, an actual rotor can have several critical speeds which have to be considered. Besides the bending oscillating a rotor also oscillates rotational. This rotational behaviour also has to be taken in account while designing a rotor.

Part of the thesis-work is the development of a demonstration device that shows the effect of imbalanced excited bending vibrations. The critical speeds of the rotor can be affected by adjusting the position of the bearings as well as the position and amount of the attached disks. The development is completely made from the idea until the, for the manufacturing needed drawings and documents in the development process steps: planning, concept, drafting and elaboration.

Keywords/tags (subjects)
Vibrations, bending vibrations, development project, design project, imbalanced excited vibrations, critical speed

Miscellaneous:
-

Table of contents

Figures

Tables

1 Introduction and objectives

I got the possibility to finish my Automotive Engineering studies in the double degree program which is provided in cooperation of my home institution, the Hochschule Esslingen University of Applied Sciences and the JAMK University of Applied Sciences. Therefore I have spent the autumn semester 2014 and the spring semester 2015 at the JAMK in Jyväskylä, Finland. Part of the double degree program is creating the bachelor's thesis abroad. In the end of the autumn semester 2014, Jorma Matilainen who is principal lecturer in the School of Technology, proposed me to make the, in this document introduced, development project within my thesis work. At this point I want to thank Jorma for the opportunity to do the thesis work at the JAMK and for his supervision as his role as representative of the host organisation. Furthermore I want to thank Matti Kurki who accompanies the thesis work as the supervisor.

The objective of this thesis work is to develop a laboratory device which demonstrates imbalance excited bending vibrations of a shaft. The device's purpose is to illustrate the in the lecture taught theory about critical shaft revolution speeds and to sensitise the students for the thereby arising risks.

The thesis is separated into two main parts, the theoretical part (chapter 2) and the actual development project (chapter 3). The theoretical part deals with the modelling and mathematically description of the oscillating rotor and serves as fundament for the designing of the device. Chapter 3 includes all steps which are passed while developing the demonstration device.

2 Theoretical part

2.1 Introduction and motivation

Bending vibrations of a shaft which are caused by an unbalanced mass distribution have a big influence of the runnability and the stability of machines. On bearings transmitted vibrations stress the bearings and reduce their life expectancy. The vibrations also can generate noises and rattling which are disturbing the machine users and the environment. The oscillating bending of the shaft increase the strain in the shaft which can cause an earlier destruction. High displacements of the shaft bring the risk of a collision between the shaft and the housing. Because of the named hazards it is necessary to consider imbalances while designing and operating a machine with a turning shaft.

In the theoretical part the effect of this vibrations are illustrated. It basically examines two different types of vibrations, the imbalanced excited bending vibrations (2.2, 2.3) and the imbalanced excited torsional vibrations which are studied in brief in chapter 2.4. In chapter 2.2 the bending vibrations are deduced in the simplified one degree of freedom model. Based on the in chapter 2.2 gained knowledge the chapter 2.3 introduces shortly bending vibrations in systems with two and more degrees of freedom.

2.2 Laval Rotor

2.2.1 Modelling

The simplest model to understand and calculate the effect of an imbalanced rotor is the so called Laval Rotor which is in English-written literature often introduced as Jeffcott-Rotor. The Laval Rotor was first described and patented by the Swedish engineer Gustav de Laval (Gasch, Nordmann, & Pfützner, 2006, 15). The Laval Rotor consists of a bending flexible and massless shaft with a disk attached on its half-length (Figure 1). The most elementary bearing model are two bearings which are infinite stiff in vertical directions to the shaft and torque-free for bending. In the technical mechanics this bearings are called pinned-supporting.

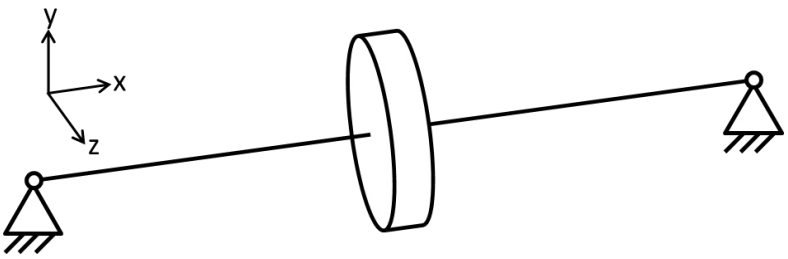

Figure 1: Laval Rotor with blocked translatory motion

Because of the symmetric structure of the system the disk is only free to shift vertically to the shaft (y- and z- direction) as well as to rotate around the shafts axis (x-direction) and does not tilt around the y- and z- axis. Due the simplification of the shaft as massless and the fact that in this particular system the disk is just moving in a plane the shaft is substitutable for a spring with an equivalent stiffness k (Figure 2). Another simplification of the system is the negligence of the gravity so that there is no static bending caused by the gravity force. In an imbalanced rotor the centre of the disk's mass C is not the same then its geometrical centre M. If the disk is not displaced its geometrical centre is on the bearings centres' connection line. To simplify the calculations it is functional to place the origin of co-ordinates into the connection line of the bearings.

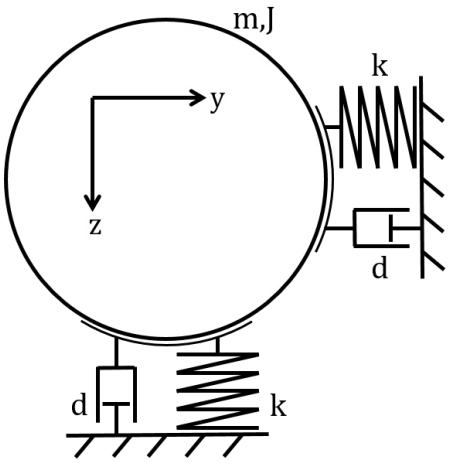

Figure 2: Laval Rotor with equivalent Springs and damping

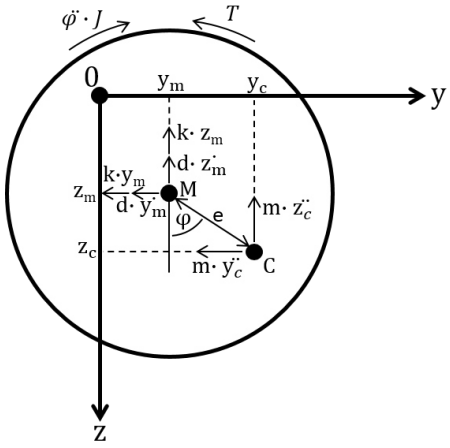

Figure 3: Laval Rotor with forces

Figure 3 shows the force-diagram of the in y- and z-direction displaced Laval Rotor. z_m and y_m are the displacement of the rotor. z_c and y_c are the positions of the disk's centre of mass. e is the constant value of the disks eccentricity. The determination of the mathematically determination of the eccentricity e is described in the equation (2.7). φ is the current rotation angle of the disk. φ is for calculation reasons determined as counter clockwise (mathematical positive) and begins on the z-axis. The active forces in this model of the Laval Rotor are the inert forces $m \cdot \ddot{y_c}$ / $m \cdot \ddot{z_c}$, the spring forces $k \cdot y_m$ / $k \cdot z_m$ and the forces which are caused by the damping $d \cdot \dot{y_m}$/ $d \cdot \dot{z_m}$. The damping in this model is implemented as a viscose damping which is the mathematically simplest way to describe damping. The accurateness and weakness of this damping model will be discussed later. According to the Newton's Law of Motion the rotor has to be in balance of forces (2.1).

$$\begin{aligned} m \cdot \ddot{y_c} + d \cdot \dot{y_m} + k \cdot y_m = 0 \\ m \cdot \ddot{z_c} + d \cdot \dot{z_m} + k \cdot z_m = 0 \end{aligned} \tag{2.1}$$

Beside the forces the torques also have to be in balance. The moments which act around C are the rotor's moment of inertia $\ddot{\varphi} \cdot J$, the inertia of the rotor's mass multiplied by the effective eccentricity $e \cdot \cos\varphi \cdot y_m$ / $e \cdot \cos\varphi \cdot y_m$ and the external driving torque T.

$$\begin{aligned} e \cdot \sin(\varphi) \cdot (k \cdot z_m + d \cdot \dot{z_m}) - e \cdot \cos(\varphi) \cdot (k \cdot y_m + d \cdot \dot{y_m}) \\ + \ddot{\varphi} \cdot J - T = 0 \end{aligned} \tag{2.2}$$

With help of the trigonometric functions and the two-times derivation $\ddot{y_c}$ and $\ddot{z_c}$ are expressible as a function of y_m / z_m and φ.

$$
\begin{aligned}
y_c &= y_m + e \cdot \sin(\varphi) \\
\dot{y}_c &= \dot{y}_m + e \cdot \dot{\varphi} \cdot \cos(\varphi) \\
\ddot{y}_c &= \ddot{y}_m - e \cdot \dot{\varphi}^2 \cdot \sin(\varphi) + e \cdot \ddot{\varphi} \cdot \cos(\varphi) \\
\\
z_c &= z_m + e \cdot \cos(\varphi) \\
\dot{z}_c &= \dot{z}_m - e \cdot \dot{\varphi} \cdot \sin(\varphi) \\
\ddot{z}_c &= \ddot{z}_m - e \cdot \dot{\varphi}^2 \cdot \cos(\varphi) - e \cdot \ddot{\varphi} \cdot \sin(\varphi)
\end{aligned}
\tag{2.3}
$$

Equation (2.3) inserted in (2.1) makes a differential equations with the geometrical centre (y_m/z_m) of the rotor and its first and second derivation ($\dot{y}_m/\dot{z}_m$, $\ddot{y}_m/\ddot{z}_m$). For a better comprehension of the differential equation the terms with y_m/z_m, $\dot{y}_m/\dot{z}_m$ and $\ddot{y}_m/\ddot{z}_m$ are brought on the left side of the equality sign and the equation is transposed so that the highest derivation ($\ddot{y}_m/\ddot{z}_m$) is an own term.

$$
\begin{aligned}
\ddot{y}_m + \frac{d}{m} \cdot \dot{y}_m + \frac{k}{m} \cdot y_m &= -e \cdot \ddot{\varphi} \cdot \cos(\varphi) + e \cdot \dot{\varphi}^2 \cdot \sin(\varphi) \\
\ddot{z}_m + \frac{d}{m} \cdot \dot{z}_m + \frac{k}{m} \cdot z_m &= e \cdot \ddot{\varphi} \cdot \sin(\varphi) + e \cdot \dot{\varphi}^2 \cdot \cos(\varphi)
\end{aligned}
\tag{2.4}
$$

Equations (2.4) are inhomogeneous differential equations of second order. The left side of the equality sign is the homogeneous part. The homogeneous part is the differential equation of a free, damped oscillation. The undamped natural frequency of those systems is ω_0 (2.5).

$$
\omega_0 = \sqrt{\frac{k}{m}} \tag{2.5}
$$

The differential equation's right side is the perturbation function which describes the excitement of the system caused by the imbalance. To predict the behaviour of a Laval Rotor the equivalent spring stiffness (k) is needed. It depends on the geometry and material of the shaft and the kind of its bearing.

The equivalent spring stiffness is for small bending nearly constant and can be approximated with equations (2.6). The influence of the kind of bearing (C) is listed in Figure 4. E describes the Young's modulus, I the second moment of area and r and l are the radius and length of the shaft.

with:

$$k = \frac{C \cdot E \cdot I}{l^3} \qquad (2.6)$$

$$I = \frac{\pi \cdot r^4}{4}$$

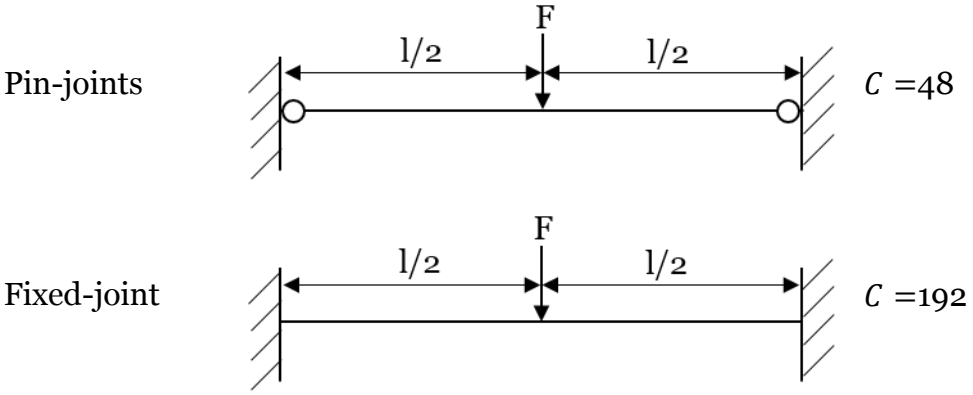

Figure 4: Bearing's influence of the equivalent stiffness

The eccentricity (e) can be calculated by the unbalanced mass (m_{unb}) and its position (r_{unb}) according equation (2.7). Both parameters are known in the case of the demonstration device, in which the imbalance is constructed.

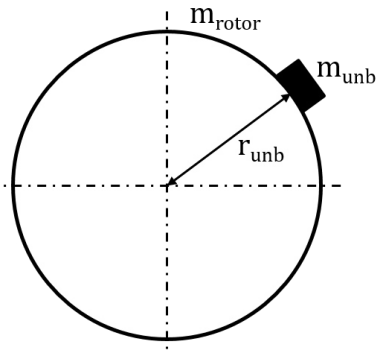

Figure 5: Unbalance

$$e = r_{unb} \cdot \frac{m_{unb}}{m_{rotor}} \tag{2.7}$$

Due the appearance of φ and its second derivation in non-linear terms like sine, cosine and quadratic functions in the equation (2.4) and (2.2) the solutions of the differential equations are not trivial. Therefore the system is solved in a numerical way, which is described in chapter 2.2.2.

2.2.2 Simulation

To solve the differential equations (2.2) and (2.4) the system is built in Matlab/Simulink. Figure 6 shows the implementation of the equation (2.4). It has the angle φ and its derivations as input signals. The eccentricity (e), the damping coefficient (d), the spring stiffness (k) and the mass are constant values which are calculated outside the simulation. The model's structure of the part of equation (2.4) which contains z_m is similar to the described one.

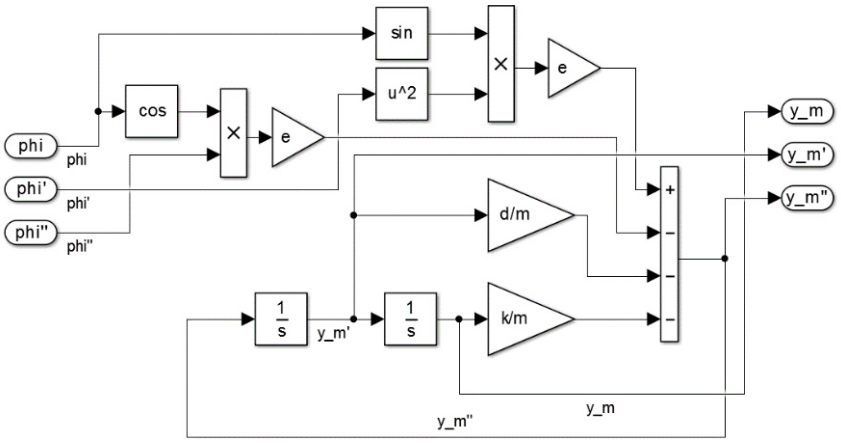

Figure 6: Simulink model equation (2.4)

The torsional moment's Simulink model is shown in Figure 7. There is the torque (T) the external control variable. The eccentricity (e) and the inertia (J) are constant values.

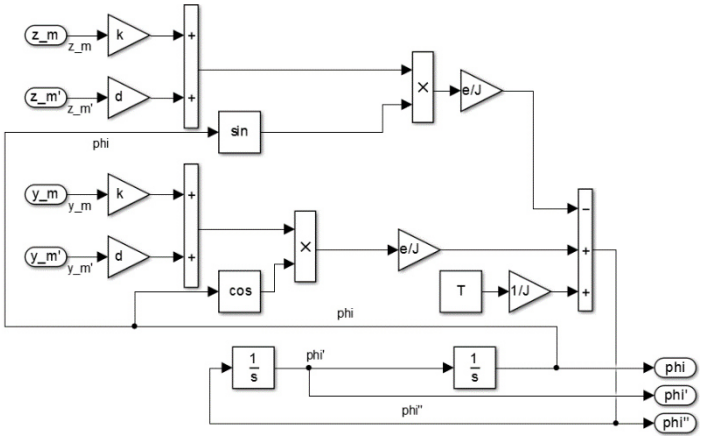

Figure 7: Simulink model equation (2.2)

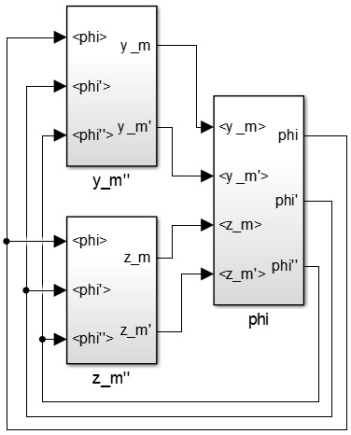

Figure 8: Simulink model

Figure 8 contains the Simulink model which executes the correlations between equations (2.4) and (2.2). To analyse the system's behaviour by constant rotations speeds and to deduce the transfer function it is viable to replace the moment's equation (2.2) with a constant angular speed ω (Figure 9). The moment's equation calculates out of the system's state and the external torque the momentary angle (φ) respectively the angular speed ($\dot{\varphi}$) and its acceleration ($\ddot{\varphi}$).

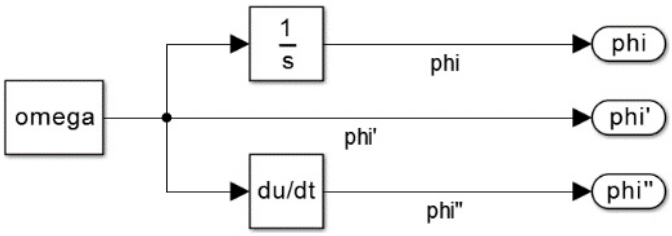

Figure 9: Simulink model constant angular speed

2.2.3 System behaviour

The transfer function (Figure 10) illustrates the vectorial sum of the rotor's displacement ($\sqrt{{y_m}^2 + {z_m}^2}$) plotted against the rotation speed by several damping ratios. The revolution speed (ω) is normalised to the system's natural frequency (ω_0) and the displacement to the eccentricity (e). The transfer function shows that there is almost no displacement low angular speeds. Next to the natural frequency the displacement ascends depending, on the damping

ratio to very high values. An undamped system reaches at its natural frequency infinite deflexion. Because of the hazard of shaft fractures this angular speed is called the critical speed. At higher angular speed the displacement stabilised to the value of the eccentricity.

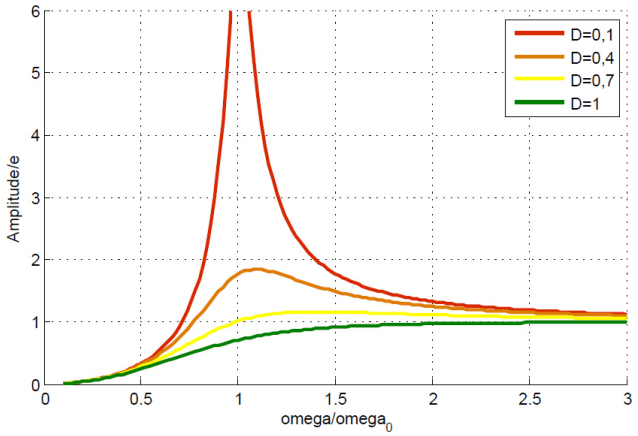

Figure 10: Transfer function Laval Rotor

The observation of the paths which the centre of the mass respectively the geometrical centre of the shaft describe are shown in Figure 11. This paths are called also called orbits. At lower rotation speed the radius of the mass centre orbit is bigger than the geometrical centre ones. By increasing the rotation speed this ratio turns. At higher speeds, the centre of mass approaches to a stable non-moving state and the centre of the shaft describes an orbit with the radius of the eccentricity.

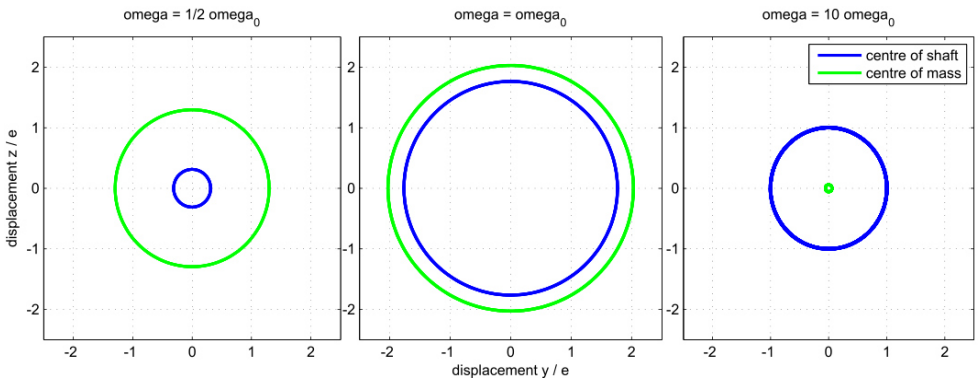

Figure 11: Orbits centre of shaft and mass

2.2.4 Supporting

The kind of the bearing has basically two factors of influence on the bending vibration of the shaft. As opposed to the assumption made in the first model of the Laval Rotor the bearings are not totally rigid in the radial direction and also not totally non-rigid for bending. The stiffness of the supporting in the radial directions (y/z) can be seen as springs in a row to the equivalent springs of the shaft (Figure 12).

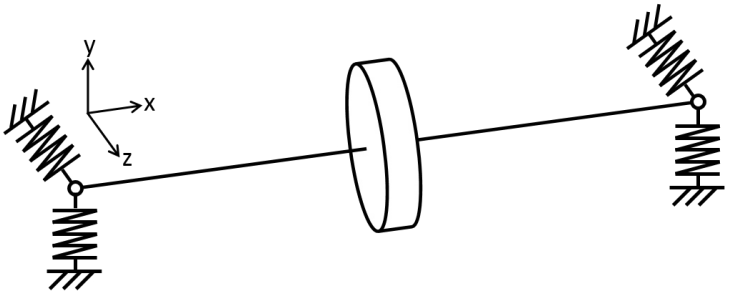

Figure 12: Laval Rotor with non-rigid bearings

For an undamped system the result stiffness can be calculated with equation (2.8). It is assumed that the supporting's stiffness is different in the y- and z- direction but symmetrically on both sides. This assumption reproduce very well the reality like it is in the demonstration device, where the same bearing supporting is used on both sides.

$$k_{tot,y} = \frac{k_{shaft} \cdot (2k_{support,y})}{k_{shaft} + (2k_{support,y})}$$
$$k_{tot,z} = \frac{k_{shaft} \cdot (2k_{support,z})}{k_{shaft} + (2k_{support,z})} \qquad (2.8)$$

Due the different stiffness in the z- and y- direction the orbits of the shaft's geometrically centre and its centre of mass are an elliptical instead of circular. Additionally to the position of the centre of mass and the geometrically centre of the shaft it is interesting to examine the displacement of the bearing. According the Hooke's law the deflexion is inversely proportional to the spring

stiffness. Referred to that the share of the displacement in the shaft and the supporting depends on the ratio of the stiffness between those. Figure 13 shows exemplarily the bending of the shaft and the deflexion of its supporting. In both cases are the totally stiffness the same so that the totally displacement of the rotor is also the same. In the upper case the equivalent stiffness of the shaft is much lower than the stiffness of the bearing. In the lower case both are similarly stiff.

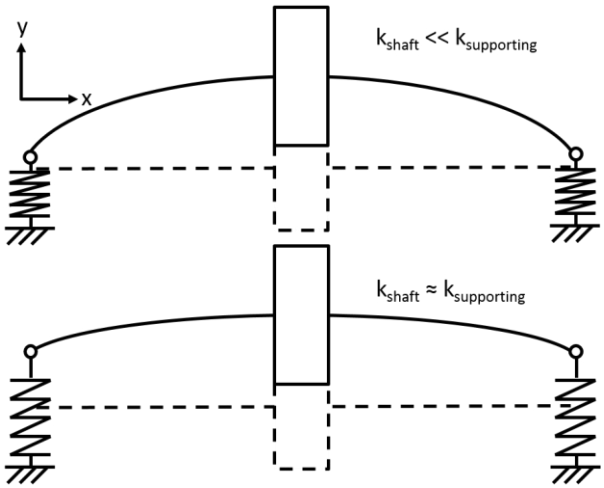

Figure 13: Comparison stiffness ratio of shaft to supporting

Since the total system stiffness is lower with a less stiff supporting, the natural frequency decreases (2.5). The influence of the stiffness in bending directions is more difficult to determine. It is contained in the constant number (C) in equation (2.6). The totally rigid bending support (Fixed-joints) leads to a four-time higher equivalent spring than the totally non-rigid bending support (Pinned-joints). Depending on the actual bearings the stiffness is somewhere between. Self-aligning ball bearing for instance are nearly non-rigid in bending direction as against plain bearings are rather rigid.

2.2.5 Weaknesses of the model

The described model of the Laval-Rotor is just an approximation to an actual system. Depending on the actual system characteristics, the model has different weaknesses with different impact to the system's accurateness. In this

chapter are the negligence of the gravity, the influence of the damping, the negligence of the shaft's mass and the determination of the shaft's stiffness discussed.

The negligence of the gravity is just in case of a completely balanced shaft exact. In this case the bending vibrations are added to the static, of the gravitation force caused bending of the shaft. Imbalanced, horizontal mounted shafts have according to Stodola (1918, 1-3) an additional critical speed. Is the rotor central on the shaft this critical speed is the half of the shafts first critical speed. The derivation of this new critical speed is with following concept possible (Stodola, 1918, 1-3). The view on the system should be from a with the shaft speed (ω) rotating co-ordinate system. Due the elastic vibration the shafts centre follows a circle with the velocity of the critical speed (ω_c). The motion seen by the rotating system has the relative speed $\omega_c - \omega$. The gravity impacts the centre of mass with the rotating force $g \cdot m \cdot \sin(\omega t)$ respectively $g \cdot m \cdot \cos(\omega t)$ which generate vibrations with the angular frequency (ω). The gravity caused vibration and the natural vibration are in resonance if $\omega_c - \omega = \omega$. In this case is $\omega = \omega_c/2$ and the amplitudes of both vibrations can be added.

Another aspect which brings inexactness into the model is the assumption that the damping is a totally viscose. This assumption simplifies the mathematical model but reflects the reality not completely accurate. Furthermore even if the system is precisely described with a viscose damping the determination of the damping ratio is not easy. The most practical procedure to determinate the damping ratio is to measure the decay time of the actual system which is obviously not feasible when the system is still in development.

The most-reaching simplification of the system is probably the consideration of the shaft as massless. The accurateness of this simplification depends on the ratio between the rotor mass and the shaft mass. A continuous shafts has its own vibration behaviour. The determination of the influence of this vibrations should not be done here because it requires a highly more complex model than

the model of the Laval-Rotor is. For more exactly outcomes with consideration of the shafts mass and geometry it is recommendable to calculate the system with the finite element method.

As earlier discussed the kind of the supporting has a big influence of the stiffness of the shaft. And even if the correct equation for the equivalent stiffness is found it is valid for small bending magnitudes. For higher bending magnitudes the shaft gets stiffer. Moreover the model assumes a linear-elastic material behaviour which is just valid in certain limits.

2.3 System with two and more degrees of freedom

2.3.1 Introduction

Each multi-degree of freedom system with n degree of freedoms has n natural frequencies with the belonging n natural modes (Rao, 2010, 461). Due the continuous distribution of mass and rigidity on the shaft, the in the previous chapter introduced Laval-Rotor actually has an infinite number of natural frequencies. Basically this applies for all actual systems, but the influence of the higher natural frequencies is different in different systems. In this chapter a system similar to the Laval-Rotor but with two disks as well as a shaft without attached disks are discussed. Due the disks' slim shape orthogonal to the shaft-axis, they have a high mass at a marginal length on the shaft. The shaft is contrary to the disks relative lightweight by its comparatively high length. Therefore the disk mass' influence on the rotor's vibration behaviour is much higher than the shaft mass'. This is why systems with attached disks are more accurately describable with a lower number degrees of freedom then it is the case of a rotor without attached disks.

2.3.2 Natural frequencies and natural modes of a continuous shaft

According to Rao (2010, 527) the shape of a continuous beam's respectively a shaft's nth natural mode is described with the formula (2.9). l is the length of the beam and C_n the particular maximal deflexion. The determination of C_n which is depending on the beam's material, dimensions and damping is not

described in this thesis. The natural frequencies of continuous beams which are pinned-supported are computed in equation (2.10) (Rao, 2010, 526). Figure 14 shows the three lowest mode shapes according formula (2.9).

$$w_n(x) = C_n \cdot sin\left(n \cdot \pi \cdot \frac{x}{l}\right) \tag{2.9}$$

$$\omega_n = (\pi \cdot n)^2 \sqrt{\frac{EI}{\rho A l^4}} \tag{2.10}$$

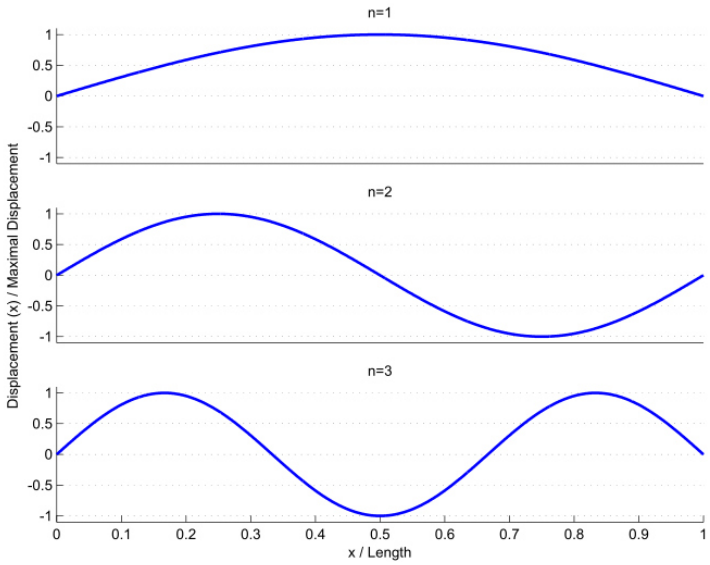

Figure 14: Beam's three lowest mode shapes

2.3.3 Rotor with two attached disks

Basically the in the previous chapter 2.2 about the Laval- Rotor got findings are also valid for the rotor with two masses (Figure 15). The mechanism of unbalanced gained vibrations are the same in the system with two rotors. So it is also dangerous to run the rotor at rotation speeds which are nearby its natural frequencies. Compared to the Laval- Rotor, a Rotor with two disks has two natural frequencies which have to be considered. Both natural frequencies are important for the dimensioning of the demonstration device.

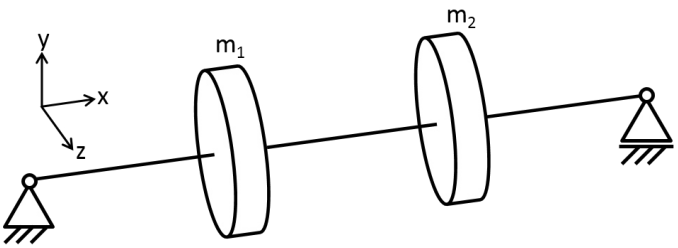

Figure 15: Rotor with two disks

To identify the natural frequencies the equation of motion has to be determined (2.11). The introduced system is undamped. Equation (2.11) is a differential equation written in matrix form with M as mass matrix and K as stiffness matrix. Solving equation (2.12) gives the natural frequencies.

$$\bar{M} \cdot \ddot{y} + \bar{K} \cdot y = 0 \tag{2.11}$$

$$\det[\bar{K} - \omega^2 \bar{M}] = 0 \tag{2.12}$$

With:

$$\bar{M} = \begin{bmatrix} m_1 & 0 \\ 0 & m_2 \end{bmatrix}, \bar{K} = \begin{bmatrix} a_{11} & a_{12} \\ a_{21} & a_{22} \end{bmatrix}^{-1}$$

a_{vw} are so called factors of influence and are measuring units of the system's stiffness relating to the disk's positions. Technically they are the shaft's deflexion on position w caused by a force ($F_v = 1$ N) applied on position v. To determine the factors of influence, the bending line $w(x)$ (Figure 16) caused by the force F is calculated. The correlation between the bending line and a_{vw} is $a_{11} = w_1(F_1 = 1N)$ and $a_{12} = w_2(F_1 = 1N)$. Since the symmetrical structure of the rotor, the equations $a_{22} = a_{11}$ and $a_{21} = a_{12}$ are valid.

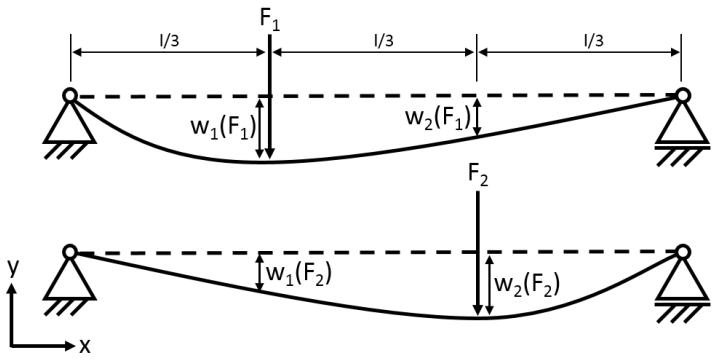

Figure 16: Bending line w(F,x)

The approach to calculate the bending is the Bernoulli beam theory (2.13).

$$E \cdot I \cdot \ddot{w}(x) = -M(x) \tag{2.13}$$

To determine $M(x)$ the beam is cut twice (Figure 17). At their cross section the equations of the moments (2.14) is formulated.

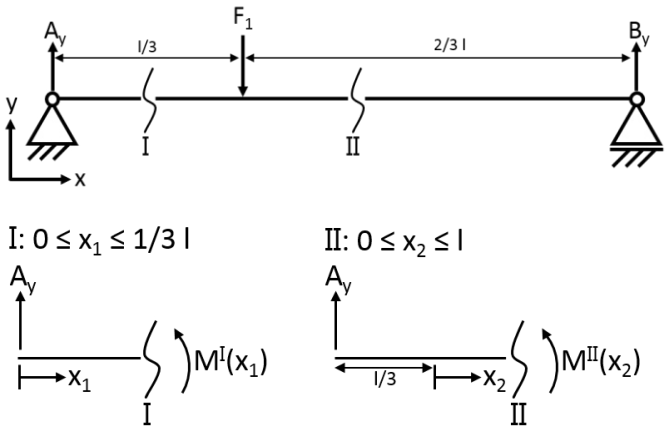

Figure 17: Force diagram at position I and II

$$\begin{aligned} A_y &= \frac{2}{3}F \\ M^I(x_1) &= x_1 \cdot \frac{2}{3}F \\ M^{II}(x_2) &= \frac{2}{9}Fl - \frac{1}{3}F \cdot x_2 \end{aligned} \tag{2.14}$$

The moment's equations (2.14) inserted into the Bernoulli beam theory (2.13) and two times integrated gives the equation of the bending line (2.15) with the integration constants C_1, C_2, C_3 and C_4.

$$\begin{aligned} E \cdot I \cdot \ddot{w}(x_1) &= -x_1 \cdot \frac{2}{3} F \\ E \cdot I \cdot \dot{w}(x_1) &= -\frac{1}{3} \cdot F \cdot {x_1}^2 + C_1 \\ E \cdot I \cdot w(x_1) &= -\frac{1}{9} \cdot F \cdot {x_1}^3 + C_1 \cdot x_1 + C_2 \end{aligned} \tag{2.15}$$

$$\begin{aligned} E \cdot I \cdot \ddot{w}(x_2) &= \frac{1}{3} F \cdot x_2 - \frac{2}{9} F l \\ E \cdot I \cdot \dot{w}(x_2) &= \frac{1}{6} \cdot F \cdot {x_2}^2 - \frac{2}{9} \cdot l \cdot F \cdot x_2 + C_3 \\ E \cdot I \cdot w(x_2) &= \frac{1}{18} \cdot F \cdot {x_2}^3 - \frac{1}{9} \cdot l \cdot F \cdot {x_2}^2 + C_3 \cdot x_2 + C_4 \end{aligned}$$

There are four boundary conditions needed to determine the four integrations constants. Boundary conditions (I) and (II) result from the supporting at both ends of the shaft which do not allow displacements. Boundary conditions (III) and (IV) are formed out of the fact that $x_1 = 1/3\ l$ and $x_2 = 0$ are the same point and therefore their displacement and their sloping are the same.

$$\begin{aligned} (I) \quad & w(x_1) = 0 \\ (II) \quad & w(x_2 = 2/3\ l\ ) = 0 \\ (III) \quad & w(x_1 = 1/3\ l) = w(x_2 = 0) \\ (IV) \quad & \dot{w}(x_1 = 1/3\ l) = \dot{w}(x_2 = 0) \end{aligned} \tag{2.16}$$

The four boundary conditions are an equations system with four unknowns. Its solution is not shown here. The determined integrations constants inserted in equation (2.15) gives the equation of the bending line (2.17).

$$E \cdot I \cdot w(x_1) = -\frac{1}{9} \cdot F \cdot {x_1}^3 + \frac{5}{81} \cdot F \cdot l^2 \cdot x_1$$
$$E \cdot I \cdot w(x_2) = \frac{1}{18} F \cdot {x_2}^3 - \frac{1}{9} lF \cdot {x_2}^2 + \frac{2}{81} Fl^2 \cdot x_2 + \frac{4}{243} Fl^3 \quad (2.17)$$

Out of the bending line's equation (2.17) the factors of influence a_{11}, a_{12}, a_{21} and a_{22} are determined with the above described conditions.

$$a_{11} = a_{22} = w\left(x_1 = \frac{1}{3} l, F = 1N\right) = \frac{2}{81} \cdot \frac{1N}{E \cdot I} \cdot l^3$$
$$a_{12} = a_{21} = w\left(x_2 = \frac{1}{3} l, F = 1N\right) = \frac{7}{486} \cdot \frac{1N}{E \cdot I} \cdot l^3 \quad (2.18)$$

The in chapter 2.2.5 described weaknesses of the Laval-Rotor which are the negligence of the gravity, the inadequacy of the damping model, the negligence of the shafts' mass and the inexactness in the determination of the system's stiffness are also valid for the rotor with two attached disks. Beside those there is a further influence factor. Due the bending of the shaft the rotors do not only move translational and rotatory around the x-axis but also in small angles rotatory around the z-axis (Figure 18).

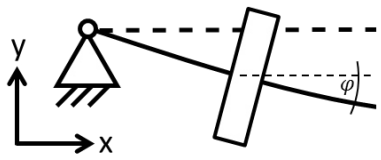

Figure 18: Rotatory motion of the disk

According the law of conservation of angular momentum or colloquially called the gyro effect the rotating disk pursues because of its inertia to stay in its actual state. For the described system, that means that depending on the inertia around the shaft axis and the rotating speed there arises a moment which is opposite directed to the slope of the shaft (φ). This moment acts against the

shafts deflexion and stabilize the system against the vibration. A numeral determination of this moment is not part of this thesis but should be considered by fast running systems with heavy hubs.

2.4 Torsional vibrations

Beside the in the previous chapters described motions and vibrations in translational directions a shaft also has a rotatory behaviour which should not be neglected. This chapter deals with the determination of the torsional vibrations of a shaft with two rotors.

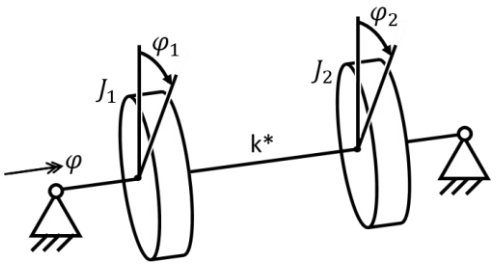

Figure 19: Torsional system

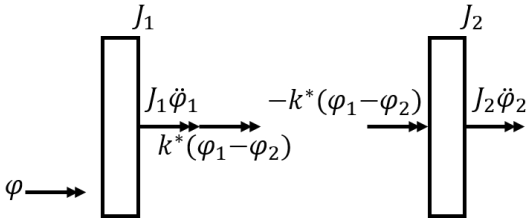

Figure 20: Diagram of moments

The system shown in Figure 19 is a shaft with two attached masses and a neglected inertia. Since both disks have generally different rotation angles, they are cut free (Figure 20). On both disks act their respective moment of inertia as well as the moment emerging by their torsion against each other. The oscillating differential equations (2.19) are derived out of the principle of the moment equilibrium.

$$\begin{aligned} J_1\ddot{\varphi}_1 + k^*(\varphi_1 - \varphi_2) &= 0 \\ J_2\ddot{\varphi}_2 + k^*(\varphi_2 - \varphi_1) &= 0 \end{aligned} \tag{2.19}$$

The oscillating differential equations (2.19) written in matrix-form makes the equation (2.20). The natural frequencies are determined by solving the equation (2.21).

$$\bar{M} \cdot \begin{bmatrix} \ddot{\varphi}_1 \\ \ddot{\varphi}_2 \end{bmatrix} + \bar{K} \cdot \begin{bmatrix} \varphi_1 \\ \varphi_2 \end{bmatrix} = \begin{bmatrix} 0 \\ 0 \end{bmatrix}$$

With:

$$\bar{M} = \begin{bmatrix} J_1 & 0 \\ 0 & J_2 \end{bmatrix}; \bar{K} = \begin{bmatrix} k^* & -k^* \\ -k^* & k^* \end{bmatrix} \tag{2.20}$$

$$\det[\bar{K} - \omega^2 \bar{M}] = 0 \tag{2.21}$$

The torsional rotating system responses analogue to the in chapter 2.2.3 described behaviour of the Laval-Rotor on external oscillating excitations. If the excitation frequency is nearby a natural frequency of the rotating system, its torsional vibrations gets high amplitudes. A kind of excitement are like in the case of the Laval-Rotor, imbalanced caused forces.

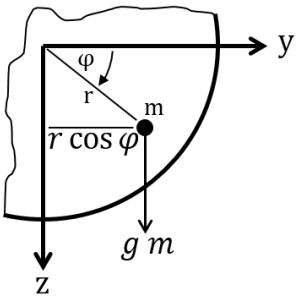

Figure 21: Unbalanced caused force

Figure 21 shows the, by the off-centred mass caused force ($g \cdot m$). This force causes with the on the rotors angular position (φ) depending lever arm a moment ($g \cdot m \cdot r \cdot \cos \varphi$). Since generally both rotors are imbalanced, the oscillating differential equations (2.19) changes to the non-linear differential equation (2.22).

$$\bar{M} \cdot \begin{bmatrix} \ddot{\varphi}_1 \\ \ddot{\varphi}_2 \end{bmatrix} + \bar{K} \cdot \begin{bmatrix} \varphi_1 \\ \varphi_2 \end{bmatrix} = \begin{bmatrix} g\ mr_1 \cos \varphi_1 \\ g\ mr_2 \cos \varphi_2 \end{bmatrix}$$

With:

$$\bar{M} = \begin{bmatrix} J_1 & 0 \\ 0 & J_2 \end{bmatrix}; \bar{K} = \begin{bmatrix} k^* & -k^* \\ -k^* & k^* \end{bmatrix} \tag{2.22}$$

3 Development of the demonstration device

3.1 Introduction

Based on the in the previous chapters generated knowledge about bending vibrations a demonstration device is developed. The demonstration device should be used in the context of lectures and laboratory-works to visualize the imbalanced-caused bending vibrations and the possibilities to influence them by changing the system properties. This work contains all steps of the product development from the request to the finished designed and documented product. The process is split in four main stages: the planning-, the concept-, the drafting- and the elaboration-stage. The planning-stage contains mainly the elaboration of the list of requirements in agreement with the customer. The list of requirements consists all features which are required of the finished product. The scheduling is also part of the planning. It determines periods of time for the different development stages and also consists milestones to set specific project-events. Based on the list of requirement the concept is described. During the concept-phase an abstract working principle is developed. It describes the particular functions of the system without specifying its technical realization. The technical realization is developed in the drafting-stage. The overall design is executed and the system is divided in functional groups. Additionally main attributes like functional-dominating dimensions or the speed-range are defined during the drafting-stage. The elaboration-stage is mainly the construction respectively designing of the particular parts and the producing of the technical drawings for manufacturing. A complete product documentation which contains an operational manual as well as an assembly guidance is done in the developing process. The manufacturing of the parts will be done in the JAMK's mechanical workshop and is not part of this thesis work.

3.2 Features of the device

The list of requirements is elaborated together with Jorma Mattilainen and Matti Kurki. The requirements are derived from the demand of the device as a lecture and laboratory-work supporting apparatus. It should be able to show unbalanced excited bending vibrations with amplitudes which are high enough to see with the naked eye. The systems arrangement should be changeable in the position and amount of the masses. It also should be able to influence the bending stiffness of the shaft. Since of the purpose of the device, it should be easily moveable and the operating should be fast, safety and easy.

3.3 Concept

The working concepts for the different rotor arrangements are directly derived out of the list of requirements. There are basically three different kinds of arrangement which are shown in Figure 22. All of those modes are controlled by a by the user predetermined revolution speed. The shaft with the rotor respectively rotors should be as good as possible uncoupled from the environment so that the bending vibrations are as free and unaffected as possible. Figure 22 a) shows the working mode with one imbalanced rotor between the two bearings. The magnitude of the imbalance, the position of the rotor as well as the effective length of the shaft are adjustable. The second working mode (Figure 22 b)) has a second rotor with adjustable position and imbalance. The last mode as shown in Figure 22 c) has a cantilevered adjustable rotor.

a)

b)

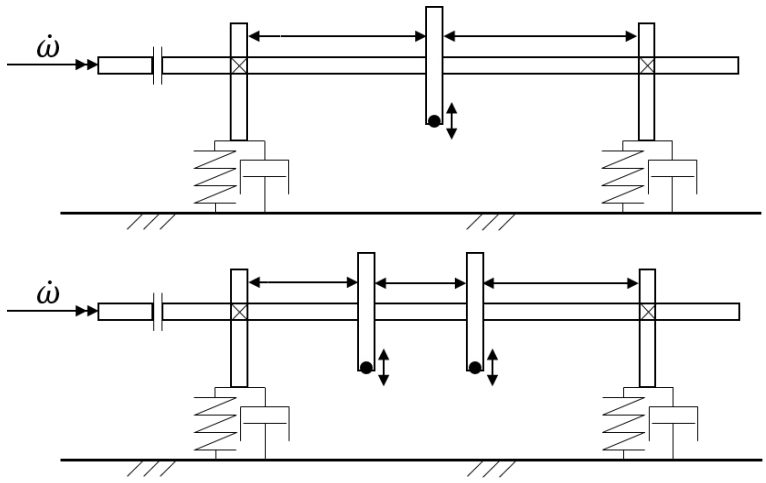

c)

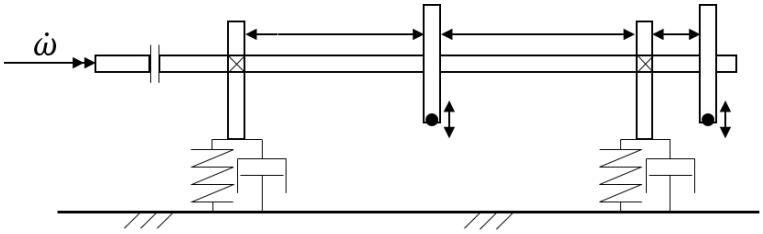

Figure 22: arrangement with a) one rotor b) two rotor c) cantilevered rotor

3.4 Drafting

The objective of the drafting is to gather, on the basic of the overall concept, the functionalities of the different parts and their main attributes. Therefore the concept is separated into different functional groups (chapter 3.4.1). By analysing the functional groups, the overall design of the different components is made. The first step is the specification of the rotor's dimensions (chapter 3.4.2) because they determine the dimensions of every other component. An important part of the drafting is the development of the safety concept which is made in chapter 3.4.6.

3.4.1 Functional groups

The device is divided into different functional groups which are under certain limitations independently designable. The first functional group is the oscillating system. It contains all parts which are directly involved in the bending vibration. The second functional group, the supporting includes all parts that are necessary to support the shaft and adjust the shaft's effective length. In the functional group driveline are all parts integrated which are necessary to provide the torque for operating the system by a certain speed. The housing contains all the equipment needed to keep the systems parts in position, hold up the forces and torques and also the mechanism to avoid accidents by touching rotating parts.

Functional group: Oscillating system

- Shaft
- Rotor
- Unbalanced mass
- Mechanism for adjusting rotor's position

Functional group: Supporting

- Bearings
- Bearing supporting
- Mechanism for adjusting bearing's position

Functional group: Driveline

- Motor
- Controlling
- coupling – motor to shaft

Functional group: Housing

- Carrier, ground plate
- Vibration absorber system
- Safety equipment

3.4.2 Dimensioning rotor

Important attributes to get the desired natural frequencies of the rotor, are beside the shaft's length, diameter and its modulus of elasticity the disk's mass and the bearing type. The calculations are based on the in the theoretical part gathered formulas. The dimensioning process is described below.

1. Determine maximal rotating speed depending on the maximal motor speed and safety issues.

   $\omega_{max} = 3000\ 1/\text{min}$

2. Determine second natural frequency lower then maximal rotating speed.

   $\omega_1 \ll \omega_{max} \rightarrow \omega_1 = 2000\ 1/\text{min}$

3. Determine material (young's modulus) and bearing type.

   Young's modulus: 200 GPa (Steel)
   Bearing types: self-aligning ball bearings (non-rigid bending support)

4. Choose shaft length, diameter and disk mass. Therefore curves with a constant second natural frequency and modulus of elasticity are plotted (Figure 23).

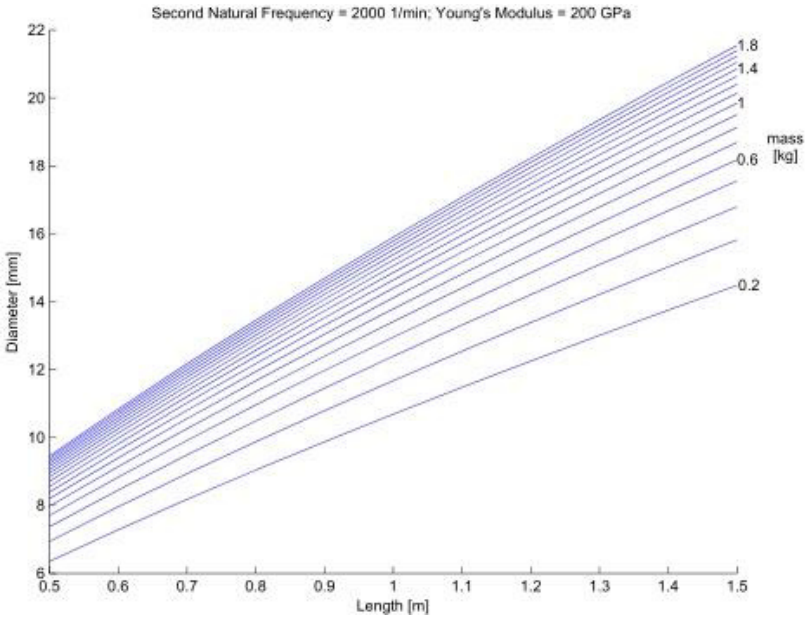

Figure 23: Curves of constant masses and frequency

In Table 1 the in agreement with the thesis supervisor chosen attributes and the expected natural frequencies are listed.

Mass	Length	Diameter	f_1	f_2	f_{Laval}
1 kg	0,6 m	9,982 mm -> 10 mm	1030 1/min	2007 1/min	1410 1/min

Table 1: Rotor dimensions

Determination unbalanced mass

The unbalanced mass and its lever arm causes the excitement of the vibrations. For the above given shaft dimensions, the maximum displacement at its first natural frequency of a Laval-Rotor is shown in Figure 24. The displacement is plotted against the unbalanced mass by a constant lever arm of 0,1 m. The displacement depends also on the damping ratio. Since the damping ratio is not accurately definable, it is practicable to choose the unbalanced mass experimentally on the finished demonstration device.

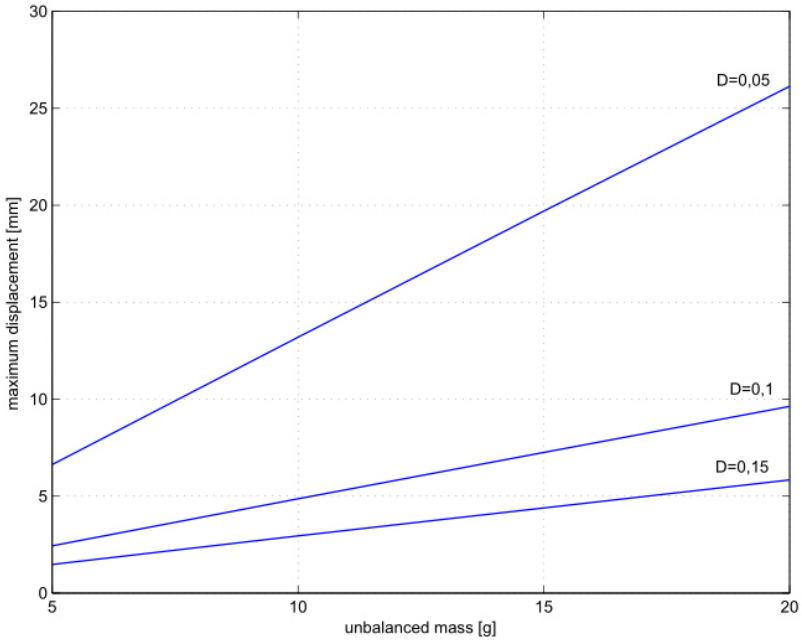

Figure 24: max. rotor displacement according unbalanced mass and damping ratio

3.4.3 Supporting

Derived from the concept, the supporting has to execute different tasks respectively it has to meet different properties. First it has to support the bearings forces properly. Part of this is to isolate the shaft's vibrations from the device's housing. This isolation is on the one hand necessary to avoid an oscillating of the device's housing and on the other hand to keep the shaft's vibration as free from external influences as possible. The supporting also has to provide the possibility to change the effective shaft length by varying the bearing distance. Summarized, the supporting has three different main tasks: supporting the bearing, isolating the vibrations and adjusting the length. Since this three tasks demand quite different properties of the supporting, they are designed separately.

Bearings supporting

The supporting has to hold the static load of the rotor which is caused by the gravitation and the forces which are caused by the oscillating of the rotor. It also has to determine the shaft's axial position. Basically there are two different main solutions to support the bearing. Either to use standardized bearing housings or to design and manufacture custom housings. This decision is made with the following decision matrix (Table 2) and in dialog with the projects supervisors. The criteria which are used for the decision are:

- Overall dimensions:

  Since the standardized housings for bearings are designed for about the maximum bearing load, they have presumably way bigger overall dimensions than special for the demonstration devices designed ones.

- Weight:

  Because of the same reason as for the overall dimensions, the weight of a custom housing will be presumably way lower than a standardized housing.

- Costs:

  Compared to the purchase price of standardized housings, the manufacturing which includes material costs, machining costs and working times is most probably more expensive.

	Factor	Standardized housing		Custom housing	
		rating [1)]	weighted	rating	weighted
Dimensions	5	2	10	5	25
Weight	2	2	4	5	10
Costs	4	5	20	1	4
Sum			34		39

[1)] 1 - very poor; 5 –very good

Table 2: Decision matrix supporting

According the decision matrix a custom manufactured housing is the more matching solution.

Adjusting of the effective length

To adjust the shaft's effective length at least one of both bearings has to be moveable. Since the shaft's axial positions has also to be fixed by the supporting and it is difficult feasible to have an adjustable bearing which also should fix the shaft's axial position, it is practicable to separate those two tasks onto both bearings. This is realized by setting the motor-sided bearing as static and the other one as shiftable. The static, motor-sided bearing has to fix the shaft's axial position. This layout of the supporting is a so called locating and non-locating bearing arrangement (Figure 25).

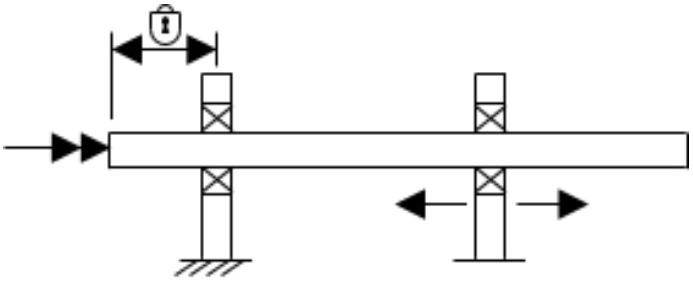

Figure 25: Bearing arrangement

There are several different possibilities to realize the shifting and fixing of the adjustable bearing. There are three basically different solutions gathered. Figure 26 a) shows the first solution. It is based on the mechanism like it is used to move the slide of a milling-machine or a bench vice. It has a turnable-supported threaded bar which is as long as the adjusting range of the bearing should be. The threaded bar is on one side axially fixed and has on the other side a handle. The bearing supporting is located on a slide which is routed on two guide rails. The slide-supporting unit has an inside thread in which is the threaded bar stuck. Thereby the slide moves by turning the threaded bar. On Figure 26 b) and c) are the second solution for shifting and fixing the bearing shown. They consist out of four different main units. A slide-supporting unit, guide rails, a clamping plate and clamping screws. The slide is axially free supported on the guide rails and clamped with the clamping plate and screws against them. The slide-supporting unit is manually shiftable into the desired position after loosening the clamping screws. The third solution (Figure 26 d)) acts similarly to the previous one. The clamping is performed by screws which push against the upper face of the rail. The slide and the rail are shaped in a way that they are clamped to each other by tightening the screws.

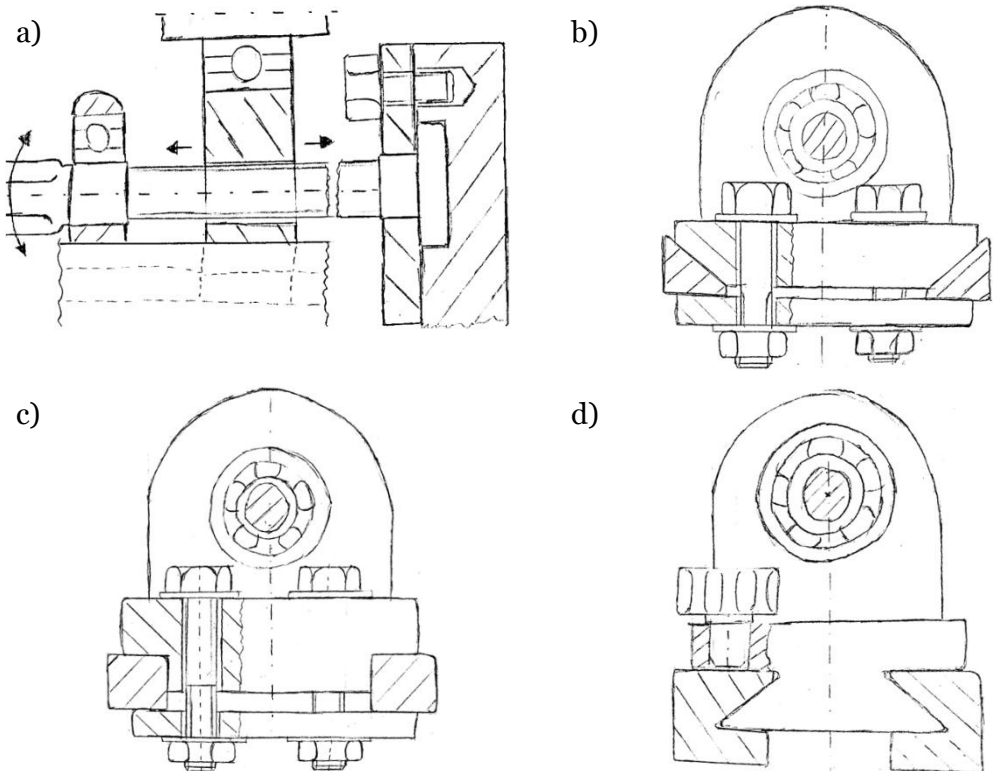

Figure 26: Design proposals bearing shifting

The selecting of the adjusting and fixing principle is executed by using a decision matrix. Therefore the solutions are evaluated by the following criteria:

- Usability

  Since the solution a) just requires a turning of the threaded bar to adjust the bearing's positions, it is quite easy to use. Especially the fine-tuning is comfortable but a larger changing takes a quite long time. The usage of the solution b)/c) and d) are similar. They require a loosening and tightening of the screws for the positioning of the bearing. A larger changing of the positioning is compared to solution a) much faster.

- Costs

  The manufacturing of solution a) is pretty extensive. Especially the threaded bar and its supporting is expensive. Since the rails of solution d) have a complex shape, they are not realizable with standard profiles but have to be manufactured out of solid profiles which leads to higher

costs. For the rails of solution b)/c) can be standardized profiles used. The solution b)/c) has, compared to solution d) an additional part.

- Dimensions and weight

  The solutions b)/c) and d) have comparable dimensions and weights. Since of the threaded bar and its supporting, the solution a) is heavier and needs additional space.

- Clamping capability

  Since of the threaded bar's self-locking, it has a good clamping capability. The solution d) has a between the screws and the rails just a small contact surface a therefore a lower axial fixation. The solution's a) and d) fixation in the plane vertically to the shaft is because of the rail's shape very strong. The clamping of solution b)/c) has to be supplied by its screws initial tension and has therefor a lower clamping capability.

	Factor	Solution					
		a)		b)/c)		d)	
		r[1)]	w[2)]	r	w	r	w
Usability	4	3	12	4	16	4	16
Costs	5	2	10	5	25	4	20
Dimensions and weight	3	2	6	5	15	5	15
Clamping capability	2	5	10	3	6	4	8
Sum			38		62		59

[1)] rating: 1 - very poor; 5 –very good; [2)] weighted rating

Table 3: Decision matrix bearing adjusting

According the decision matrix the solutions b) and c) are the concepts with the highest potential. Since the solution b) has because of its triangular rail a self-aligning while clamping, it is used as concept for the further elaboration.

Vibration isolation

Since the bearing housing has to be stiff enough to support the bearings outer ring, it has nearly no damping capability. To provide the necessary damping capability the supporting's clamping unit should be quite solid and out of a material with a high internal damping.

3.4.4 Shaft hub joint

According the concept the disks have to be shift- and removable attached onto the shaft. Since there appears between the disk and the shaft only the torque which results of the disk's inertness, the holding force does not affect the choosing of the shaft hub joint much. Beside the fulfilment of its main tasks, the shaft hub joint has to satisfy different demands. It should be fast to strain and loose, around the shaft axis balanced and as low priced as possible. Since the connection has to be re-adjustable, it should to be friction-locked. There are several different principles for the shaft hub connection. Proposal a) (Figure 27 a)) is to separate the disk into two part which are clamped with stretching screws and an interference fit onto the shaft. The manufacturing of this solution is complicated because the accurateness of the fit is difficult to achieve on the open hole. Since the point symmetrical shape, the solution a) is balanced. Its loosing and straining is quite fast. Figure 27 b) shows the second proposal for the shaft hub connection. It is a screw-strained cone clamping connection. It has on one or both sides of the hub a loose element with a conical plane which clamps due tightening against a further conical plane on the inner-side of the hub. This kind of shaft hub joint is as standardized part available and has therefore low manufacturing costs. Since this shaft hub joint has several screws to strain, it is more time-intensive to adjust the position of the disks than by systems with fewer screws. The last (Figure 27 b)) solution which is taken into account is also a cone clamping connection and has basically the

same working principle like the previous one. Instead of multiple screws which strains the conical faces against each other it has just a single nut. This brings the advantage of a fast adjusting of the disk by just loosing and straining one nut. This kind of element is also available as standard purchasing part and also needs no additional machining.

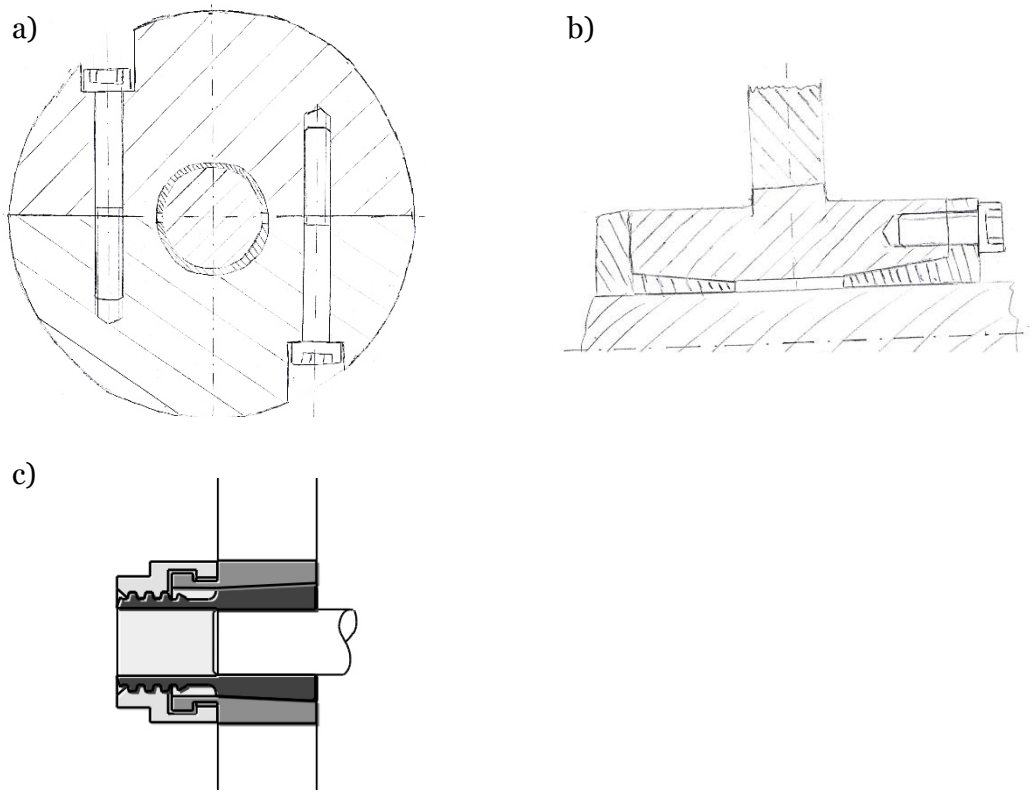

(Ringspann GmbH, 2014)

Figure 27: Design proposals shaft hub connection

The selection of the used system is made with a decision matrix. Evaluated are the properties:

- Costs

  Considered are the purchasing costs as well as the manufacturing costs.

- Ease of use

  The ease of use is mostly depending on the time which is needed for adjusting the time. Solution a) has compared to the other solutions the advantage that the rotor is completely attach- and removable at any position of the shaft. The other solutions has to be putted on the end of the shaft.

	Factor	Solution					
		a)		b)		d)	
		r[1)]	w[2)]	r	w	r	w
Costs	1	2	2	4	4	4	4
Ease of use	1	3	3	2	2	4	4
Sum			5		6		4

[1)] rating: 1 - very poor; 5 –very good; [2)] weighted rating

Table 4: Decision matrix shaft hub joint

According the decision matrix the cone clamping element which is strained with a single nut is the best solution. The in the device used clamping element is the Ringpspann Trantorque Mini. It is available for shaft dimension between 3 mm and 16 mm and supports a maximum transmissible torque of 68 Nm which is way more than needed. Its outer diameter of the clamping element is 23 mm and the seat length for the hub is 13 mm. This dimensions has to be considered by designing the disk.

Figure 28: Ringspann Trontorque Mini (Ringspann GmbH, 2014)

3.4.5 Housing

The housing's main function is to keep all the different parts like the motor, the bearing supporting and the safety-cap in position and provide them a sufficient supporting as well as the needed space to execute their functions. The housing has to be stiff enough to keep in shape while carrying but also resistant against stimulation of the shaft's vibration. It should be easy to transport and therefore lightweight. Since an usage of standard parts is mostly more cost-effective than the manufacturing of custom-parts, they are preferred. The ease of assembling should also be considered. The first developed concept (Figure 29 a)) for the housing consists of a base frame assembled out of standard aluminium profiles and a plastic cover plate where the different units are mounted on. At Matti Kurkis suggestion a concept (Figure 29 b)) with a massive base plate out of plastic is considered, too. The different parts are mounted directly onto the base plate.

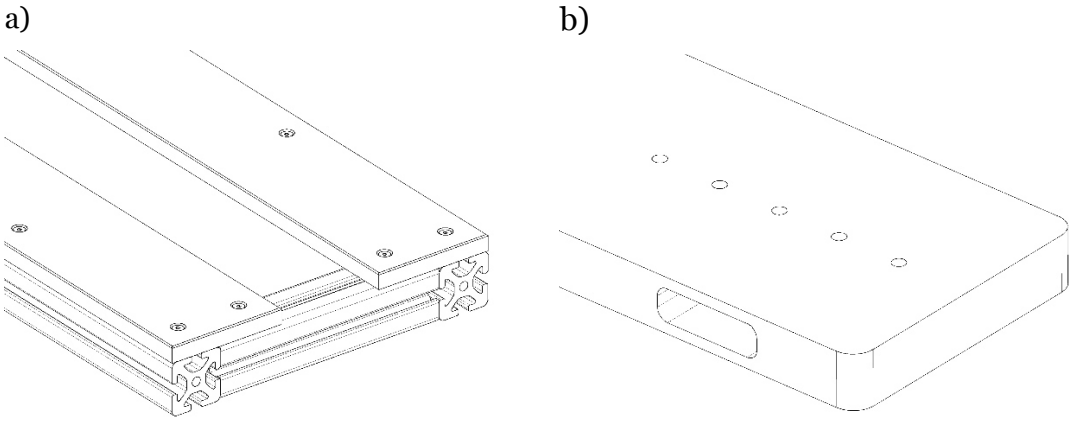

Figure 29: Design proposals housing

The choosing of the housing concept is executed by using a decision matrix. Therefore the solutions are evaluated by the following criteria:

- Costs

  The costs of proposal a) are mostly determined by the material costs of the standard profiles and their connecting elements. A roughly estimated price by using parts of the company Item is about 270 € (item Industrietechnik GmbH, 2015). A massive 50 mm PA6 plate is for comparable dimensions about 320 €. Additionally to the higher material costs the machining of proposal b) is more extensive.

- Weight

  The estimated weight of the aluminium frame and the cover plate (proposal a)) is about 14 kg. The weight of a comparable PA6 plate is about 22 kg (B & T Metall- und Kunststoffhandel GmbH, 2015).

- Stiffness and damping capability

  The damping capability of proposal a) is probably for the same stiffness, compared to all in proposal b) applicable plastics much lower.

	Factor	Solution			
		a) Al-Profiles		b) Solid plate	
		r[1)]	w[2)]	r	w
Costs	4	4	16	3	12
Weight	3	4	12	3	9
Stiffness and damping	2	3	6	5	10
Sum			34		31

[1)] rating: 1 - very poor; 5 –very good; [2)] weighted rating

Table 5: Decision matrix housing

According the decision matrix the aluminium-frame solution is the better concept for the requirements and serves as draft for the further development.

3.4.6 Safety concept

The elaborated safety concept is based on the approach of risk assessment like it is described in ISO- Norm 12100 (Mattilainen, 2015). Therefore, the possible hazards are identified. For this purpose, all tasks which are proceed by using the device have to be considered. After the identification, the risks of the hazards are evaluated. Depending on the risks their countermeasures are elaborated.

Identified hazards

- Turning parts

  The fast turning shaft during the operation involves the risk of injuries if a part of the body comes into contact with it. Also clothes or other fabrics can be dangerous if they winding up on the turning shaft.

- Unintentional restart

  An unintentional start of the device during the adjusting, cleaning and maintaining can lead to a physically contact with fast turning parts.

- High shaft deflexions

  If the device is operated next to the shaft's critical speed, the deflexion of it can be improper high. This can cause a fracture of the shaft or other components.

- Loosening of imbalance-screw

  If a screw which are attached onto the rotating disk for apply an imbalance get loose while operating, it can become a dangerously projectile.

Risk evaluation

The evaluation of the risk is done by rating the severity of the harm and the probability of its occurrence. The severity of the harm is grouped into the categories slight (normal reversible) injury or health hazards, serious (normal irreversible) injury or health hazards and death. The probability of the harm's occurrence is evaluated by the user's expose to the hazard, the probability of occurrence of a hazardous event and the possibility to avoid or limit the harm (Mattilainen, 2015).

Severity of harm	**A**		**1)** slight injury or health hazards **2)** serious injury or health hazards **3)** death
PROBABILITY OF OCCURRENCE OF HARM	**B**	Person's exposure to hazard	**1)** seldom … quite often **2)** regularly … constantly
	C	Probability of occurrence of a hazardous event	**1)** low **2)** average **3)** high
	D	Possibility to limit the harm	**1)** possible under certain conditions **2)** seldom possible

Table 6: Harm evaluation categories (Mattilainen, 2015)

After evaluating each hazard according Table 6 the Level of risk can be read out of Table 7. The higher the number the more dangerous is the rated hazard. The result of the risk level affects the priority of the countermeasure.

A	B	C						
		1)		2)		3)		
1)	1)	1*	2	3	4	5	6	Level of risk
2)	1)	3	4	5	6	7	8	
	2)	5	6	7	8	9	10	
3)	1)	7	8	9	10	11	12	
	2)	9	10	11	12	13	14	
		1)	2)	1)	2)	1)	2)	
		D		D		D		

*1… very safe – 14… highly unsafe

Table 7: Levels of risk (Mattilainen, 2015)

Table 8 shows the evaluated criteria and the out of Table 7 derived risk level of the identified hazards. According this the hazard of turning parts and the loosening of an imbalance-screw involve the highest danger. But every other single hazard is also not to neglect and it also has to be a countermeasure developed against them.

Hazards	A) Severity of harm	B) Person's exposure to hazard	C) Probability of occurrence	D) Possibility to limit the harm	Level of risk
Turning parts	2	2	3	1	9
Unintentional re-start	2	1	2	1	5
High shaft deflexions	2	1	2	1	5
Loosening of screw	3	2	1	1	9

Table 8: Risks of the identified hazards

Countermeasures

To avoid the danger of an accidently grabbing into turning parts or other contact with it, a safety-cap is practicable. The safety-cap has to be transparent to not restrict the purpose of the device. It also has to be removable or has to be able to open to adjust the arrangement of the system. This safety-cap also serves as a barrier for loosening part of the rotor.

To prevent an unintentional restart while working on the device a safety circuit, which cuts of the current if the safety-cap is open, is needed. Therefore a switch is required which cannot be accidently pressed. Since the electrical work is not part of this thesis, this countermeasure has to be considered by the person which does the wiring of the motor.

To ensure that there are no improper high shaft deflexions the maximum deflexion of the shaft has to be limited. Therefore a safety bearing is used. It restricts the shaft deflexion as a mechanical barrier.

3.4.7 Safety bearing

In chapter 3.4.6, the safety bearing as a countermeasure against too high shaft deflexions is introduced. It restricts the deflexion to a maximal amplitude of 5 mm (Figure 30 a)). If the shaft deflexion reaches 5 mm the rotor collides with the safety bearing and stops the swinging up. The safety bearing has to be out of a plastic material which does not damage the rotor while touching. The safety bearing has beside the restriction of the shaft deflexion a second purpose. It serves as an additional supporting if the shiftable bearing is removed. Therefore the rotor has an additional shoulder with the same diameter as the inner diameter of the safety bearing. The shaft can be supported due sliding the safety bearing onto the rotors shoulder (Figure 30 b)). The adjustment of the safety bearing position is similar to the of the supporting.

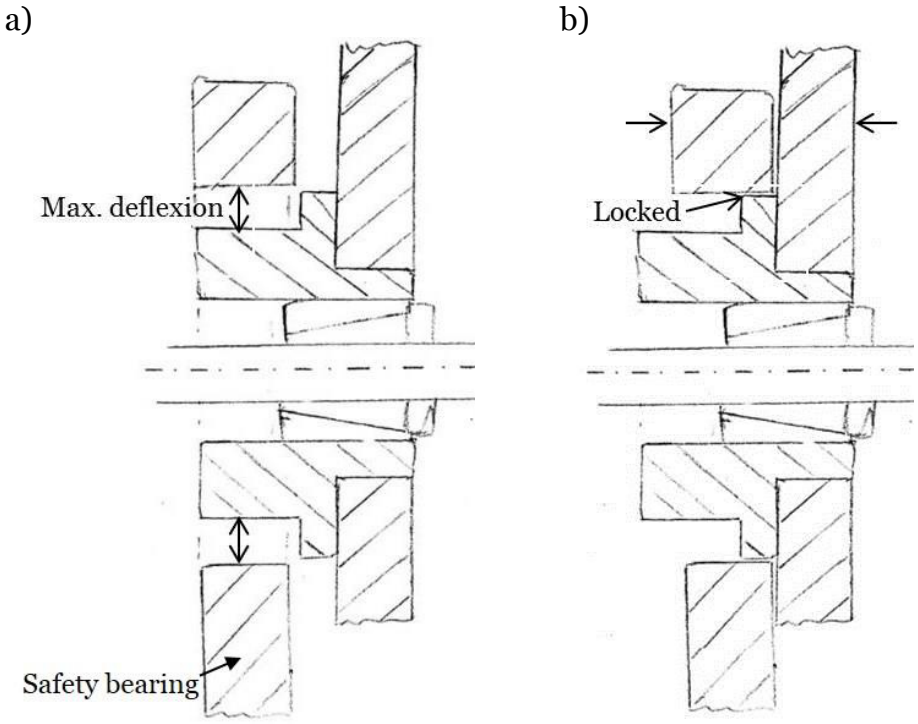

Figure 30: Safety bearing concept

3.5 Elaboration

3.5.1 Introduction

Chapter 3.5 deals with the elaboration of the in the drafting specified concepts. In the elaboration are the custom components designed and standard parts selected. Part of the elaboration are also the material selection of the custom parts and, if required, their strength calculation. The order of the subchapters are in accord with the order the elaboration process is made. Basically the elaboration is made “from inside to outside”. This means that firstly the bearing is selected. The dimensions of the bearing sets the dimension of the support which affects the housing and the safety-cap. Obviously, this process cannot be made completely sequential since sometimes loops are necessary. Part of the results of the elaboration process are the manufacturing and assembly drawings which can be found in the attachment.

3.5.2 Bearing choosing

Since the dimension of the bearings determines the design of the complete supporting, it is chosen at the beginning of the elaboration process. The bearings has to fulfil different requirements in its application at the demonstration device. The most apparently requirements are to hold the forces which are transferred from the shaft and enable the shafts almost torque free rotation. Beside these, the bearing should be as non-rigid as possible against angular-displacements in the shafts direction (Figure 31). This allows the shaft a nearly free bending without high restraints caused by the supporting. The bearings should also be almost maintenance-free and should have a life-cycle which is at least as long as the demonstration device is in business.

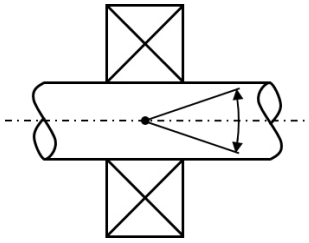

Figure 31: non-rigid bearing axis

Because of the requirement of the bearing as mostly non-rigid against turning in the shaft direction, the selection of possible bearing-types is limited. Every type of plain bearing restricts this angular movement too much. The for this angular displacement most non-rigid rolling-element bearings are the so called self-aligning ball bearings (Figure 32). Self-aligning ball bearings are bearings with two ball rows, which are running in two grooves on the inner ring. The contact surface on the outer ring is spherically shaped and allows the balls to move some degrees around the bearing centre (Figure 32b)). Typically, self-aligning ball bearings allow an angular displacement of about 4 to 7 degrees (NSK Ltd., 2015).

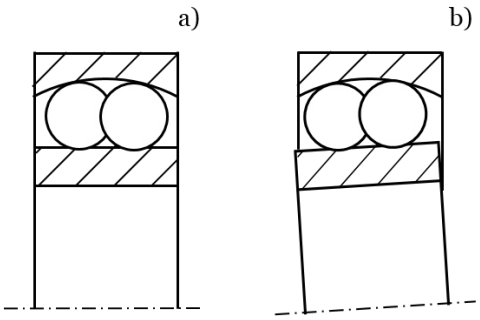

Figure 32: self-aligning ball bearing

The maximal load is the decisive parameter for choosing a suitable bearing. The radial load is a combination of the static gravity force and the rotary force. During a proper operating of the demonstration device there does not occur noteworthy axial forces. The rotary forces are centrifugal forces which results from the rotation of the disks with a particular displacement at a particular angular speed. Figure 33 shows the force diagram with the gravity force and the centrifugal force marked.

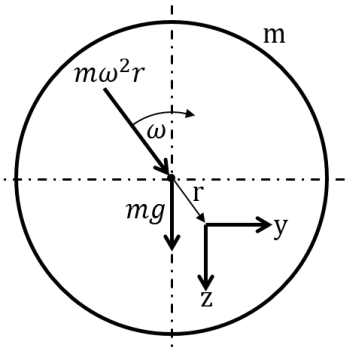

Figure 33: Force diagram disk

The maximal centrifugal forces occur at the second natural frequency of the system, with both disks attached and their maximal allowable displacement of 5 mm (3.1).

$$2 \cdot F_{r,revolving} = F_{centrifugal} = m\omega^2 r$$
$$2 \cdot F_{r,static} = m \cdot g$$

with:

$$m = \sim 2 \cdot m_{Rotor} \approx 2\ kg$$
$$\omega = f_2 \approx 2000\ min^{-1} \approx 210\ s^{-1}$$
$$r = 5\ mm \tag{3.1}$$

$$2 \cdot F_{r,revolving} \approx 2\ kg \cdot \left(210 \frac{1}{s}\right)^2 \cdot 5 \cdot 10^{-3}\ m \approx 441\ N$$
$$F_{r,revolving} \approx \frac{1}{2}\ 441\ N \approx 220\ N$$
$$2 \cdot F_{r,static} \approx 2\ kg \cdot 9{,}81\ \frac{m}{s^2} \approx 20\ \mathrm{N}$$
$$F_{r,static} \approx \frac{1}{2}\ 20\ N = 10\ N$$

The determination of the required dynamic (C) and static (C_0) basic load ratings are done according the Roloff/Matek guideline (Wittel, Muhs, Jannasch, & Voßiek, 2013, 506) in (3.2). The used parameters are listed in Table 9. All parameters are selected either out of Roloff/Matek or, if not named, calculated in this thesis.

Symbol	Parameter	Value	Source
P	Dynamic load	0,22 kN	-
p	Life-time exponent	3	Roloff/Matek 14.2.6
n	Rotating speed	2000 min^{-1}	-
L_{10h}	Desired life-time	2000 h	Roloff/Matek TB 14-7
P_0	Static load	0,01 kN	-
S_0	Static safety factor	1,5	Roloff/Matek 14.2.6

Table 9: Parameter bearing calculation

$$C_{req} \geq P \sqrt[p]{\frac{60\ n\ L_{10h}}{10^6}}$$

$$C_{req} \geq 0{,}22\ kN \sqrt[3]{\frac{60\ 2000\ 1/\min 2000\ h}{10^6}} = 1{,}37\ \text{kN} \tag{3.2}$$

$$C_{0,req} \geq \mathrm{P_0} \cdot \mathrm{S_0}$$

$$C_{0,req} \geq 0{,}01kN \cdot 1{,}5 = 0{,}015\ \text{kN}$$

The, by the leading ball bearing manufacturers SKF and NSK offered self-aligning ball bearings with the lowest load ratings and an inner diameter of 10 mm are listed in Table 10.

Manufacturer	Type	C	C_0
SKF	1200 ETN9	5,53 kN	1,18 kN
NSK	1200	5,55 kN	1,19 kN

Table 10: Bearing load ratings

The actual dynamic (C) and static (C_0) basic load ratings of the bearings are way higher than the required basic load rating (C_{req}, $C_{0,req}$) and are therefore not in danger to be destroyed by the load. The bearing life-time and the minimum load of the bearing is also calculated with the SKF Bearing Calculator which is available on www.skf.com. The SKF Bearing Calculator attests a life-time (L_{10h}) of 132400 hours which exceeds the desired life-time multiple. To ensure an operation without slippage a minimum radial load is needed. Especially at high angular accelerations and at high revolution speeds ball bearings tent to slip what could cause damages of the bearings. The risk of slipping increases with the viscosity of the lubricant. To keep the risk of slipping down the demonstration device should not be operated at high revolution speeds if there is no disk attached. A fast raise of the motor should also be avoid.

3.5.3 Supporting design

The supporting is separated into two main units: the bearing housing and the clamping unit. The bearing housing is a milled aluminium part. It has to support the bearing with an appropriate fit. The clamping unit consists of two plastic plates which are strained by four screws and nuts on a guidance. The upper plate has a milled pocket where the housing is bolted into. The guidance are two triangular Item aluminium profiles and two aluminium L-profiles which are mounted onto the baseplate.

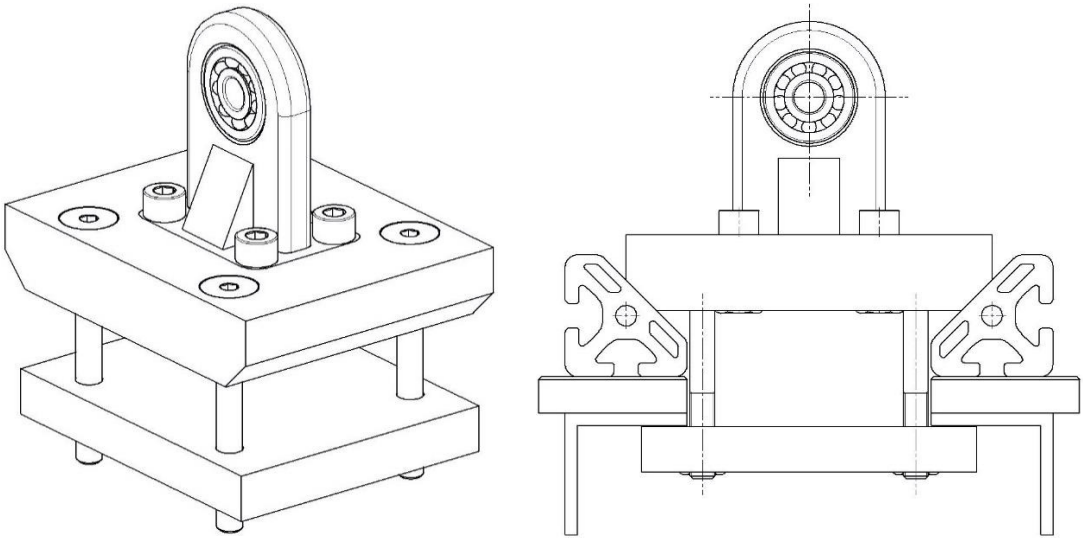

Figure 34: Supporting

Selection of fit

Since of the imbalanced excited force, the load on the bearing rotating inner ring is a point loading (Figure 35). The stationary outer ring has a circumferential load. The bearing manufacturer recommend for this type of load a transition fit at the outer ring and clearance fit at the inner ring (Haberhauer & Bodenstein, 2014, 134). The specific load is low (P / C = 0,22 kN / 5,53 kN= 0,04) and therefore the more loose recommended fits allowed. The used bore tolerance is K7 and the shaft tolerance is g6 (Figure 36).

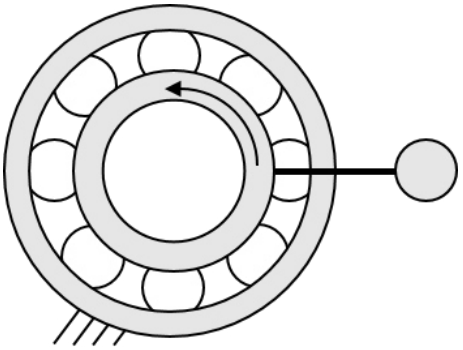

Figure 35: Bearing loading

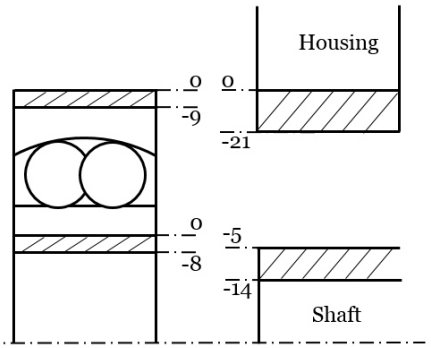

Figure 36: Fittings bearing

For a forceless joining of the bearing housing and the bearing, the housing has to be heated. Since of the thermal expansion the inner diameter of the housing increases depending on its temperature. The required joining temperature ($t_{housing}$) of the housing is calculated in formula (3.3) (Haberhauer & Bodenstein 2014, 134).

$$t_{housing} = t_{env} + \frac{C_m + \Delta D}{\alpha\ D}$$

$$t_{housing} = 20°C + \frac{0{,}021\ mm + 0{,}03\ mm}{23{,}1\ 10^{-6}K^{-1} \cdot\ 30\ mm}$$

$$t_{housing} = 80{,}6\ °C \qquad (3.3)$$

with:

$$\mathrm{D}\Delta = 0{,}03\ mm \quad \text{(join clearance)}$$

$$t_{env} = 20\ °C \quad \text{(ambient temperature)}$$

$$C_m = 0{,}021\ \mathrm{mm} \quad \text{(maximum clearance)}$$

$$\alpha = 23{,}1\ 10^{-6}K^{-1} \quad \text{(thermal expansion)}$$

$$D = 30\ mm \quad \text{(nominal Diameter)}$$

Material selection of the plastic parts

The material for the clamping unit has to fulfil different requirements. Firstly, it has to be good to machine. It also has to have a sufficient mechanical

strength and good damping properties. In the group of the established structure plastics Polyamide 6 (PA6) and Polyacetal (POM) meets this properties best. PA6 has a slightly higher mechanical strength and also a higher ductility as well as better damping characteristics and suits therefore better for the application.

Properties	PA6	POM-C
Density	1.14 g/cm3	1,41 g/cm3
Modulus of elasticity	3300 MPa	2800 MPa
Tensile strength	79 MPa	67 MPa
Elongation at break	130 %	32 %
Damping characteristics	Very good	good

(Ensinger GmbH, 2015)

Table 11: Properties PA6 and POM-C

Stress analyses bearing housing

The stress which acts in the bearing housing is a combination of the static stress resulting of the shrink fit between the bearing and the housing and the dynamic, rotating load. The stress analyses is made with the finite element tool of CATIA V5. The following calculations have the purpose to get a rough scale of the stress in the housing. If the stress is in a critical range the analyses has to be done more precisely. To calculate the stress, the load of the fit and the dynamic load are needed. As dynamic load the number which is calculated for the bearing dimensioning is used (3.1). For a rough calculation of the pressure in the shrink fit, the bearing is assumed as a solid part. This assumption reduces the shrinkage of the bearing and increases the result of the calculation and is therefore uncritical. The bearing housing is assumed as a hub with an outer diameter appropriate the upper part of the housing (D_o). The maximal possible pressure results of the highest interference (I_h), the bearing's and housing's elasticity ($E_i; E_o$), Poisson's ratio ($\mu_i; \mu_o$) and the housing's geometry.

$$p = \frac{I_h \cdot E_O}{D \cdot K}$$
$$p = \frac{0{,}021\ mm \cdot 70\ kN/mm^2}{30\ mm \cdot 2{,}70}$$
$$p = \frac{0{,}021\ mm \cdot 70\ kN/mm^2}{30\ mm \cdot 2{,}70}$$
$$p = 18{,}15\ N/mm^2 \tag{3.4}$$

with:

$$K = \frac{E_o}{E_i}(1 - \mu_i) + \frac{1 + {Q_O}^2}{1 - {Q_O}^2} + \mu_o$$
$$K = \frac{70\ kN/mm^2}{210\ kN/mm^2}(1 - 0{,}3) + \frac{1 + 0{,}6^2}{1 - 0{,}6^2} + 0{,}34 = 2{,}70$$
$$Q_O = \frac{D}{D_o} = \frac{30\ mm}{50\ mm} = 0{,}6$$

The fixation which are simulated in the finite element analyses are not like in the actual case made with bolts and surface contacts. The bolts are neglected and the fixation is realised with three so called surface slider on the bearing housings base (Figure 38). Surface slider lock the displacement vertically to the restrict surface. This simplification does affect the result of the finite element result just insignificantly, as the critical locations are in the upper part of the housing. The load of the shrinkage fit is simulated as a surface pressure on the contact face to the bearing. This loading type conforms to the actual loading precisely. The equivalent stress (Von Mises stress) resulting from the shrinkage fit has a local maximum of about 50 MPa at the flange of the bearing contact surface. This enhancement of the stress evolves from the notching effect on this position. This maximum stress is uncritical because it is far lower than the tensile strength of every aluminium alloy. If commercially available pure aluminium (tensile strength: ~90 MPa, yield strength: ~35 MPa) is used, local non-critically plasticity can occur. The stress caused by the dynamic load is computed statically in different directions. In that way the maximal stress of the rotating load can be found. The maximum Von Mises stress is about 4 MPa

and therefore negligible. Since of the low dynamic stress, a fatigue strength calculation is not made.

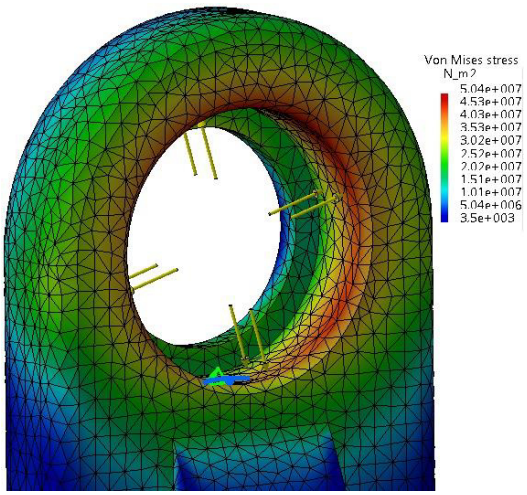

Figure 37: Stress due to shrinkage fit

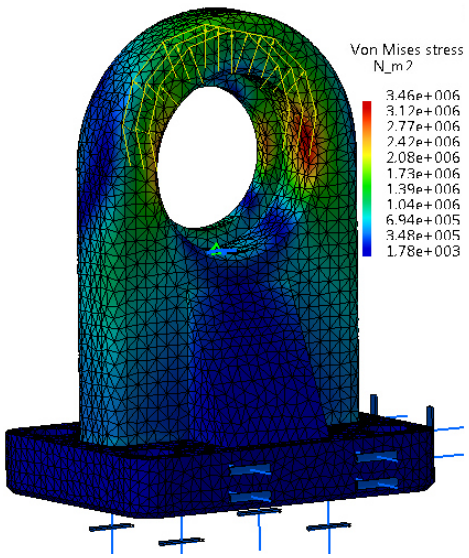

Figure 38: Stress due to dynamic loading

3.5.4 Rotor design

The rotor's purpose is to be the "mass" in the mass-spring system. Beside this it has to provide the possibility to attach the imbalance. The major property of the rotor is its weight which is determined in chapter 3.4.2. It is clamped with the in chapter 3.4.4 selected shaft hub joint on the shaft. Therefore it needs a suitable fit. Additionally the rotor has a shoulder that limits together with the safety bearing the maximal shaft deflexion. This function is described in chapter 3.5.5. The rotor is divided into two parts. The outer rotor (Figure 39) which is a disk with a constant thickness and the inner rotor (Figure 40) that has the shoulder for the safety bearing, the fit for the shaft hub joint and a fit for the outer rotor. The separation into two parts saves a lot of material and machining cost as the outer part can be made out of a sheet with a way lower thickness than the inner part needs. The outer rotor has threaded holes where bolts can be mounted, to apply the desired imbalance. The holes are on four different diameter, so that is it possible to adjust four different magnitudes of imbalance with one bolt. A combination of several bolts increases the possible

steps of the imbalance's magnitude. Since the rotors are in touch with skin while adjusting their position, they are exposed to sweat. To avoid rusting, the rotors material is stainless steel. Since there are no highly requirements on the material strength, the used stainless steel can be chosen by its cost and availability. Because of its cheap price, the well-established stainless steel V2A steel (x5CrNi18-10) is selected.

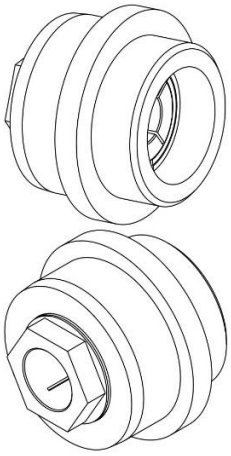

Figure 39: Inner rotor

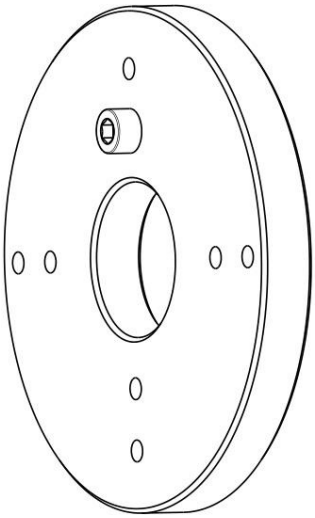

Figure 40: Outer rotor

Fit calculation

The connection between the outer and the inner rotor is made with an interference fit. The calculation are made according Roloff / Matek (Wittel, Muhs, Jannasch, & Voßiek, 2013, 389 – 395). The maximum requried transferable torque is the torque which is needed to tight the shaft hub joint ($T = 44\ Nm$).

Symbol	Parameter	Value	Source
μ	coefficient of adhesion	0,19	Roloff/Matek TB 12-6 (steel – steel)
S_A	Adhesion safety factor	1,5	Roloff/Matek 12.3.1 (static loading)
S_y	Yielding safety factor	1,2	Roloff/Matek 12.3.1 (ductile material)
R_{zi}	Roughness inner rotor	25 μm	Roloff/Matek TB 2-12 (milled surface)

R_{zo}	Roughness outer rotor	25 μm	Roloff/Matek TB 2-12 (milled surface)
$R_{p0,2}$	Yield strength inner rotor	190 MPa	V2A (x5CrNi18-10)
E	Modulus of elasticity	200 GPa	V2A (x5CrNi18-10)
D_F	Diameter of fit	35 mm	Drawing 2
D_{Oo}	Outer diameter outer rotor	114 mm	Drawing 2
D_{Ii}	Inner diameter inner rotor	23 mm	Drawing 3
l_F	Length of fit	11 mm	Drawing 2

Table 12: Parameter for fit selection

First the lowest required joint compression is calculated (p_l) (3.5). It results of the fit's surface (A_F) and diameter (D_F), the coefficient of adhesion (μ) and the required transferable torque (T).

$$p_l = \frac{F \cdot S_A}{A_F \cdot \mu} = \frac{2514\ N \cdot 1{,}5}{1210\ mm^2 \cdot 0{,}19} = 16{,}4\ N/mm^2 \tag{3.5}$$

With:

$$F = \frac{T}{D_F/2} = \frac{44\ Nm}{17{,}5 \cdot 10^{-3}\ m} = 2514\ N$$

$$A_F = \pi \cdot D_F \cdot l_F = \pi \cdot 35\ mm \cdot 11\ mm = 1210\ mm^2$$

With the lowest required joint compression, the lowest required allowance of interference can (I_l) be calculated (3.6). The grading (g) of the fit surface caused by the compression is also considered.

$$I_l = \frac{p_l \cdot D_F}{E} \cdot K + g = \frac{16{,}4 \frac{N}{mm}^2 \cdot 35\ mm}{200\ GPa} \cdot 3{,}76 + 40\ \mu m = 51\ \mu m$$

With:

$$\begin{aligned} K &= \frac{1 + Q_i^2}{1 - Q_i^2} + \frac{1 + Q_o^2}{1 - Q_o^2} = \frac{1 + 0{,}66^2}{1 - 0{,}66^2} + \frac{1 + 0{,}31^2}{1 - 0{,}31^2} = 3{,}76 \\ Q_i &= \frac{D_{Ii}}{D_F} = \frac{23\ mm}{35\ mm} = 0{,}66 \\ Q_o &= \frac{D_F}{D_{Oo}} = \frac{35\ mm}{114\ mm} = 0{,}31 \\ g &= 0{,}8 \cdot (R_{zi} + R_{zo}) = 0{,}8 \cdot (25\ \mu m + 25\ \mu m) = 40\ \mu m \end{aligned} \tag{3.6}$$

The highest allowed joint compression (p_h) is determined by the strength of the used material of the inner and outer rotor and is calculated in (3.7). The highest allowed joint compression sets the highest allowed interference (I_h) (3.8).

$$\begin{aligned} p_{ho} &= \frac{R_{p0,2}}{S_y} \cdot \frac{1 - Q_o^2}{\sqrt{3}} = \frac{190\ MPa}{1{,}0} \cdot \frac{1 - 0{,}31^2}{\sqrt{3}} = 99\ N/\ mm^2 \\ p_{hi} &= \frac{R_{p0,2}}{S_y} \cdot \frac{1 - Q_i^2}{\sqrt{3}} = \frac{190\ MPa}{1{,}0} \cdot \frac{1 - 0{,}66^2}{\sqrt{3}} = 62\ N/\ mm^2 \\ p_{hi} &< p_{ho} \Rightarrow p_h = p_{hi} = 62\ N/\ mm^2 \end{aligned} \tag{3.7}$$

$$I_h = \frac{p_h \cdot D_F}{E} \cdot K + g = \frac{62 \frac{N}{mm^2} \cdot 35\ mm}{200\ GPa} \cdot 3{,}76 + 40\ \mu m = 81\ \mu m \tag{3.8}$$

The difference of the highest and lowest allowed allowance of interference determines the possible dimension variation (P_t) of the fit. The dimension variation is separated into the tolerance of the inner and outer diameter (T_i, T_o). The tolerances are chosen according the ISO- tolerance table (ISO 286). Because of machining reasons a hole basic fit is chosen.

$$P_t = I_h - I_l = 81\ \mu m - 51\ \mu m = 30\ \mu m$$

⇒inner dimension:

H6 (EI=0 µm; ES=16 µm)

⇒outer dimension: (3.9)

$$ei = ES + I_l = 16\ \mu m + 51 \mu m = 67\ \mu m$$

$$es = EI + I_h = 0 + 81\ \mu m = 81\ \mu m$$

u6 (ei=60 µm; eo=76 µm)

To join the parts forceless, the inner rotor has to be cooled down or the outer rotor heated up. The calculation of the required temperature difference is mad in (3.10) (Haberhauer & Bodenstein, 2014).

$$t_\Delta = \frac{C_m + \Delta D}{\alpha\ D}$$

$$t_\Delta = \frac{0{,}081\ mm + 0{,}03\ mm}{10{,}1 \cdot 10^{-6} K^{-1} \cdot\ 35\ mm} = 300\ °C \quad (3.10)$$

with:

$D\Delta = 0{,}035$ mm	(join clearance)
$C_m = 0{,}076$ mm	(maximum clearance)
$\alpha = 10{,}1 \cdot 10^{-6} K^{-1}$	thermal expansion)
$D = 35\ mm$	(nominal Diameter)

3.5.5 Safety bearing design

The safety bearing consists out of the bearing itself, a strain plate, two metal plates and a countersunk bolt. Since the safety bearing does not have to support high loads it is strained with just one bolt. To hold the strain plate while straining the bolt, it has two shoulders which are in contact to the ground plate. The metal part which is inserted into the strain plate is threaded and transmits the bolts stress into the strain plate. The material requirements for the bearing and the strain plate are similar to them for the supporting's plastic

parts. Therefore the in chapter 3.5.3 selected material is also used for the safety bearing.

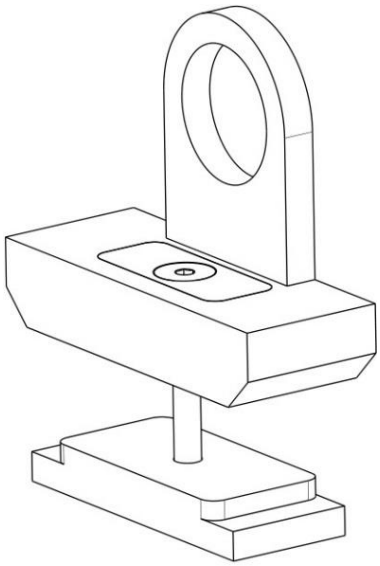

Figure 41: Safety bearing

3.5.6 Shaft design

The main properties of the shaft are determined in chapter 3.4.2. Its diameter is 10 mm and the maximal effective length which means the distance between the bearings is about 600 mm. The shaft's material is in drafting defined as a steel material. To adjust or remove the supporting, safety bearing and the rotor, the shaft has to have a constant diameter on his complete length. This is also necessary to meet the theoretical assumptions which are made for transforming the shaft into an equivalent spring (chapter 2.2.1). The axial fixation of the shaft is done in the motor-sided supporting. Therefore the bearing is fixed with a retaining ring on the shaft.

Coupling

The shaft is driven by the electric motor. The electric motor is already at hand and therefore the shaft has to be adapted to the given dimensions. The connection between the shaft and the motor should be as non-rigid against bending

as possible to get a free bending of the shaft. Beside this, the connection should isolate vibrations and rotation oscillating. A shaft coupling with a rubber element is practicable and common to satisfy this requirements. Since the required transferable torque is quite low, it plays just a minor role for the selecting of the coupling. There are lot of different supplier which offer very similar solutions. The chosen coupling are the ROTEX torsionally flexible coupling of the company KTR (Figure 42, Table 13).

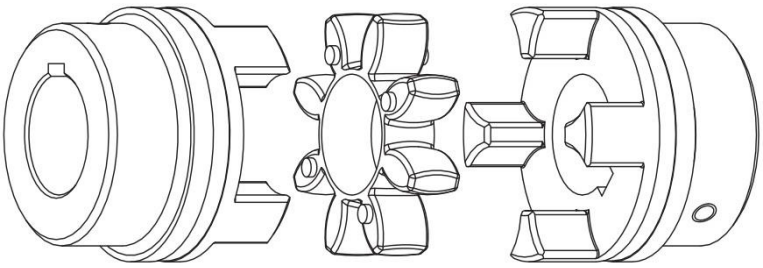

Figure 42: ROTEX coupling (KTR Kupplungstechnik GmbH , 2015)

Property	Value
Maximal angular displacement	0,9°
Maximal radial displacement	0,85 mm
Nominal torque	10 Nm
Shaft hub joint	Key connection

(KTR Kupplungstechnik GmbH , 2015)

Table 13: Main properties ROTEX coupling

The coupling is non-rigid against bending until an angle of 0,9 °. To check if the coupling is non-rigid for the complete displacement of the rotor the bending line of the shaft is as parabolic approximated. For an exemplary calculation (3.11), the distance between the bearings is 600 mm and the maximal allowed rotor displacement is centric of the shaft (Figure 43).

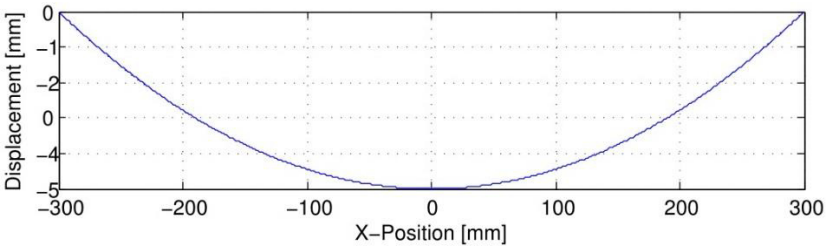

Figure 43: Bending line

The shaft bending angles which are at the bearing's position are about the same like at the coupling. For a free bending the bending angle at the bearing is 1,9 °. According this the stiffness of the system will increase for higher shaft deflexion than 0,9 °.

$$
\begin{aligned}
y(x) &= a \cdot x^2 + b \\
y(x) &= \frac{1}{18000} \cdot x^2 - 5 \\
\dot{y}(x) &= \frac{1}{9000} \cdot x \\
\dot{y}(300) &= \frac{1}{9000} \cdot 300 = 1/30 \\
\alpha_{max} &= \arctan\big(\dot{y}(300)\big) = \arctan\left(\frac{1}{30}\right) = 1{,}9\,^\circ
\end{aligned}
\tag{3.11}
$$

With:

$$
\begin{aligned}
y(0) &= -5 \\
y(300) &= 0 \\
\Rightarrow\ b &= -5 \\
\Rightarrow\ a &= 1/18000
\end{aligned}
$$

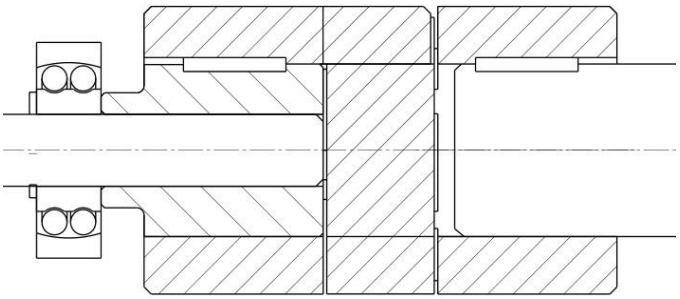

Figure 44: Shaft connection

Since the diameters of the shaft and the motor's output shaft are different, an adapter needed (Figure 44). This adapter is connected with a key to the RO-TEX coupling. The connection between the adapter and the shaft is made with a glued joint. A glue joint is the favourable connection because it does not require an additional machining of the shaft. An interference fit is not used because it would either require a second diameter of the shaft or the hole of the adapter cannot made according the hole basic system (H). Usual industrial metal glues can hold high shear forces up to 25 N/mm². A suitable glue is the Loctite 638. For this glue connection the maximal transferable torque is about 100 Nm. The used fit between the adapter and the shaft is a H7/g6. This fit is a clearance fit with a clearance of 5 to 29 µm which features an optimal bonded joint and a force-less mounting.

Property	Value
Maximal shear forces	> 25 N/mm²
Maximal gap	250 µm
Curing time (hand-tight)	4 min

(Henkel AG, 2015)

Table 14: Properties Loctite 638

Strength calculation

The strain in the shaft is caused by two different effects. The bending of the shaft and the contact pressure of the Ringspann shaft hub joint. The tension caused by the bending is oscillating and the contact pressure static. Since there is an oscillating load, the shaft is verified on fatigue strength. The calculations are made by hand with supporting by finite elements methods. For the calculation the rotor is centric assumed. In this case the highest shaft deflexion is on the same length as the contact pressure of the shaft hub joint. The strain caused by the bending (φ_b) is calculated in (3.12).

$$\varphi_b = \frac{F \cdot \frac{l}{4}}{I_y} \cdot r = \frac{115\ N \cdot \frac{600\ mm}{4}}{491\ mm^2} \cdot 5\ mm = 176\ MPa \tag{3.12}$$

With:

$$F = \frac{r \cdot 48 \cdot E \cdot I}{l^3} = \frac{5\ mm\ \cdot 48 \cdot 210\ GPa \cdot 491\ mm^2}{600\ mm^3} = 115\ N$$

$$I_y = \frac{\pi \cdot (2r)^4}{64} = \frac{\pi \cdot (10\ mm)^4}{64} = 491\ mm^2$$

Its solution is evaluated with a finite elements calculation (Figure 45). The restraints in the finite elements calculation are blocked translator deflexions of the shaft ends. The load is a forced deflexion at the centre of the shaft. This constraints causes a parabolic bending of the shaft. The solution of the maximal equivalent stress is 169 MPa and therefor about the same than the maximal stress calculated by hand (176 MPa).

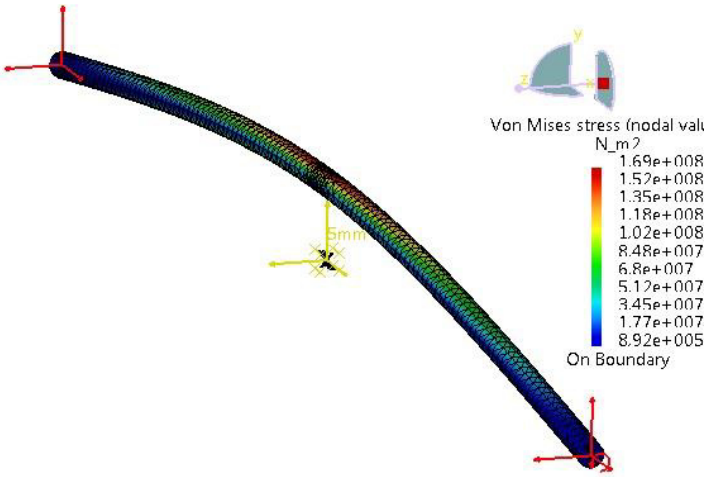

Figure 45: FE calculation strain caused by bending

The static stress caused by the clamping force of the hub joint connection is for the lowest recommended tightening torque of the damping nut 197 MPa (Ringspann GmbH, 2014). According the finite element solution, the combined stress is on the stretched side of the shaft (σ_h) 358 MPa and on the compressed side (σ_l) 22 MPa (Figure 46).

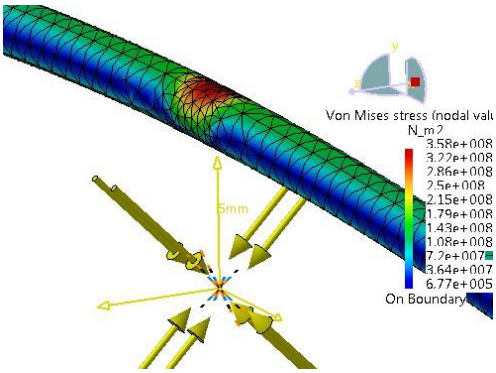

Figure 46: FE calculation combined stress

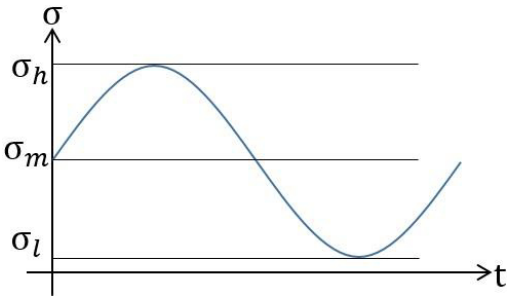

Figure 47: Stress cycle

The fatigue strength calculation is made according the strength of materials 2 script (Apel, 2012) which is based on the FKM- guidelines (research curatorship mechanical engineering). The fatigue strength of the material depends on

the nature of the load. A mean stress (σ_m) reduces the fatigue strength (σ_f). The fatigue strength for a pure alternating load (R=-1) can be estimated with its tensile strength (R_m) and its ductility. The FKM-guidelines gives experimental determined ratios between the alternating fatigue strength and the tensile strength of certain material sorts (f). The influence of the stress ratio (R) can be read in the fatigue strength diagram (Figure 48). The rate of the stress ratio's influence depends on the materials tensile strength and is specified in mean stress sensitivity (M_σ). The calculation is made for the proposed stainless steel S355 (Table 15).

Tensile strength R_m	Mean stress sensitivity M_σ	Alternating strength factor f
490..630 MPa	$3{,}5 \cdot 10^{-4} \cdot R_m - 0{,}1$	0,45

(Apel, 2012)

Table 15: Properties S355

$$
\begin{aligned}
R &= \frac{\sigma_l}{\sigma_h} = \frac{22\ MPa}{358\ MPa} = 0{,}06 \approx 0 \\
\sigma_a &= \frac{\sigma_h - \sigma_l}{2} = \frac{358\ MPa - 22\ MPa}{2} = 168\ MPa \\
\sigma_w &= f \cdot R_m = 0{,}45 \cdot 490\ MPa \\
M_\sigma &= 3{,}5 \cdot 10^{-4} R_m[MPa] - 0{,}1 = 3{,}5 \cdot 10^{-4} \cdot 490 - 0{,}1 = 0{,}072
\end{aligned}
\tag{3.13}
$$

The fatigue strength for the given stress ratio $\sigma_{f(R=0)}$ can be read out the fatigue strength diagram (Figure 48). It is $\sigma_{f(R=0)} = 205\ MPa$. The safety factor for a fatigue fracture is $S_f = 1{,}2$ (3.14). This result is just a roughly expectation and is shows just a tendency of the actual fatigue strength. Since the calculations are made with the lowest specified tensile strength the actual fatigue strength is probably higher. The fatigue strength is defined as the stress which destroys the material after 10^6 stress cycles. 10^6 stress cycles are at a mean revolution speed of 1500 1/min a run-time of about 700 minutes. The run-time by maximum shaft deflexion will be just several seconds or at least few minutes. Therefore the probability of a collapse is even less.

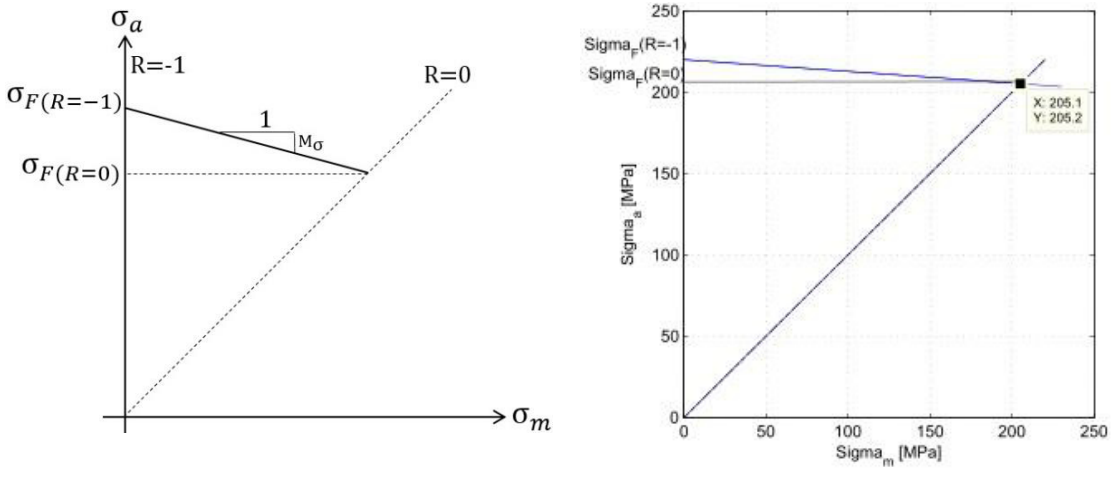

Figure 48: fatigue strength diagram

$$S_f = \frac{\sigma_{f(R=0)}}{\sigma_a} = \frac{205\ MPa}{168\ MPa} = 1{,}2 \tag{3.14}$$

3.5.7 Housing design

The housing (Figure 49) consist mainly out of an aluminium profile frame on which are two plastic plates mounted. The plates serve as basis for the motor and the supporting rails. The aluminium frame has in combination with supporting rails the needed stiffness for carrying the device and for supporting the motor and the rotor. The plates provide an additional damping between the rotor supporting and the frame as well as between the motor and the frame. This reduces a vibrating of the housing. A low vibration of the complete device is necessary to ensure an undisturbed oscillating of the rotor. The requirements of the plate material is alike those of the supporting's plastic parts. Therefore the in chapter 3.5.3 selected material can also be used for the plates.

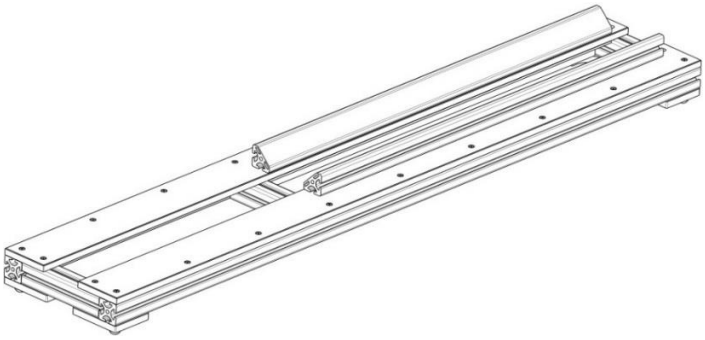

Figure 49: Housing

3.5.8 Safety-cap design

One of the in chapter 3.4.6 defined safety measures is the safety-cap. It has to avoid a harmful contact between the rotating parts of the device and the user. Additionally, it provides a barrier if rotating parts get loose or the shaft collapses. To not limit the view onto the rotor, the safety-cap is made out of Plexiglas (acrylic glass). An established glass thickness for applications like this is 8 mm. This thickness is adopted by commercial safety-caps for machine tools. For a good torsion stiffness and to close the cap on both ends, there are endcaps out of plastics (PA6 or POM). The cap is fixed with two quick clamps on each end to fastening plates. The Plexiglas cover can be either bended to shape or pieced out of several plates. The bended cover (Figure 51) needs threaded holes on its faces to join it to the cap ends. This threaded holes are critical to produce because of the occurring notch effect. There is a high risk that the Plexiglas cover cracks while cutting the tread or straining the bolts. The bending of Plexiglas is with a sufficient heating possible. If the cap will be made with a bended Plexiglas cover the processing instructions of the material has be followed. Since of the manufacturing difficulties, a cap is elaborated which does not requires threads in the Plexiglas (Figure 50). It has instead of one bended plate five several plates with milled chamfers on their long sides. The cap ends have milled slots in which the Plexiglas plates are bonded. To achieve an additionally stiffness, the cap ends are connected with two bars.

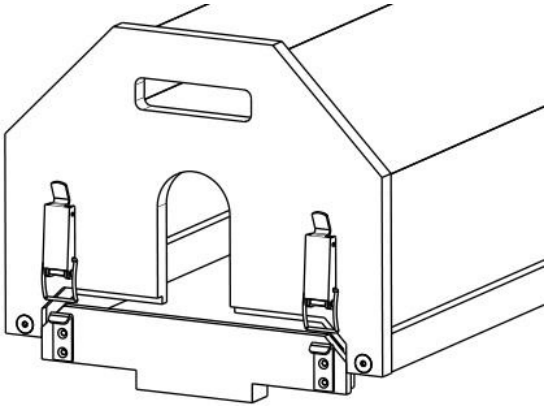

Figure 50: Safety cap with several plates

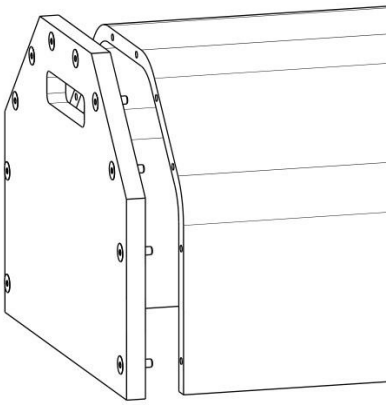

Figure 51: Safety cap with bended plate

3.6 Summary and prospects

The complete demonstration device is shown in Figure 52. The natural frequencies of the rotor can be varied by adjusting the free supporting's position as well as by adjusting the position of the disks. To remove or attach a disk the free supporting has to be slide of the shaft so that the disk and its safety bearing can be pulled out the shaft. To keep the shaft horizontally while the free bearing is taken-off, the second safety bearing is supposed to be put onto its corresponding disk. The disks can also be mounted on the cantilevered side of the shaft if desired. The combination of the thin shaft, the comparatively heavy disks and the, to a certain extend non-rigid supporting should demonstrate the critical speeds and their characteristic oscillating modes well. A sufficient operational safety is given by the safety-cap and the safety bearings. A detailed

operation manual and the assembly instructions for the device can be found in the attachment.

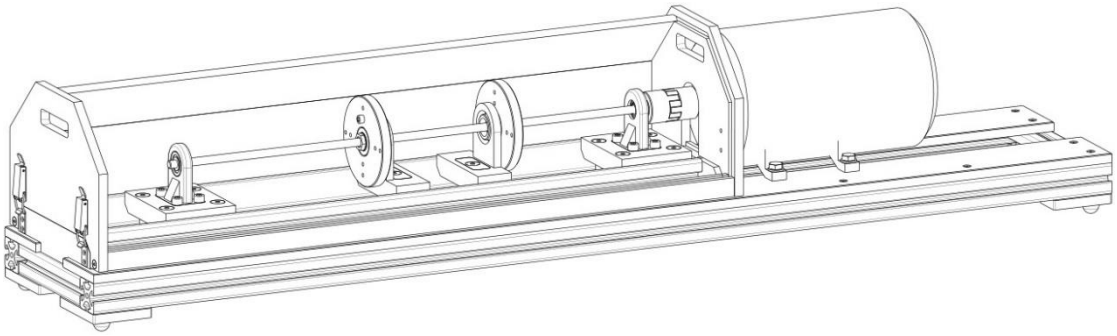

Figure 52: Complete device

Since in this work is just the mechanical design of the device made, the controlling of the motor has to be elaborated in a further work. Unfortunately the manufacturing of the custom parts is not done during my stay in Jyväskylä, so the assembling and putting into service has to be made later.

4 Summary

The introduced Laval Rotor is a simple model of a shaft-disk combination. The negligence of the shaft's mass and the assumption of a symmetrically system permits to transfer the model into a plane mass-spring system which can be simply descript with a usual linear oscillating differential equation. An imbalance combined with a turning of the rotor excites the oscillating. This excitement makes the differential equation inhomogeneous and is described in the perturbation function. Since of the imbalance the differential equation got non-linear. The solving of the model is made numerical in the software Matlab. Analysing the transfer function shows that the system's maximum deflexion is on its natural frequency. This deflexion depends on the damping and reaches in an undamped system infinite. Because of the risk of destruction, the natural frequency of a shaft is called critical speed. The Laval Rotor has because of its simplification as a one-mass system just a single degree of freedom and so just a single natural frequency. A distributed of the mass raises the number of degrees of freedom and also the number of natural frequencies. Therefore a shaft with several disks has several critical speeds. A rotor oscillates beside translational also rotational which also should be taken in account while constructing a shaft.

The development project is separated in the planning phase, the conception phase, the drafting and the elaboration. In the conception are the device's rough functions gathered. The concept describes that shaft length as well as the disks amount and positions should be adjustable. The drafting improves this concepts and specifies sub-functions and their operation methods. In the elaboration the designing process is completed and provides every documents which are necessary to manufacture and operate the device.

5 Discussion

A main objective of this thesis-work was on the one hand the gathering of the theoretical basis which is necessary to understand the effect of imbalanced excited bending vibrations of rotors and to determine the concept of the demonstration device. Furthermore, the development of an executable demonstration device was the actual objective of this work.

The theoretical basis is compiled in the theoretical part of this thesis. It provides an extensive overview and a comprehensively mathematical description of the phenomenon of imbalanced excited vibrations. The theoretical basis exceeds the, for the development demanded knowledge and deepened the author's skills in the theory of oscillations and simulation.

The development of the demonstration device for imbalanced excited bending vibrations has be done during the thesis-work. The demands on the device are mainly fulfilled. Since the designing of the motor's control circuit is not made in this thesis-work, the demonstration device is not ready for use yet. Unfortunately, the manufacturing of the custom designed parts is not made during the author's stay in Jyväskylä, so the assembling as well as the bringing into service cannot be done by the author. The development process demands capabilities in different subjects but primarily in the field of mechanical engineering design. The major challenge of the project was to meet the timetable.

The creating of the thesis was interesting, challenging and not least, because of the results satisfactory. Once more, I want to thank Matti and Jorma for supervising the thesis and the frequent, fruitful meetings.

6 References

Gasch, R., Nordmann, R., & Pfützner, H. 2006. Rotordynamik [*Rotor dynamic*]. Berlin: Springer-Verlag.

Rao, S. 2010. *Mechanical Vibrations*. New Jersey: Prentice Hall.

Wittel, H., Muhs, D., Jannasch, D., & Voßiek, J. 2013. Roloff/Matek Maschinenelemente [*Roloff/Matek machine elements*]. Wiesbaden: Springer Vieweg.

Haberhauer, H., & Bodenstein, F. 2014. Maschinenelemente [*Machine elements*]. Berlin: Springer Verlag.

Stodola, A. 1918. Eine neue kritische Wellengeschwindigkeit [*A new critical shaft speed*]. Dinglers Polytechnisches Journal, 12. January 1918.

Apel, N. 2012. Festigkeitslehre 2 [*Strength of materials 2*]. Hochschule Esslingen.

Mattilainen, J. 2015. *Machine Safety & Ergonomics*. JAMK University of Applied Sciences.

B & T Metall- und Kunststoffhandel GmbH. 20 April 2015. *Prices of PA6 and POM-C*. Retrieved from http://www.metallkunststoffhandel.de/shop/

Henkel AG. 12 May 2015. *Loctite 638 Data sheet*. Retrieved from http://tds.henkel.com/tds5/docs/638-EN.PDF

item Industrietechnik GmbH. 20 April 2015. *Prices of item products*. Retrieved from http://www.item24.com/

KTR Kupplungstechnik GmbH. 10 April 2015. *ROTEX catalogue*. Retrieved from http://ktrinternational.com/root/img/pool/pdf/produktkataloge/en/en_gesamt/001_rotex_en.pdf

NSK Ltd. 15 April 2015. *Information about self-aligning ball bearings*. Retrieved from http://www.nsk.com/products/ballbearing/selfaligning/

Ringspann GmbH. 15 December 2015. *Installation and Operating Instructions for Cone Clamping Elements*. Retrieved from http://www.ringspann.com/files_db/1417603013_46__14.pdf

7 Attachment

1. Part list

Manufacturing drawings:

2. Supporting (DWR001)
3. Outer rotor (DWR002)
4. Inner rotor (DWR003)
5. Shaft (DWR004)
6. Hull (DWR005)
7. Supporting plate (DWR006)
8. Support strainplate (DWR007)
9. Safety-bearing (DWR008)
10. Safety-bearing strainplate (DWR009)
11. Safety-bearing mountingplate (DWR010)
12. Mountingplate strainplate (DWR011)
13. Groundplate (DWR012)
14. Corner 1 (DWR013)
15. Corner 2 (DWR014)
16. Cap plexiglass corner (DWR015)
17. Cap plexiglass side (DWR016)
18. Cap face (DWR017)
19. Cap face motor side (DWR018)
20. Cap rail (DWR019)
21. Cap shoulder (DWR020)
22. L-profile (DWR029)

Assembly drawings:

23. Safety-cap (DWR021)
24. Rotor (DWR022)
25. Supporting (DWR023)
26. Frame (DWR024)
27. Housing (DWR025)
28. Safety-bearing (DWR026)
29. Complete device top-view (DWR027)
30. Complete device side-view (DWR028)

Manuals:

31. Assembly instructions
32. Operation manual

PART LIST

Custom parts

Part Nr.	Drawing Nr.	Name	Amount	Material	Weight [kg]
PART001	DWR001	Bearing housing	2	Aluminium	0,16
PART002	DWR002	Rotor outer	2	Stainless Steel (V2A)	0,93
PART003	DWR003	Rotor inner	2	Stainless Steel (V2A)	0,12
PART004	DWR004	Shaft	1	Structural Steel (S355)	0,42
PART005	DWR005	Hull	1	Structural Steel (S355)	0,08
PART006	DWR006	Supporting plate	2	Plastics (POM-C/PA6)	0,27
PART007	DWR007	Supporting strainplate	2	Plastics (POM-C/PA6)	0,17
PART008	DWR008	Safetybearing	2	Plastics (POM-C/PA6)	0,16
PART009	DWR009	Safetybearing strainplate	2	Plastics (POM-C/PA6)	0,05
PART010	DWR010	Mountingplate Safetybearing	2	Structural Steel (S235)	0,1
PART011	DWR011	Mountingplate Strainplate	2	Structural Steel (S235)	0,11
PART012	DWR012	Groundplate	2	Plastics (POM-C/PA6)	2,26
PART013	DWR013	Corner 1	2	Plastics (POM-C/PA6)	0,08
PART014	DWR014	Corner 2	2	Plastics (POM-C/PA6)	0,08
PART015	DWR015	Cap plexiglass corner	3	Acryl glass (Plexiglass)	0,81
PART016	DWR016	Cap plexiglass side	2	Acryl glass (Plexiglass)	0,85
PART017	DWR017	Cap face	1	Plastics (POM-C/PA6)	0,49
PART018	DWR018	Cap face motorside	1	Plastics (POM-C/PA6)	0,44
PART019	DWR019	Cap rail	2	Plastics (POM-C/PA6)	0,5
PART020	DWR020	CAP shoulder	2	Plastics (POM-C/PA6)	0,16

Purchasing parts				**Order Number**	
PART101		Item profile 40x40 45° x820mm	2	See Item offer	1,62
PART102		Item profile 40x40 x180mm	3	See Item offer	0,44
PART103		Item profile 40x40 x1400mm	2	See Item offer	3,46
PART104	DWR029	Item L-profile 40x40x4 x820mm	2	See Item offer	0,66
PART105		Ringspann shaft-hub-coupling	2	4202-010100-000000	0,05
PART106		Rotex coupling	1	see Rotex drawing	0,35
PART107		Self-alligning ball bearing	2	SKF 1200 ETN9	0,034
PART108		Item T-Slot Nut 8 St M4	44	See Item offer	0,011
PART109		Item T-Slot Nut 8 St M6	12	See Item offer	0,01
PART110		ItemAutomatic-Fastening Set 8	12	See Item offer	0,035
PART111		quick fastener	4		
PART112		Motor	1		13,2

Standard pts.	**Norm**	**Name**		**Position**	
PART201	ISO 10642	Countersunk Screw M4x22	40	Groundplate, Corners	0,002
PART202	ISO 10642	Countersunk Screw M6x25	12	L-Profile/45°-Profile	0,005
PART203	ISO 10642	Countersunk Screw M8x80	10	Supporting/Safetybearing	0,034
PART204	ISO 4762	Cylinder Screw M8x25	8	Supporting	0,014
PART205	ISO 4032	Hex nut M8	16	Supporting	0,004
PART206	ISO 4017	Hex Screw M10x40	4	Motor	0,032
PART207	ISO 4032	Hex nut M10	4	Motor	0,01
PART208	ISO 4762	Cylinder Screw M6x14	4	Rotor	0,005
PART209	ISO 4032	Hex Nut M5	4	Cap	0,003
PART210	ISO 10642	Countersunk Screw M5x25	4	Cap	0,002

PART213	ISO 4762	Cylinder Screw M4x40	4	Cap shoulder	0,003
PART214	DIN 125A	Washer M10	8	Motor	
PART211	DIN 6885	Feather key - Form A 8x7x18	2		
PART212	DIN 471	Retaining ring - A 10x1	1		

Device weight: 44 kg

GROUP LIST

GROUP Nr.	**Drawing Nr.**	**Name**
GROUP001	DWR021	Safety cap
GROUP002	DWR022	Rotor
GROUP003	DWR023	Supporting
GROUP004	DWR024	Frame
GROUP005	DWR025	Housing
GROUP006	DWR026	Safetybearing unit
GROUP007	DWR027	Complete device
	DWR028	

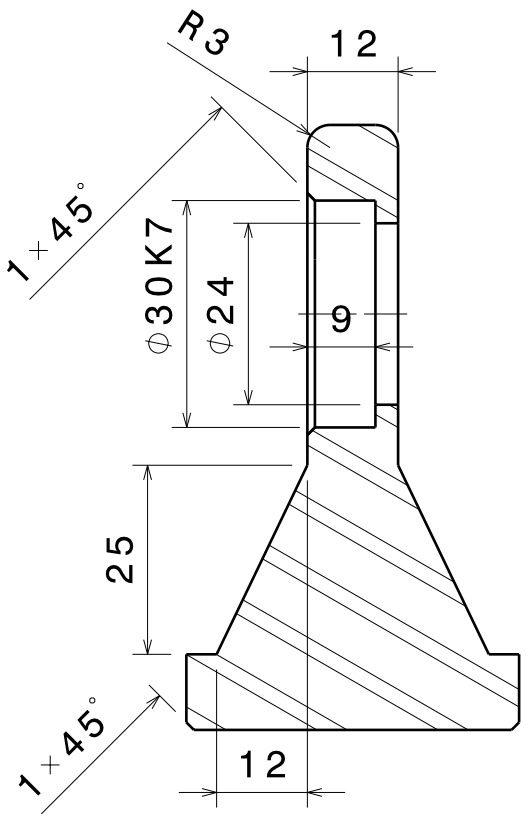

Section view A-A
Scale: 1:1

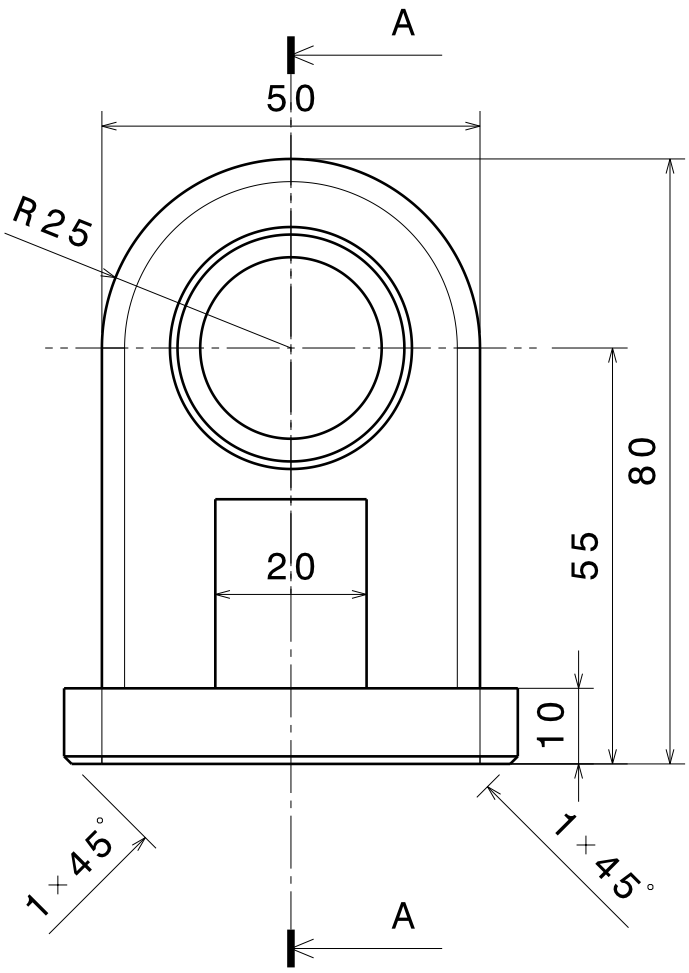

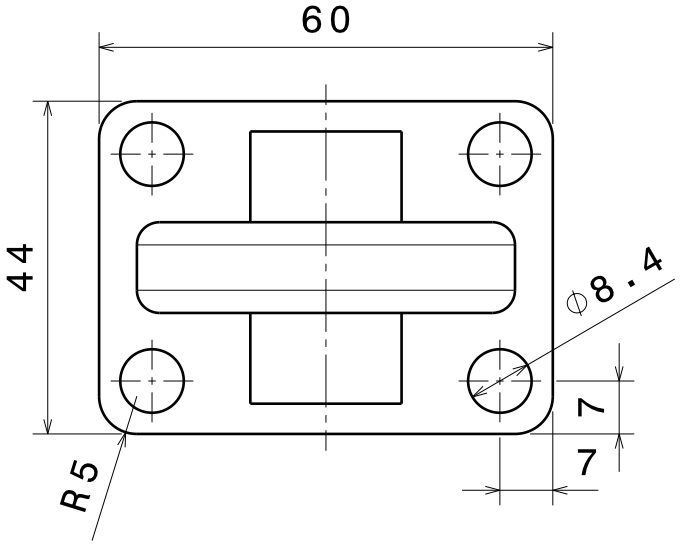

general tolerance: SFS-EN 22768-1m

DESIGNED BY: J. Gengenbach DATE: 12.04.2015			
Material: Aluminium			
SIZE: A4	Amount: 2	Supporting PART001	
SCALE: 1:1	WEIGHT (kg): 0,16	DRAWING NUMBER: DWR001	SHEET: 1/1

I	_
H	_
G	_
F	_
E	_
D	_
C	_
B	_
A	_

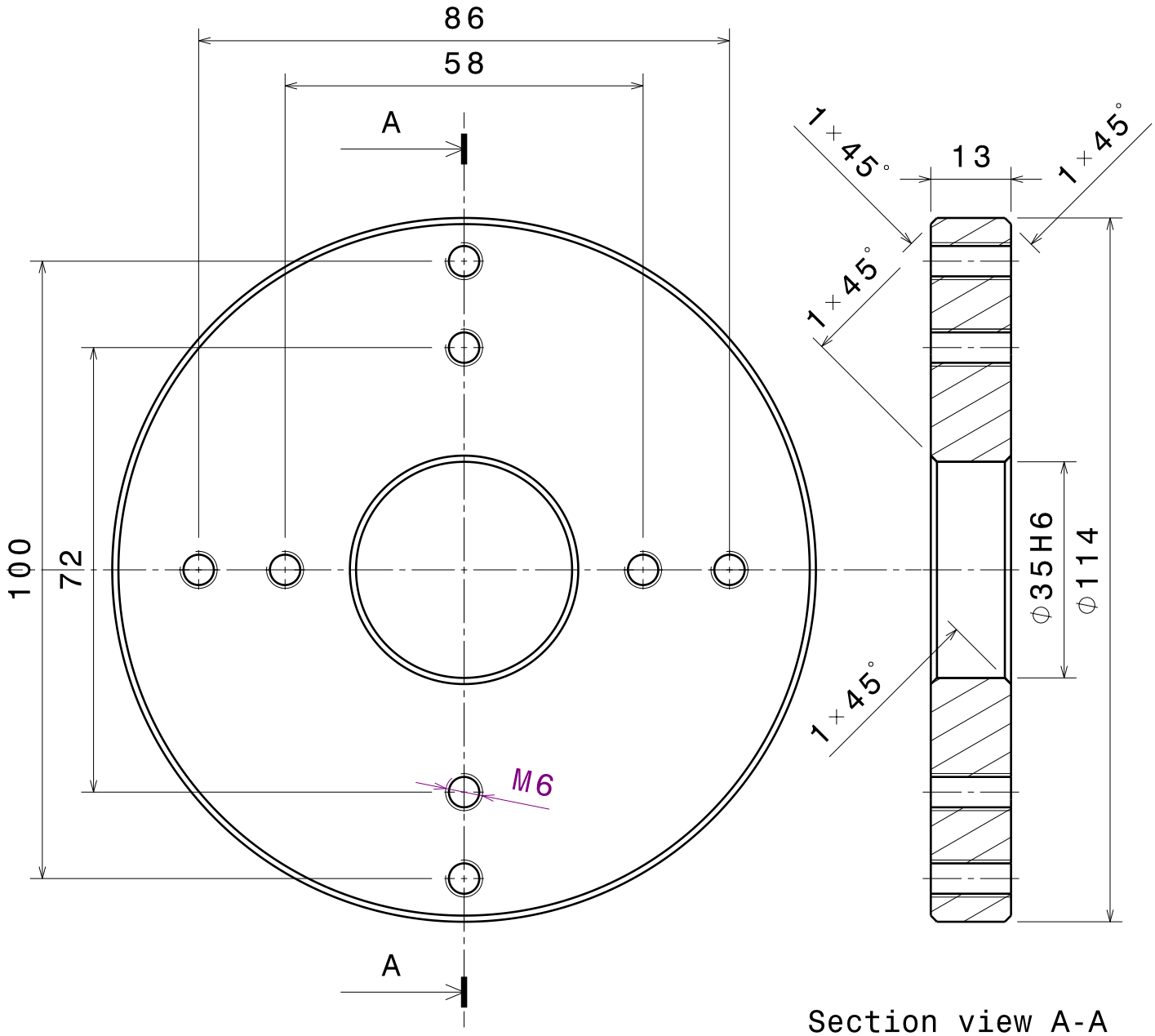

Section view A-A
Scale: 1:1

general tolerance: SFS-EN 22768-1m

DESIGNED BY: J. Gengenbach DATE: 11.04.2015				
Material: Stainless Steel (according availability)				
SIZE A4	Amount: 2	Rotor Outer PART002		
SCALE 1:1	WEIGHT (kg) 0,93	DRAWING NUMBER DWR002	SHEET 1/1	

This drawing is our property; it can't be reproduced or communicated without our written agreement.

I	_
H	_
G	_
F	_
E	_
D	_
C	_
B	_
A	_

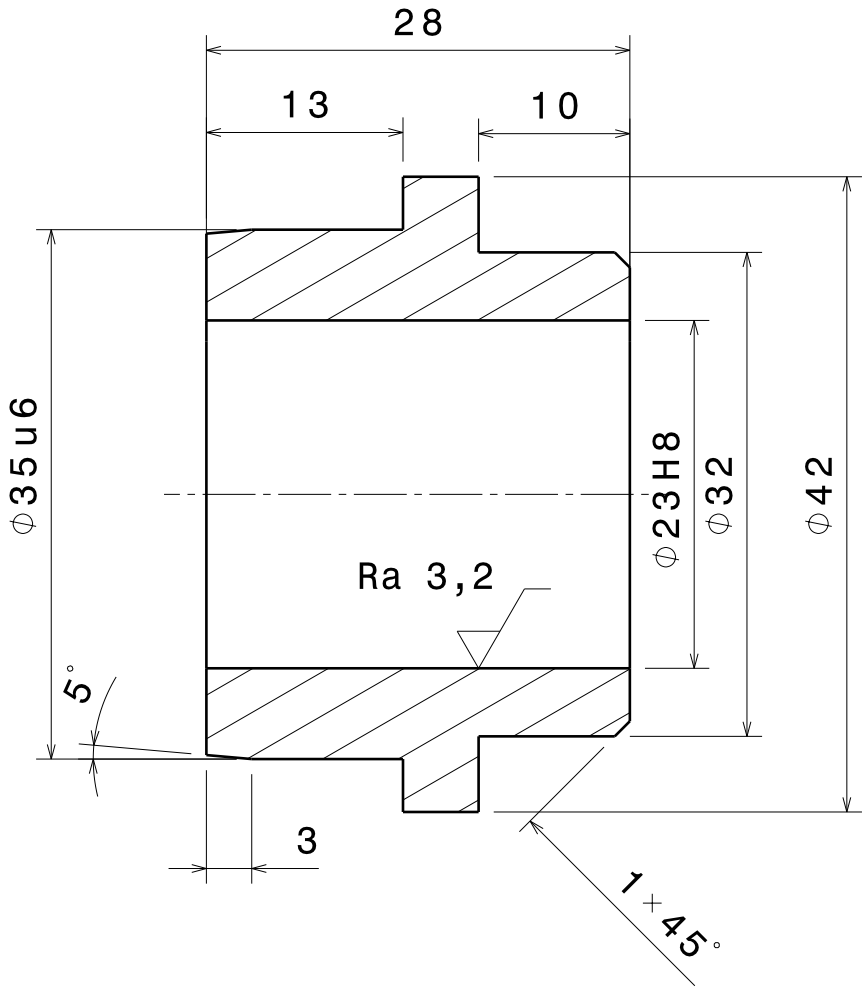

general tolerance: SFS-EN 22768-1m

DESIGNED BY: J. Gengenbach DATE: 09.04.2015			
Material: Stainless Steel (according availability)			
SIZE: A4	Amount: 2	Rotor inner PART003	
SCALE: 2:1	WEIGHT (kg): 0,12	DRAWING NUMBER: DWR003	SHEET: 1/1

I	_
H	_
G	_
F	_
E	_
D	_
C	_
B	_
A	_

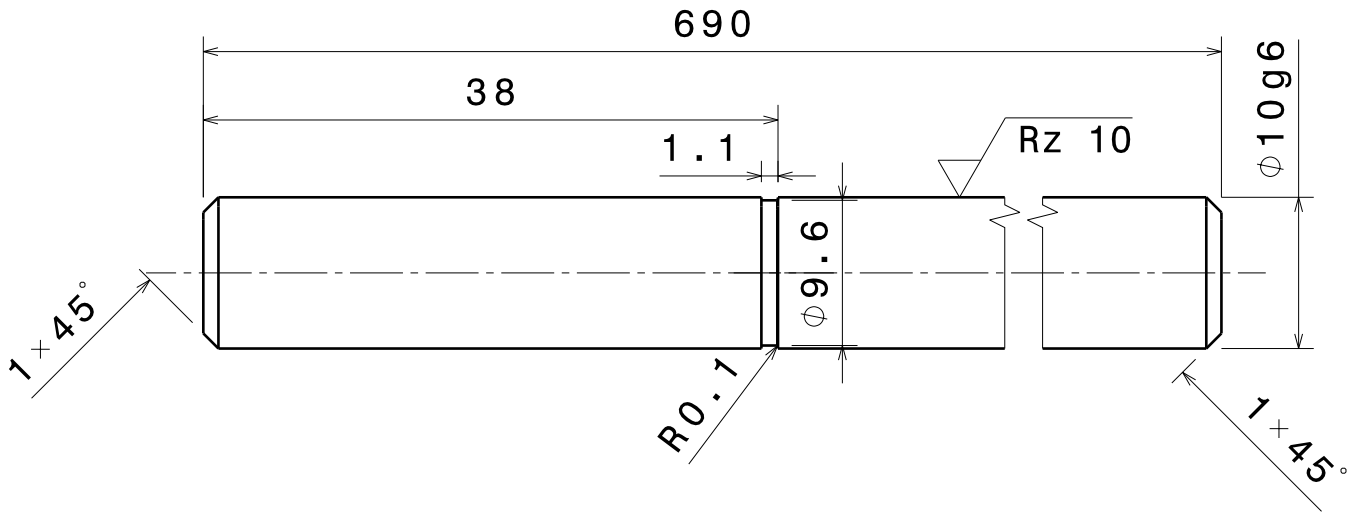

general tolerance: SFS-EN 22768-1m

DESIGNED BY: J.Gengenbach DATE: 10.04.2015				
Material: S355				
SIZE A4	Amount: 1	Shaft PART004		
SCALE 2:1	WEIGHT (kg) 0,42	DRAWING NUMBER DWR004	SHEET 1/1	
This drawing is our property; it can't be reproduced or communicated without our written agreement.				

I	_
H	_
G	_
F	_
E	_
D	_
C	_
B	_
A	_

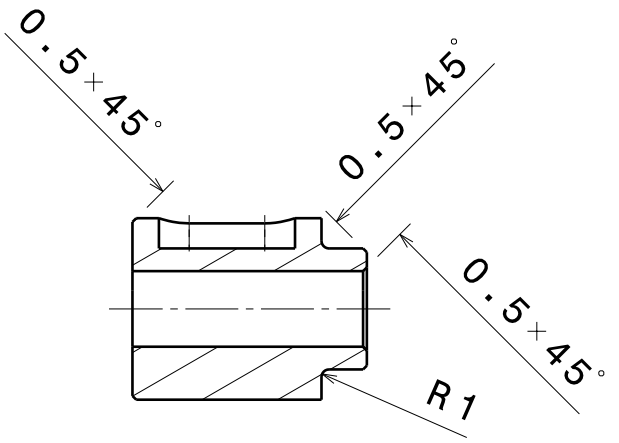

Section view B-B
Scale: 1:1

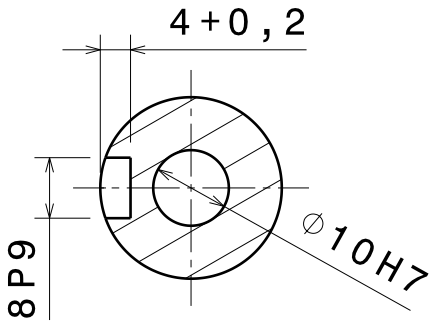

Section view A-A
Scale: 1:1

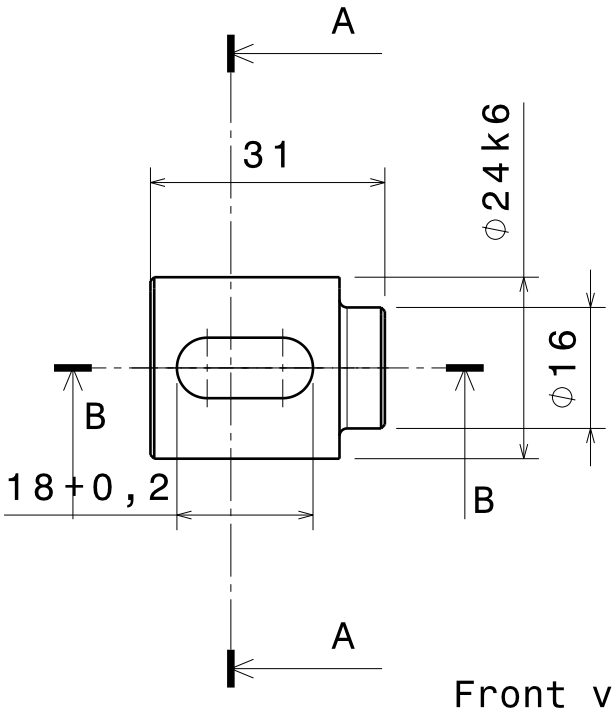

Front view
Scale: 1:1

general tolerance: SFS-EN 22768-1m

DESIGNED BY: J. Gengenbach DATE: 12.04.2015			I	_
			H	_
Material: S355			G	_
			F	_
SIZE A4	Amount: 1	Hull PART005	E	_
			D	_
SCALE 1:1	WEIGHT (kg) 0,08	DRAWING NUMBER DWR005 / SHEET 1/1	C	_
			B	_
			A	_

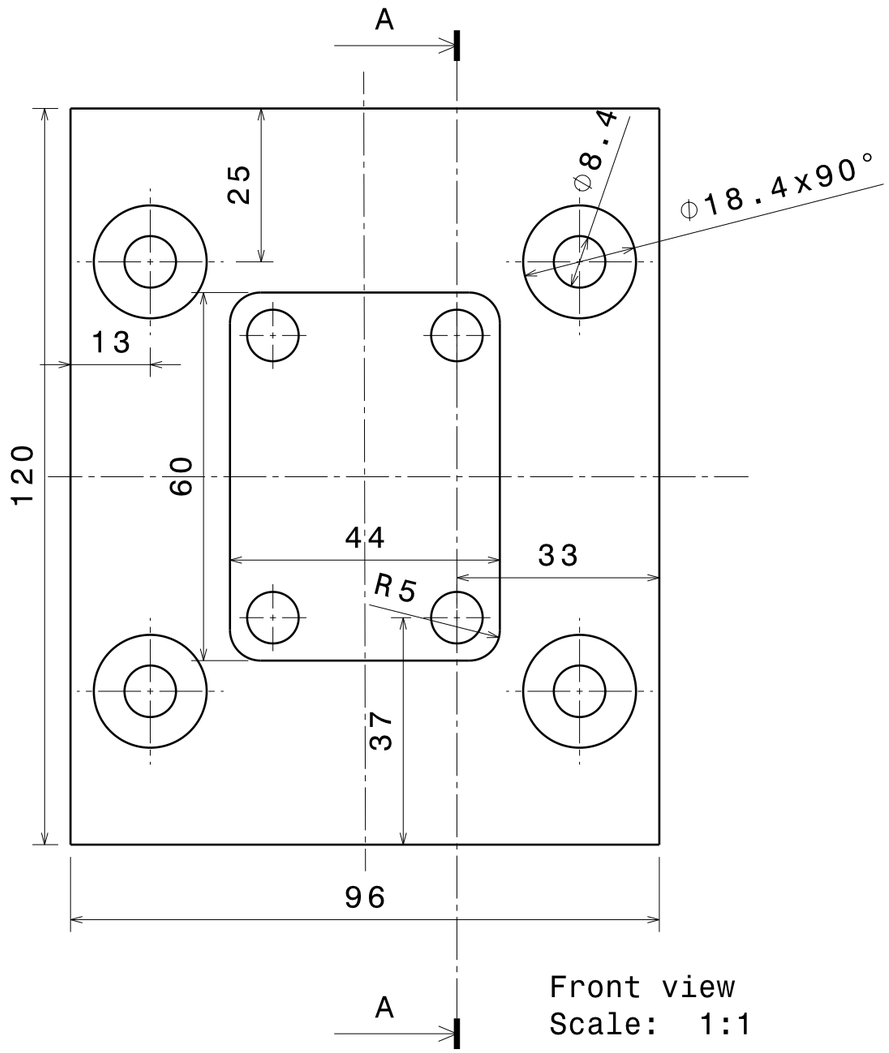

Front view
Scale: 1:1

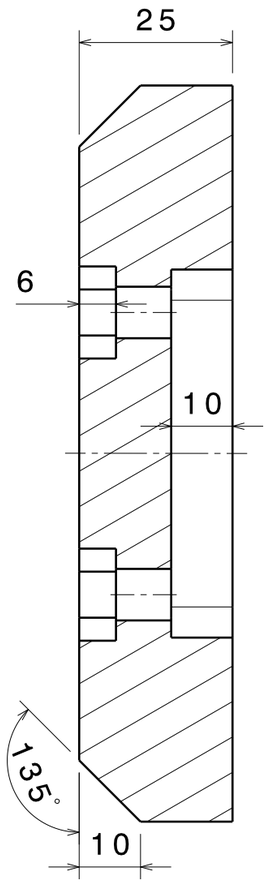

Section view A-A
Scale: 1:1

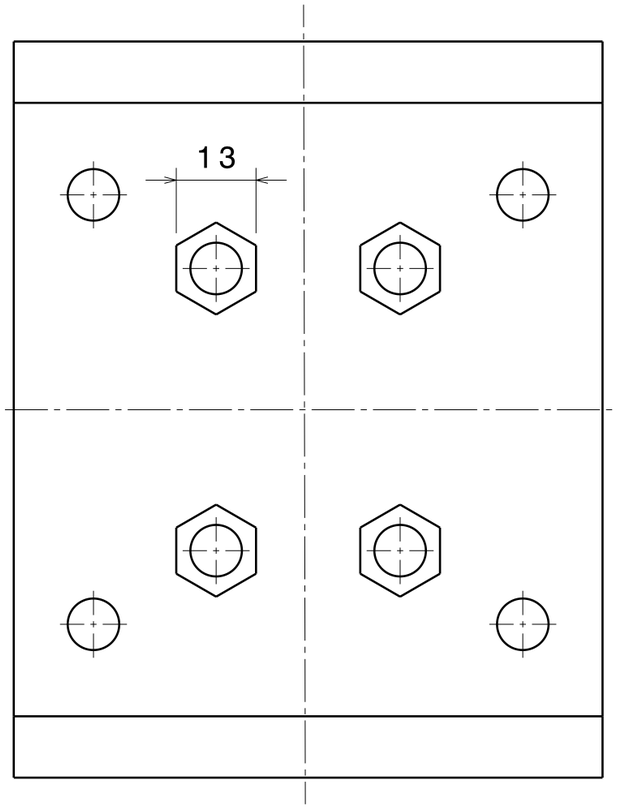

Back view
Scale: 1:1

general tolerance: SFS-EN 22768-1m

DESIGNED BY: J. Gengenbach DATE: 12.04.2015			I _
Material: PA6 / POM-C (according availability)			H _
			G _
			F _
SIZE A3	Amount: 2	Supporting Plate PART006	E _
			D _
			C _
SCALE 1:1	WEIGHT (kg) 0,27	DRAWING NUMBER DWR006 / SHEET 1/1	B _
			A _

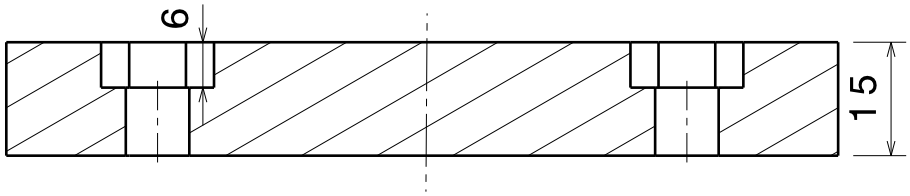

Section view A-A
Scale: 1:1

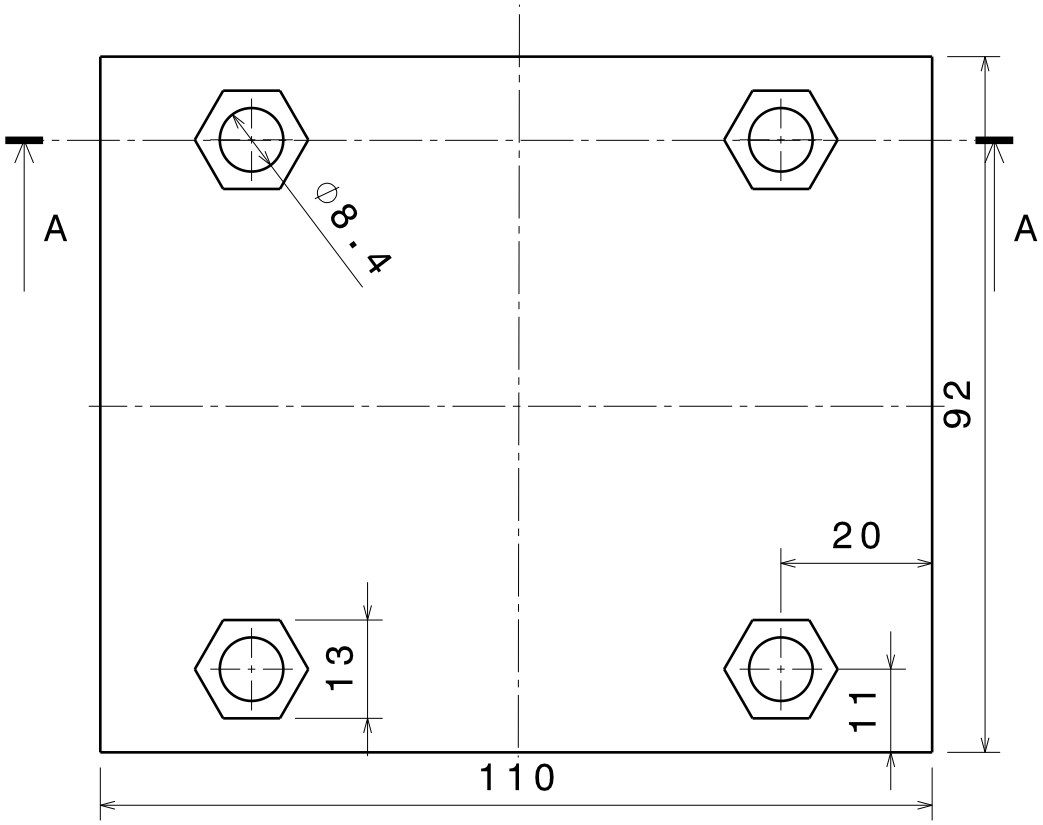

general tolerance: SFS-EN 22768-1m

DESIGNED BY: J. Gengenbach DATE: 12.04.2015			
Material: PA6 / POM-C (according availability)			
SIZE: A4	Amount: 2	Support Strainplate PART007	
SCALE: 1:1	WEIGHT (kg): 0,17	DRAWING NUMBER: DWR007	SHEET: 1/1

I	_
H	_
G	_
F	_
E	_
D	_
C	_
B	_
A	_

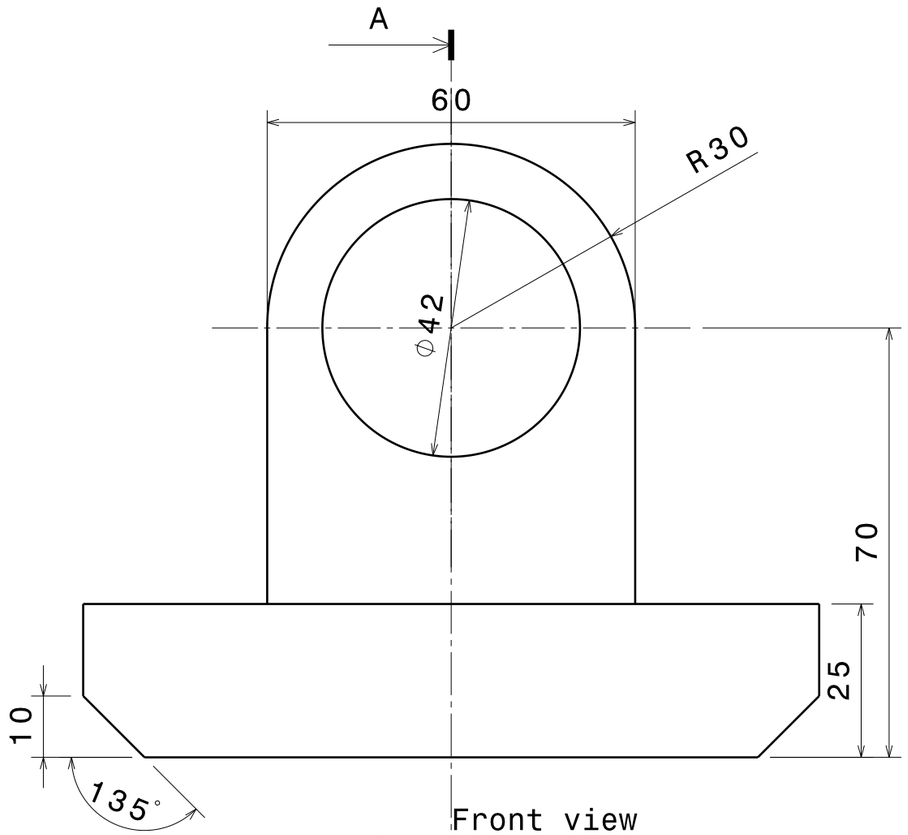

Front view
Scale: 1:1

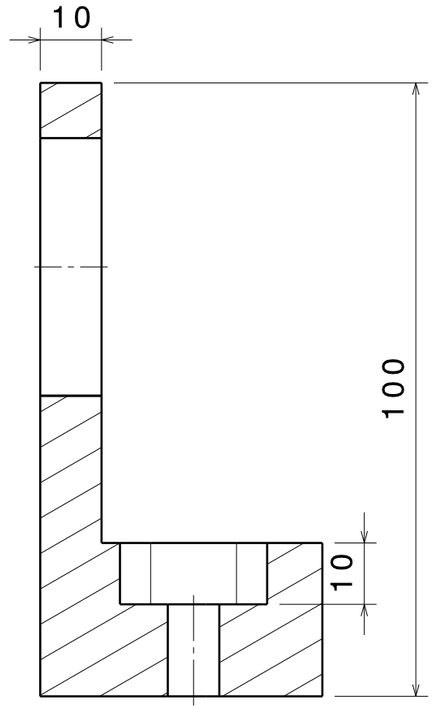

Section view A-A
Scale: 1:1

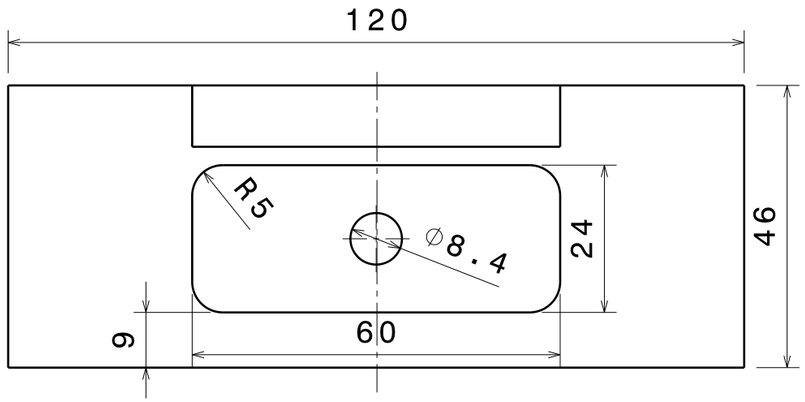

Top view
Scale: 1:1

general tolerance: SFS-EN 22768-1m

DESIGNED BY: J. Gengenbach DATE: 12.04.2015			I –
Material: PA6 / POM-C (according availability)			H –
			G –
			F –
SIZE A3	Amount: 2	Safetybearing PART008	E –
			D –
SCALE 1:1	WEIGHT (kg) 0,16	DRAWING NUMBER DWR008 / SHEET 1/1	C –
			B –
This drawing is our property; it can't be reproduced or communicated without our written agreement.			A –

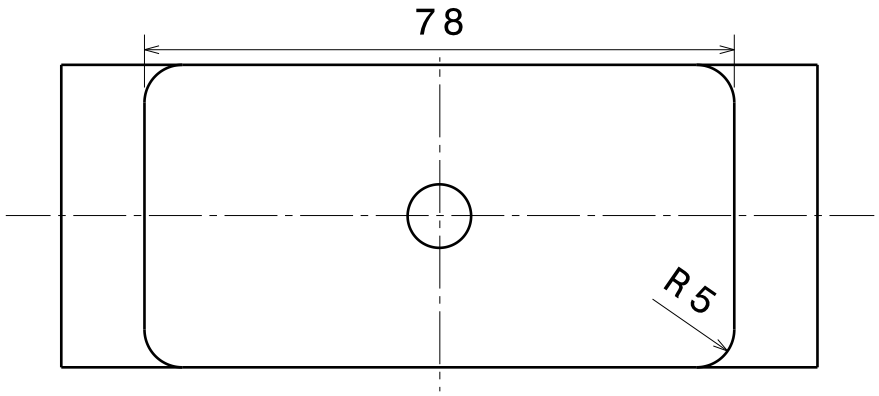

Rear view

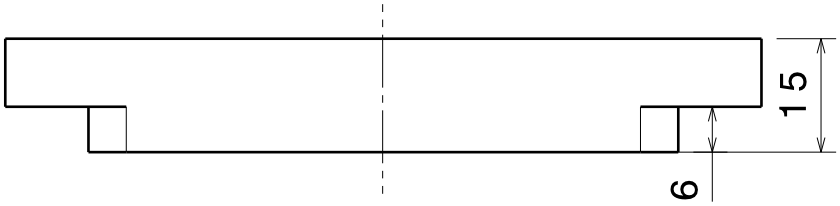

Bottom view

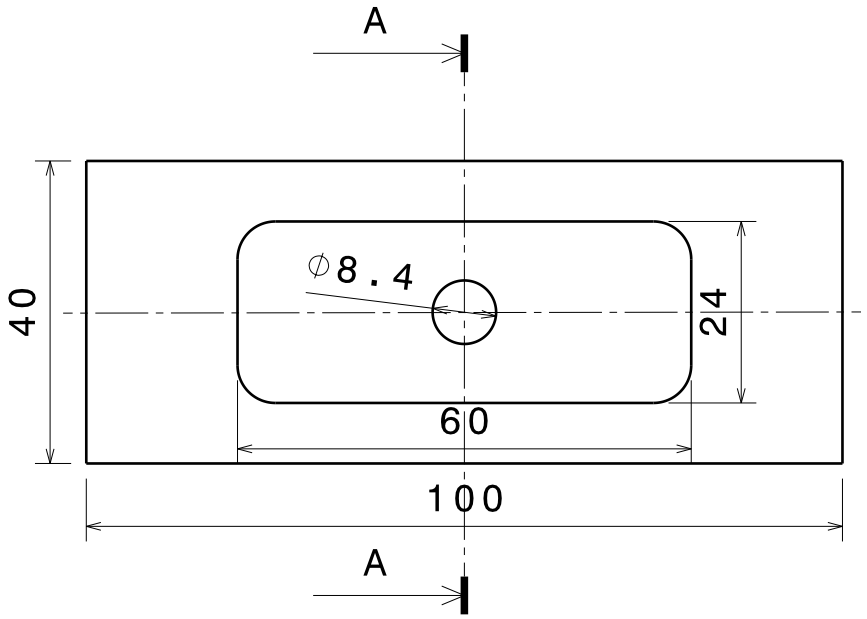

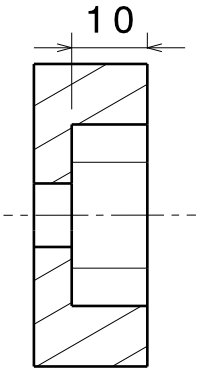

Section view A-A

general tolerance: SFS-EN 22768-1m

DESIGNED BY: J. Gengenbach DATE: 12.04.2015			I	_
			H	_
Material: PA6 / POM-C (according availability)			G	_
			F	_
			E	_
SIZE A4	Amount: 2	Safetybearing Strainplate PART009	D	_
SCALE 1:1	WEIGHT (kg) 0,05	DRAWING NUMBER DWR009	C	_
		SHEET 1/1	B	_
This drawing is our property; it can't be reproduced or communicated without our written agreement.			A	_

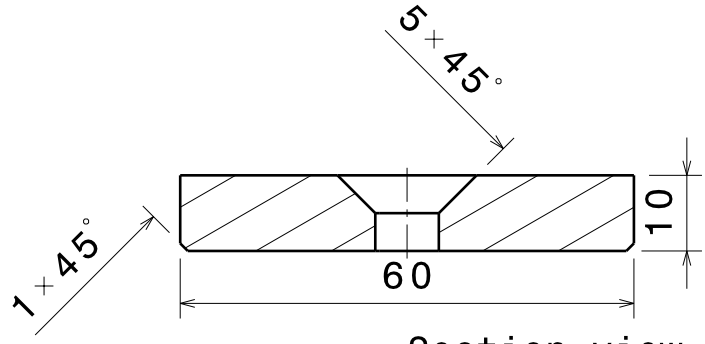

Section view A-A
Scale: 1:1

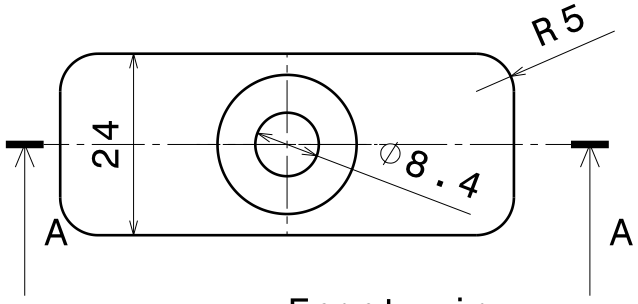

Front view
Scale: 1:1

general tolerance: SFS-EN 22768-1m

DESIGNED BY: J. Gengenbach DATE: 12.04.2015			
Material: S235			
SIZE A4	Amount: 2	Mountingplate Safetybearing PART010	
SCALE 1:1	WEIGHT (kg) 0,10	DRAWING NUMBER DWR010	SHEET 1/1

I	_
H	_
G	_
F	_
E	_
D	_
C	_
B	_
A	_

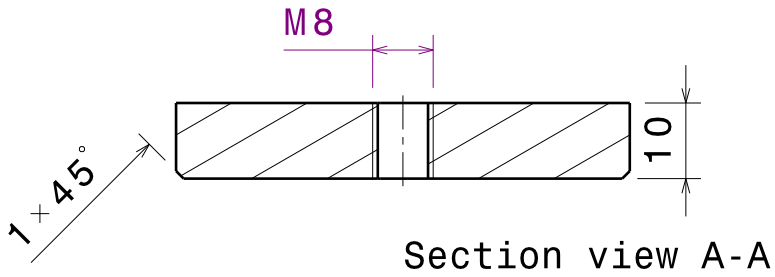

Section view A-A

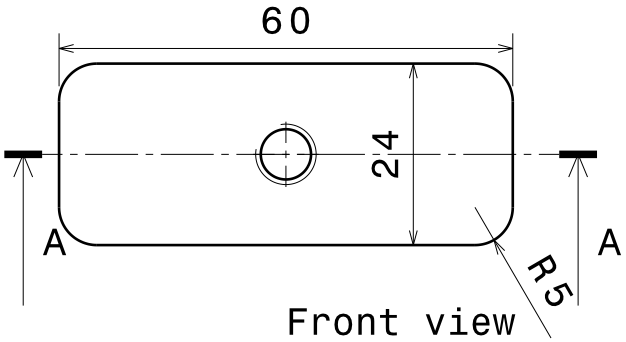

Front view

general tolerance: SFS-EN 22768-1m

DESIGNED BY: J. Gengenbach DATE: 12.04.2015			
Material: S235			
SIZE A4	Amount: 2	Mountingplate Strainplate PART011	
SCALE 1:1	WEIGHT (kg) 0,11	DRAWING NUMBER DWR011	SHEET 1/1

I	_
H	_
G	_
F	_
E	_
D	_
C	_
B	_
A	_

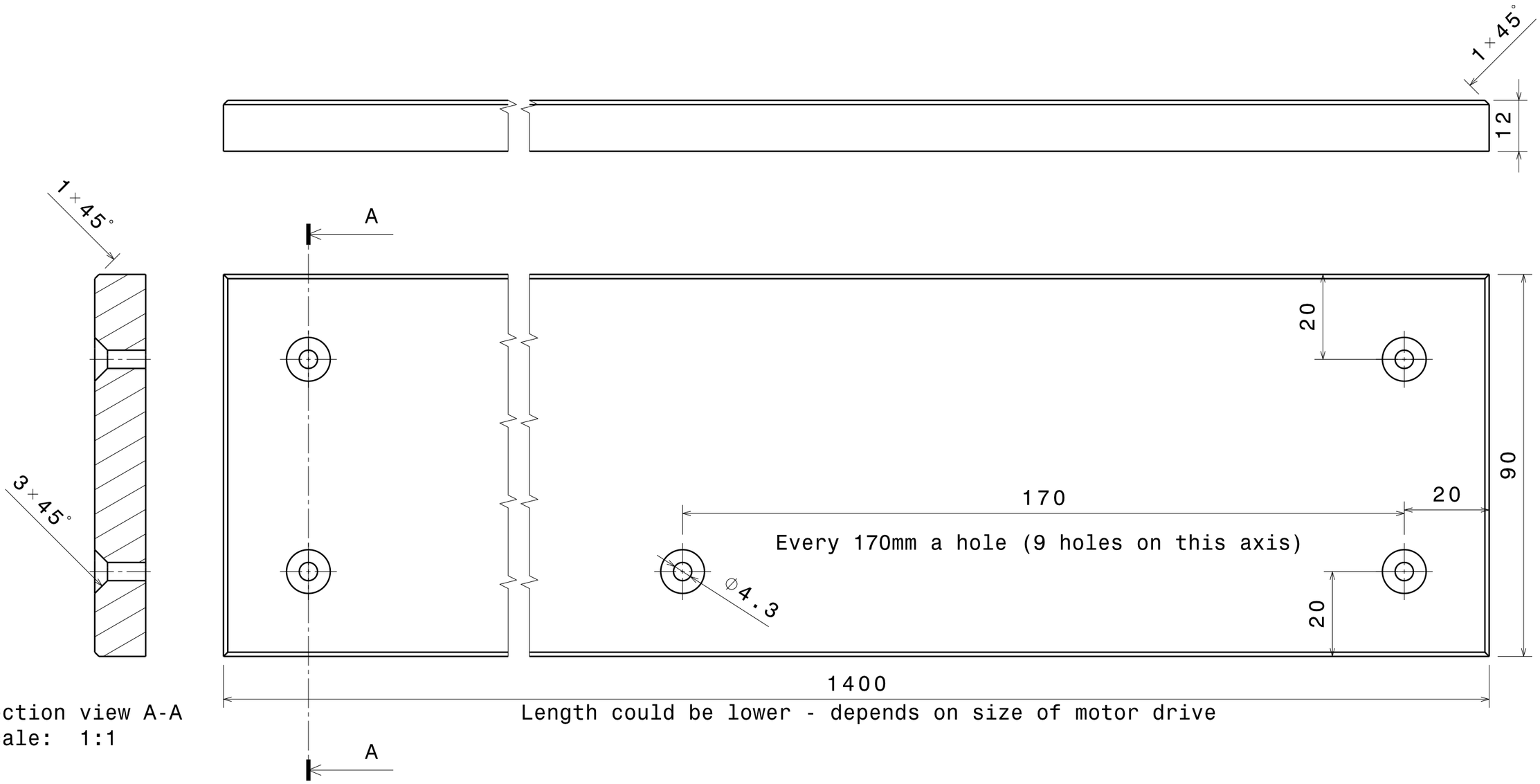

Section view A-A
Scale: 1:1

general tolerance: SFS-EN 22768-1m

DESIGNED BY: J. Gengenbach			I –
DATE: 13.04.2015			H –
Material: PA6 / POM-C (according availability)			G –
			F –
SIZE: A3	Amount: 2	Groundplate PART012	E –
			D –
SCALE: 1:1	WEIGHT (kg): 2,26	DRAWING NUMBER: DWR012	SHEET: 1/1
			C –
			B –
			A –

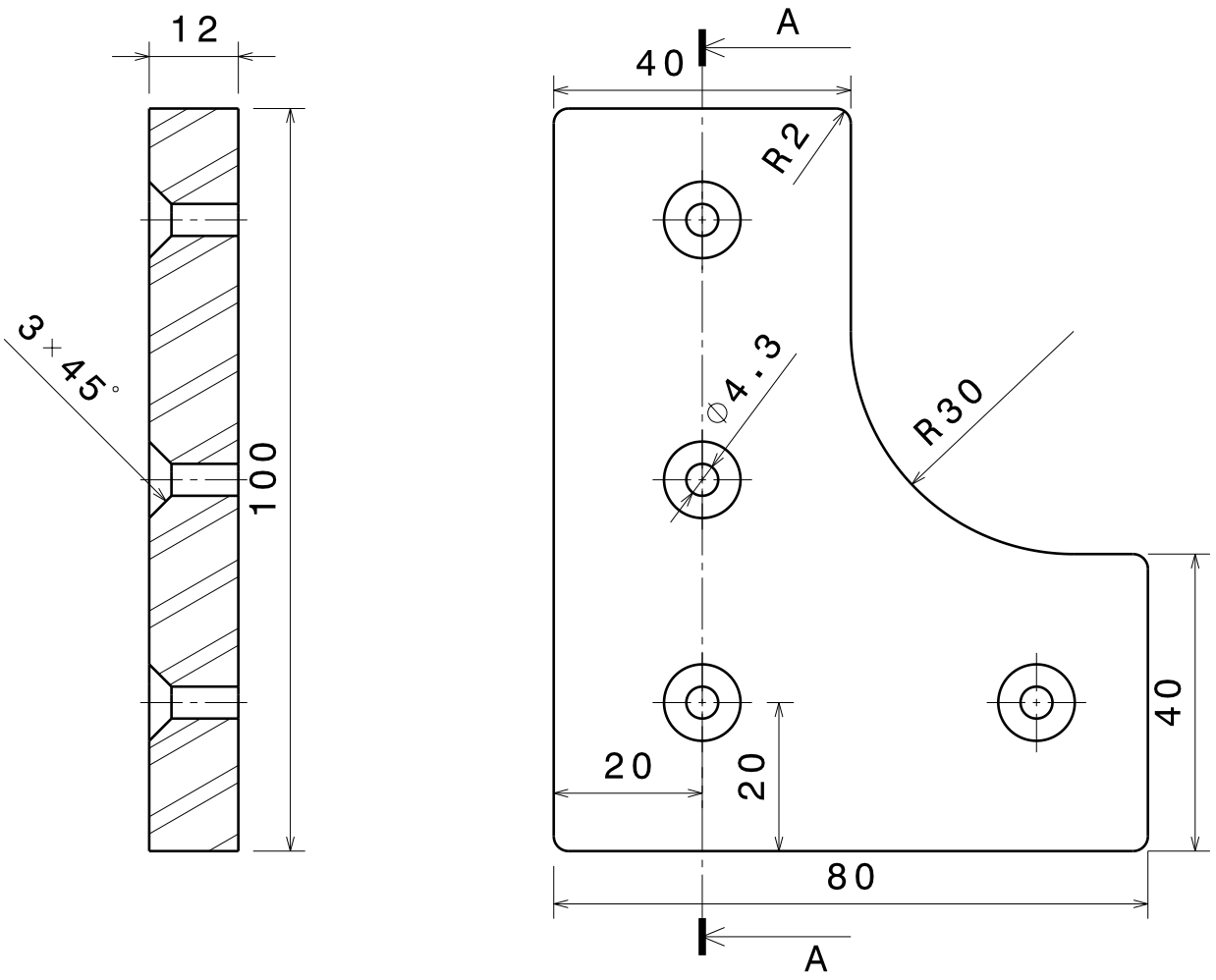

Section view A-A
Scale: 1:1

Front view
Scale: 1:1

general tolerance: SFS-EN 22768-1m

DESIGNED BY: J. Gengenbach DATE: 13.04.2015			
Material: PA6 / POM-C (according availability)			
SIZE A4	Amount: 2	Corner 1 PART013	
SCALE 1:1	WEIGHT (kg) 0,08	DRAWING NUMBER DWR013	SHEET 1/1

I	_
H	_
G	_
F	_
E	_
D	_
C	_
B	_
A	_

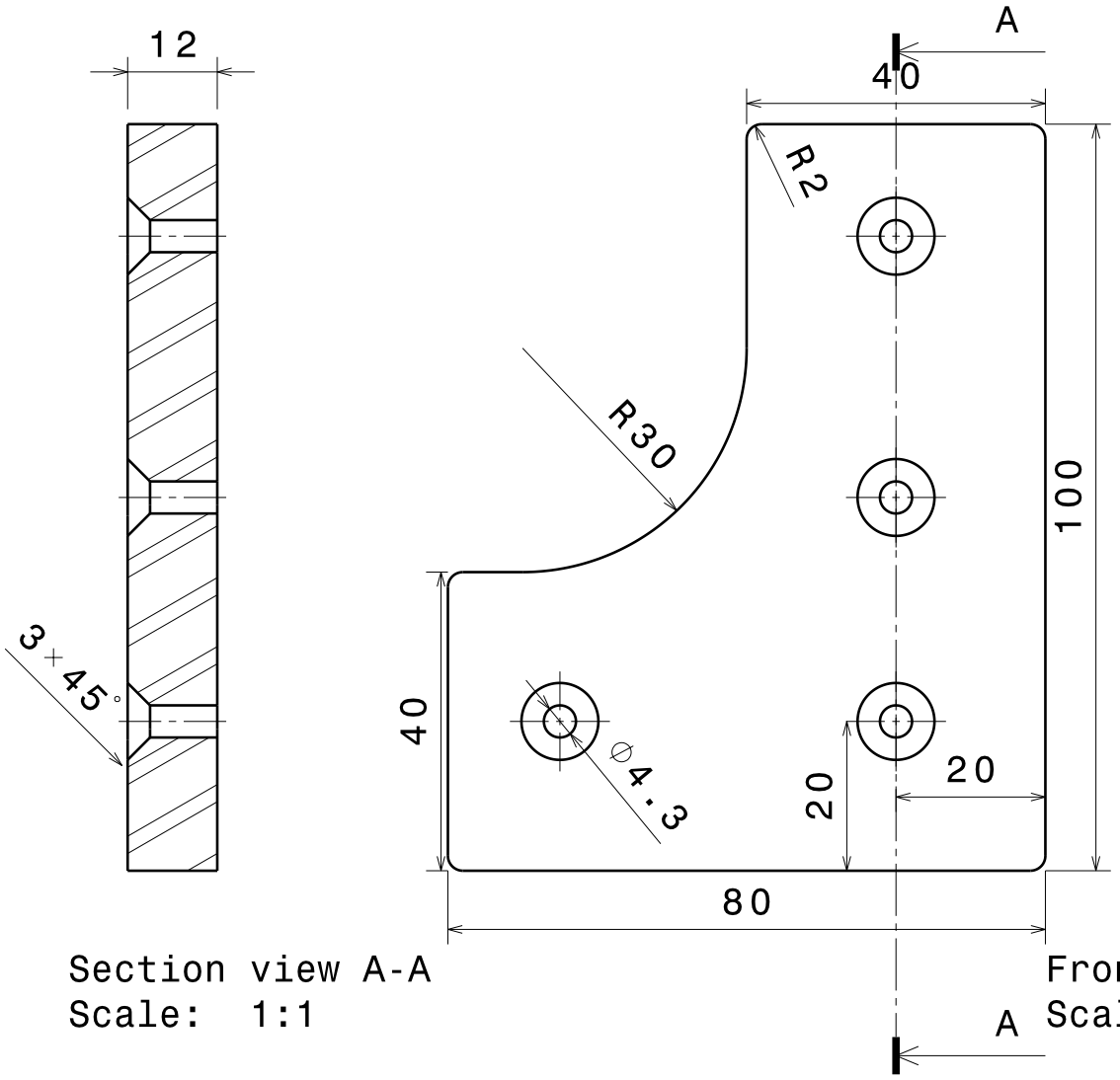

Section view A-A
Scale: 1:1

Front view
Scale: 1:1

general tolerance: SFS-EN 22768-1m

DESIGNED BY: J. Gengenbach DATE: 13.04.2015				I _
Material: PA6 /POM-C (according availability)				H _
				G _
				F _
SIZE A4	Amount: 2	Corner 2 PART014		E _
				D _
SCALE 1:1	WEIGHT (kg) 0,08	DRAWING NUMBER DWR014	SHEET 1/1	C _
				B _
				A _

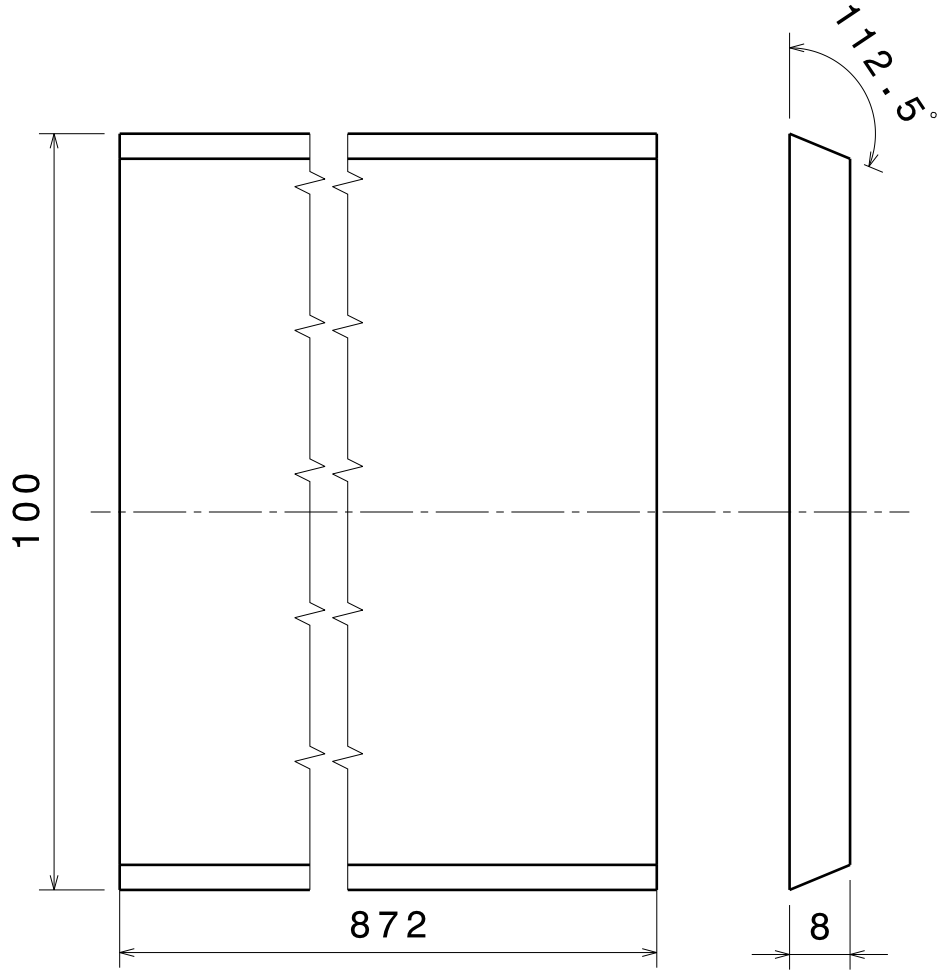

general tolerance: SFS-EN 22768-1m

DESIGNED BY: J. Gengenbach DATE: 24.04.2015			I	_
			H	_
Material: Plexiglass			G	_
			F	_
SIZE A4	SIZE 3	Cap plexiglass corner PART015	E	_
			D	_
SCALE 1:1	WEIGHT (kg) 0,81	DRAWING NUMBER DWR015	C	_
		SHEET 1/1	B	_
			A	_

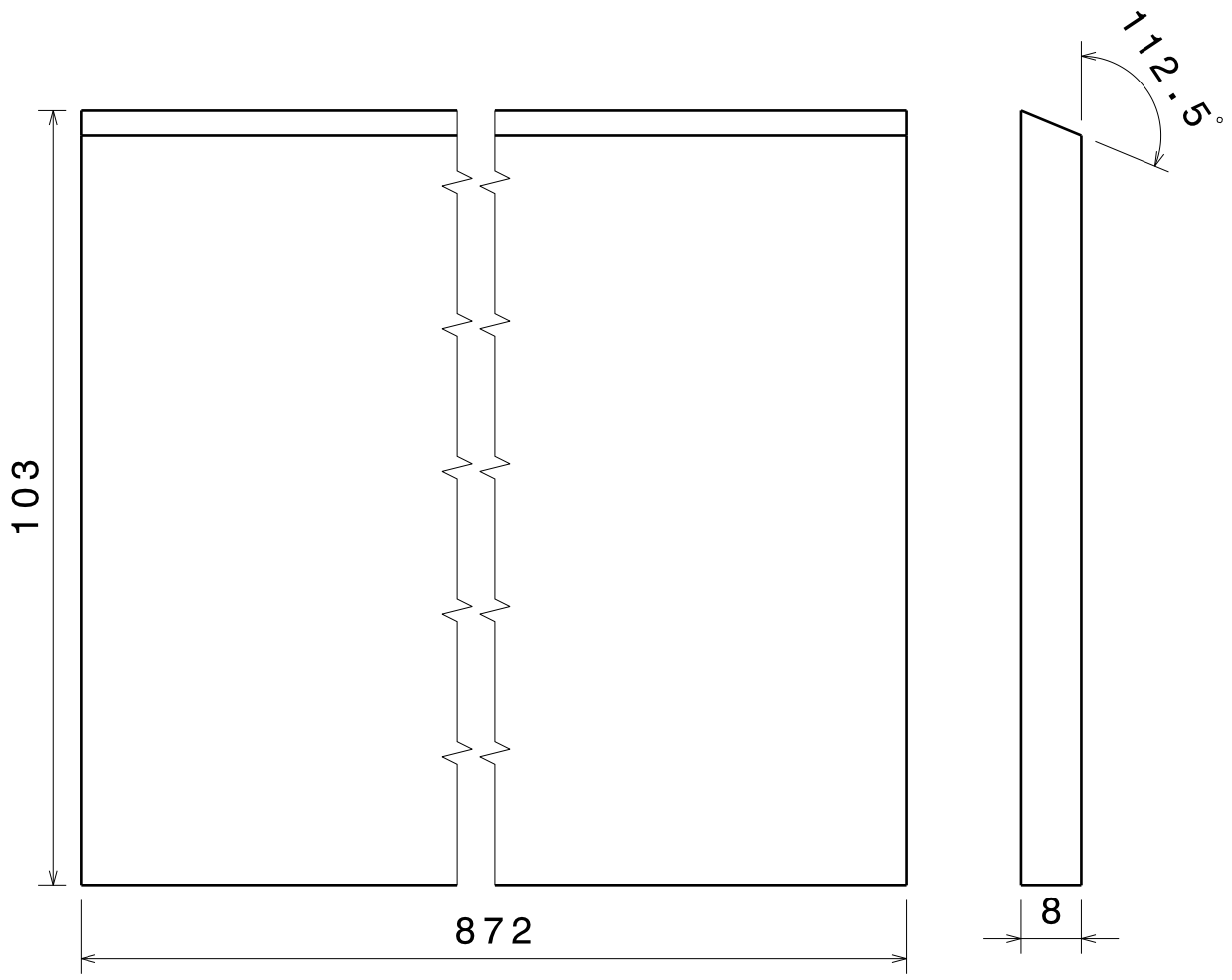

general tolerance: SFS-EN 22768-1m

DESIGNED BY: J. Gengenbach DATE: 24.04.2015			
Material: Plexiglass			
SIZE: A4	Amount: 2	Cap plexiglass side PART016	
SCALE: 1:1	WEIGHT (kg): 0,85	DRAWING NUMBER: DWR016	SHEET: 1/1

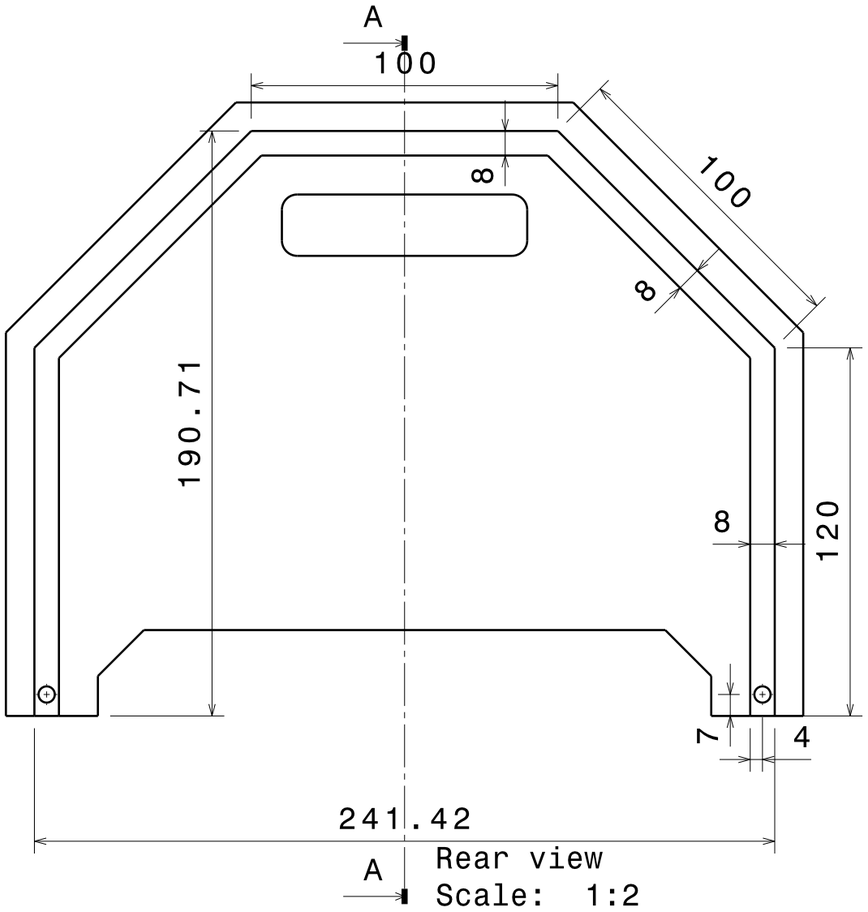

Rear view
Scale: 1:2

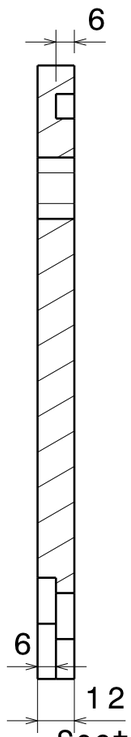

Section view A-A
Scale: 1:2

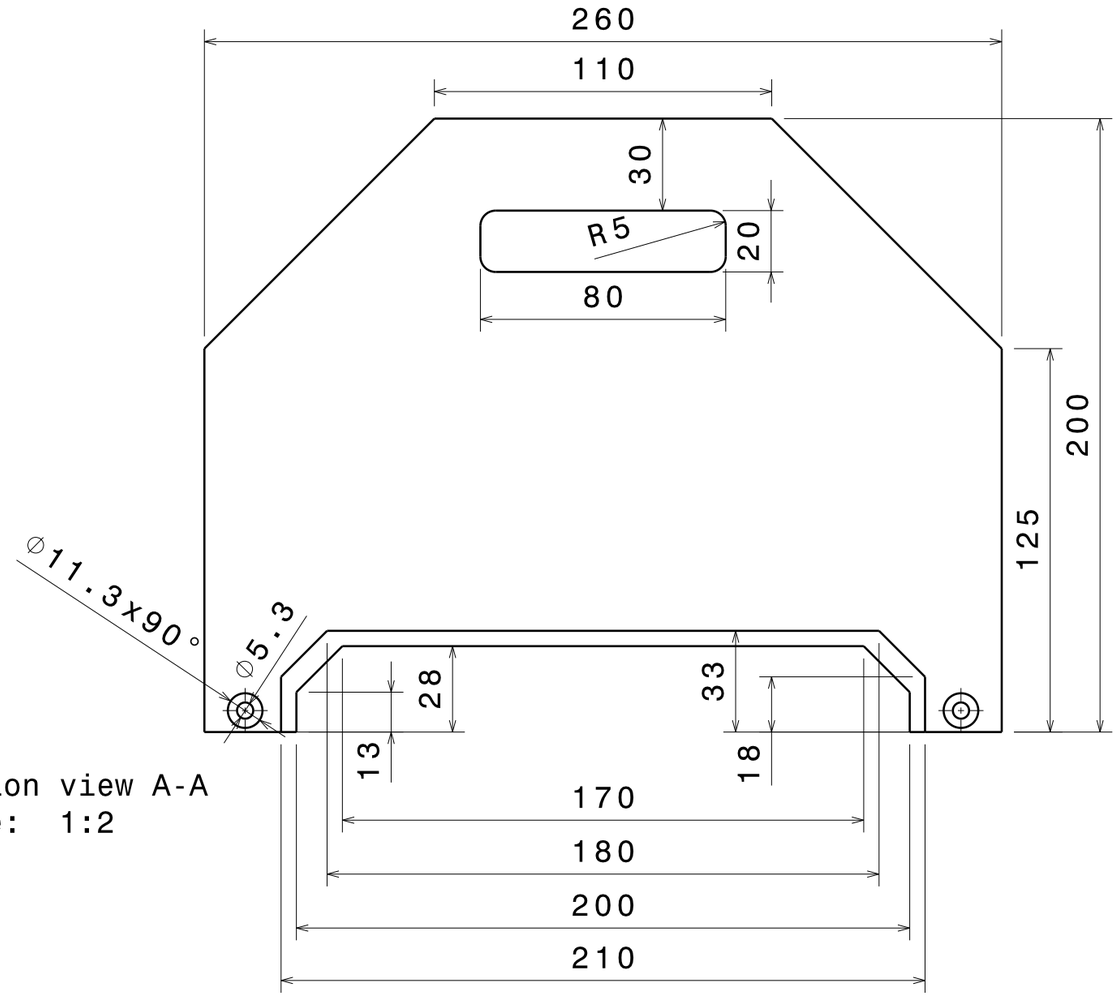

Front view
Scale: 1:2

general tolerance: SFS-EN 22768-1m

DESIGNED BY: J. Gengenbach DATE: 24.04.2015			I –
Material: PA6 / POM-C (according availability)			H –
			G –
			F –
SIZE: A3	Amount: 1	Cap face PART017	E –
			D –
			C –
SCALE: 1:2	WEIGHT (kg): 0,49	DRAWING NUMBER: DWR017 / SHEET: 1/1	B –
This drawing is our property; it can't be reproduced or communicated without our written agreement.			A –

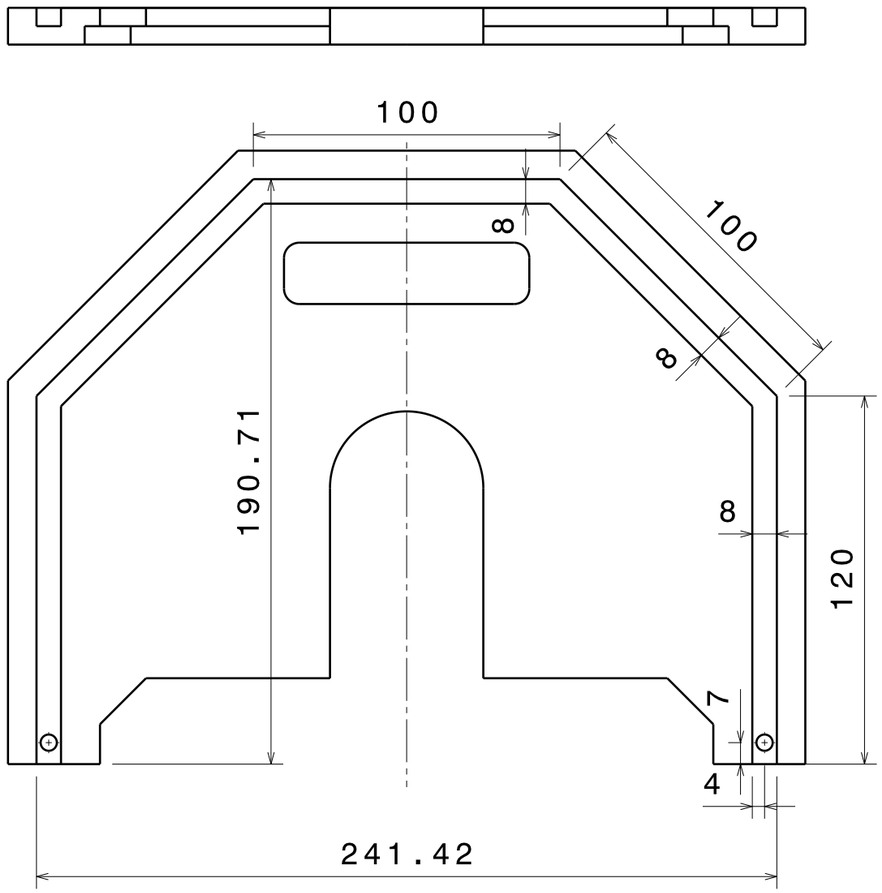

Rear view
Scale: 1:2

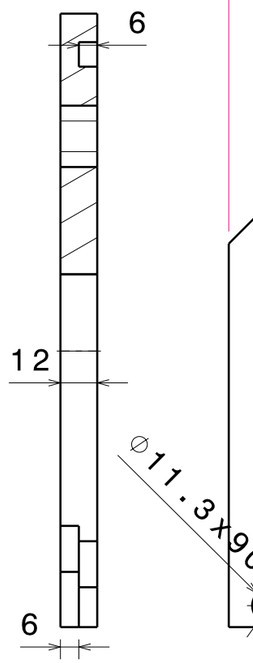

Section view A-A
Scale: 1:2

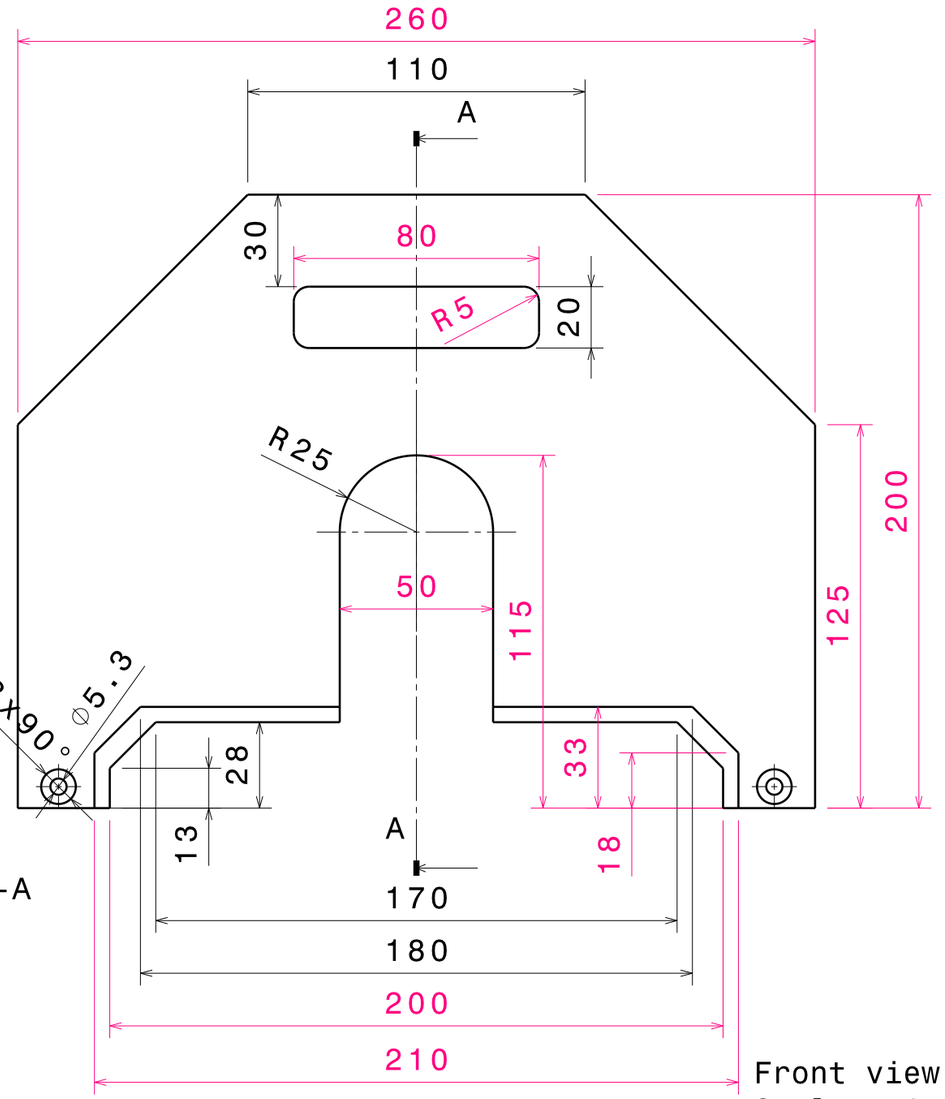

Front view
Scale: 1:2

general tolerance: SFS-EN 22768-1m

DESIGNED BY: J. Gengenbach DATE: 23.04.2015			I _
Material: PA6 / POM-C (according availability)			H _
			G _
			F _
			E _
SIZE: A3	Amount: 1	Cap face motorside PART018	D _
SCALE: 1:1	WEIGHT (kg): 0,44	DRAWING NUMBER: DWR018	C _
		SHEET: 1/1	B _
			A _

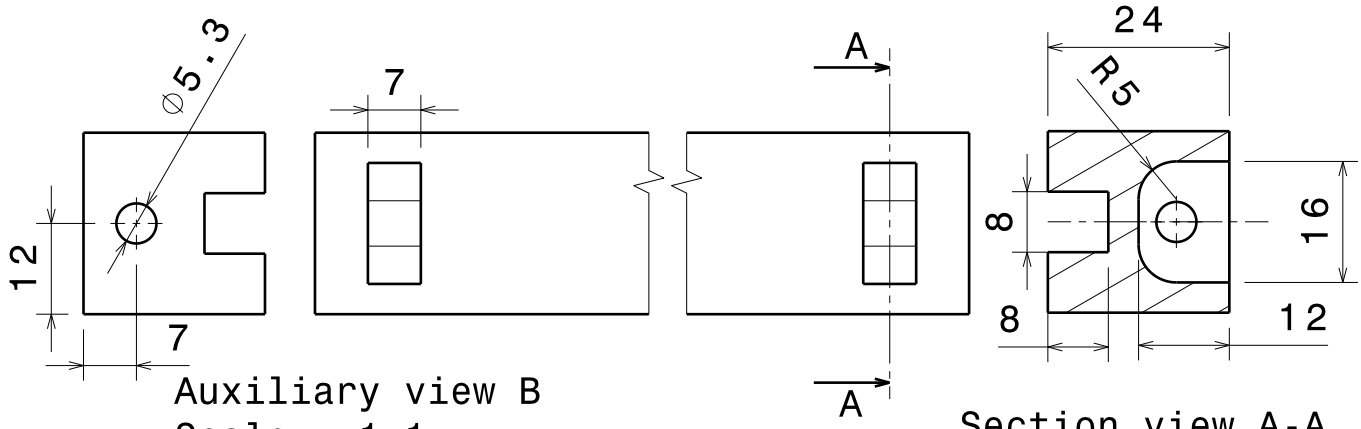

Auxiliary view B
Scale: 1:1

Section view A-A

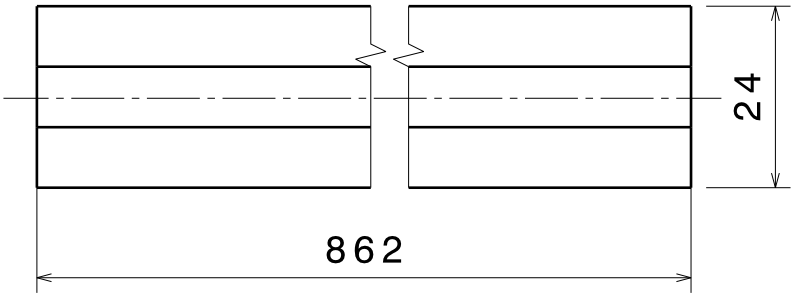

general tolerance: SFS-EN 22768-1m

DESIGNED BY: J. Gengenbach DATE: 24.04.2015			
Material: PA6 / POM-C (according availability)			
SIZE: A4	Amount: 2	Cap rail PART019	
SCALE: 1:1	WEIGHT (kg): 0,50	DRAWING NUMBER: DWR019	SHEET: 1/1

I	_
H	_
G	_
F	_
E	_
D	_
C	_
B	_
A	_

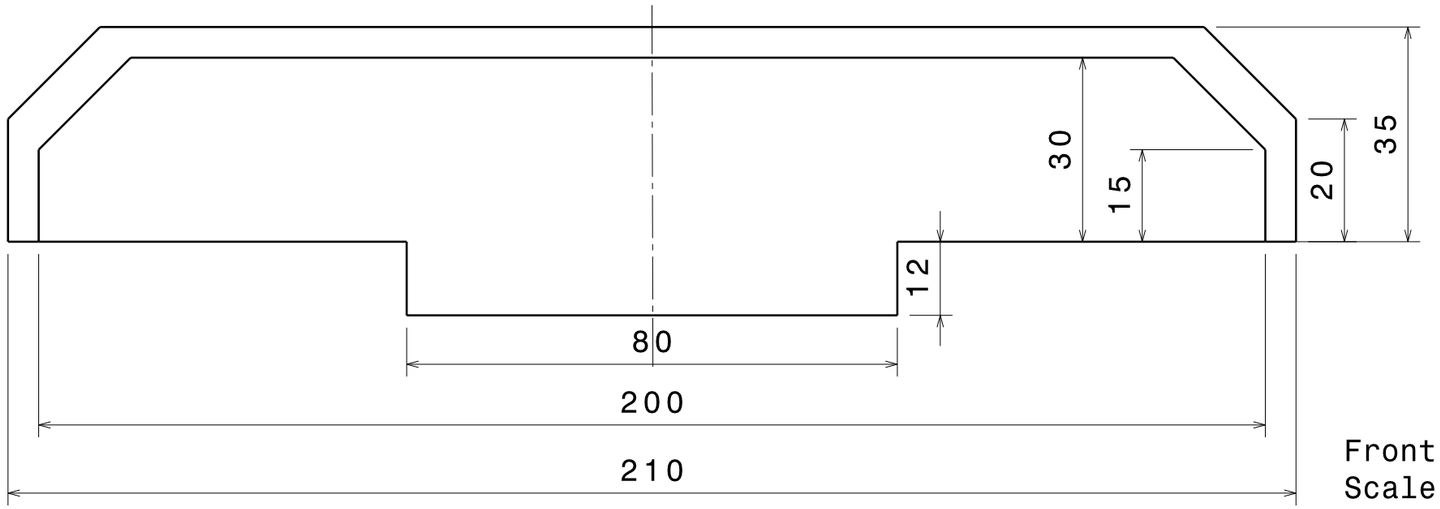

Front view
Scale: 1:1

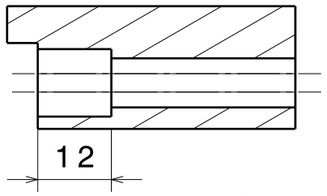

Section view A-A
Scale: 1:1

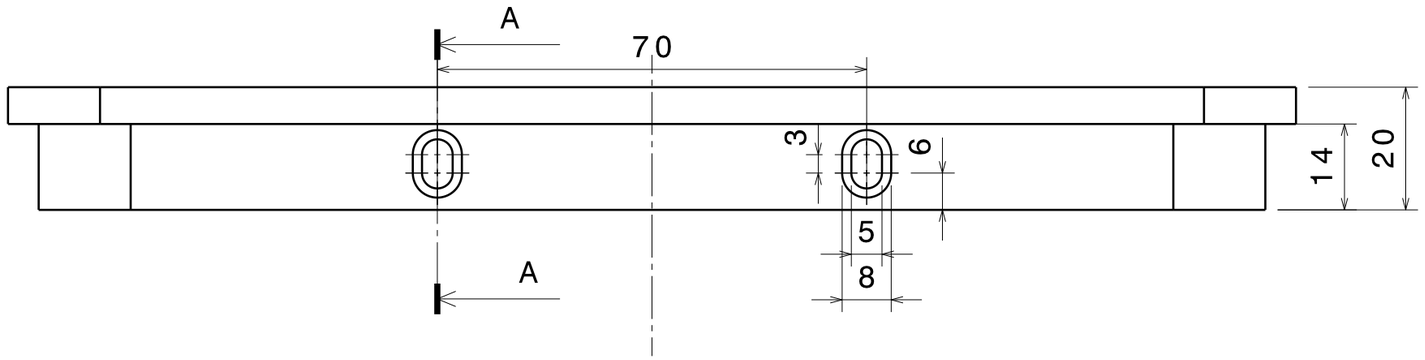

Top view
Scale: 1:1

general tolerance: SFS-EN 22768-1m

DESIGNED BY: J. Gengenbach DATE: 04.05.2015			I _
Material: PA6 / POM-C (according availability)			H _
			G _
			F _
SIZE A3	Amount: 2	Cap shoulder PART020	E _
			D _
			C _
SCALE 1:1	WEIGHT (kg) 0,16	DRAWING NUMBER DWR020 / SHEET 1/1	B _
This drawing is our property; it can't be reproduced or communicated without our written agreement.			A _

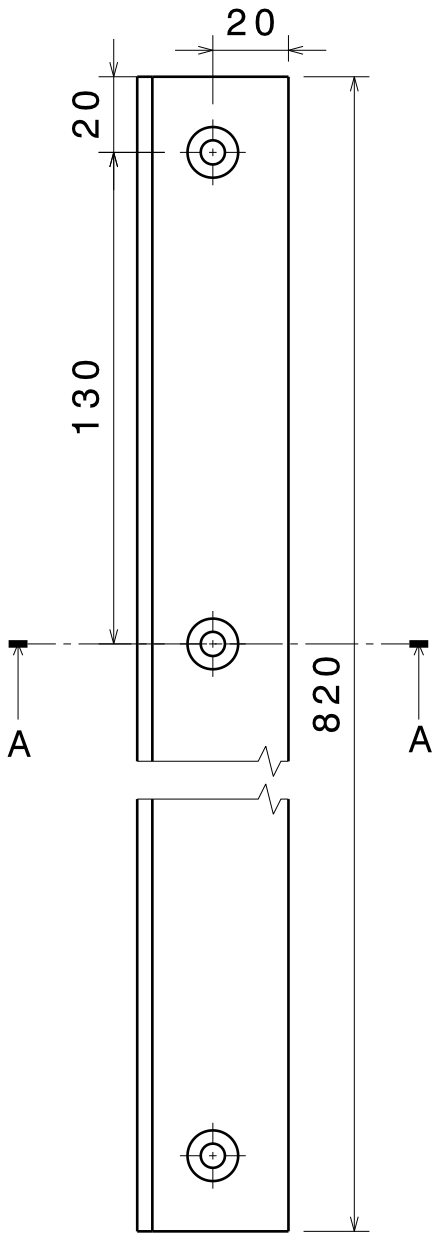

Top view
Scale: 1:2

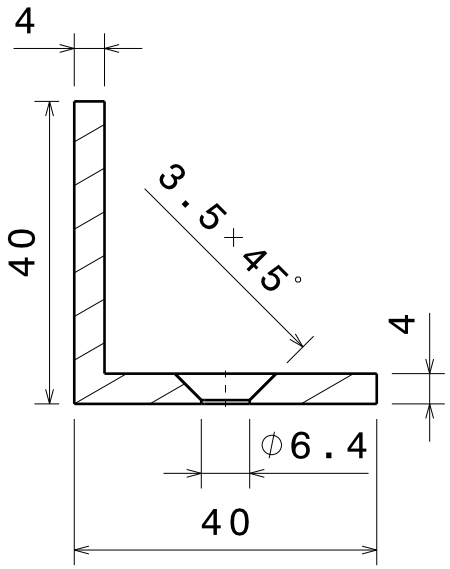

Section view A-A
Scale: 1:1

Every 130mm a hole (7 holes)

general tolerance: SFS-EN 22768-1m

DESIGNED BY: J. Gengenbach DATE: 05.05.2015			
Material: Aluminium Standardprofile			
SIZE: A4	Amount: 2	L-Profile (PART104)	
SCALE	WEIGHT (kg): 0,66	DRAWING NUMBER: DWR029	SHEET: 1/1

I	_
H	_
G	_
F	_
E	_
D	_
C	_
B	_
A	_

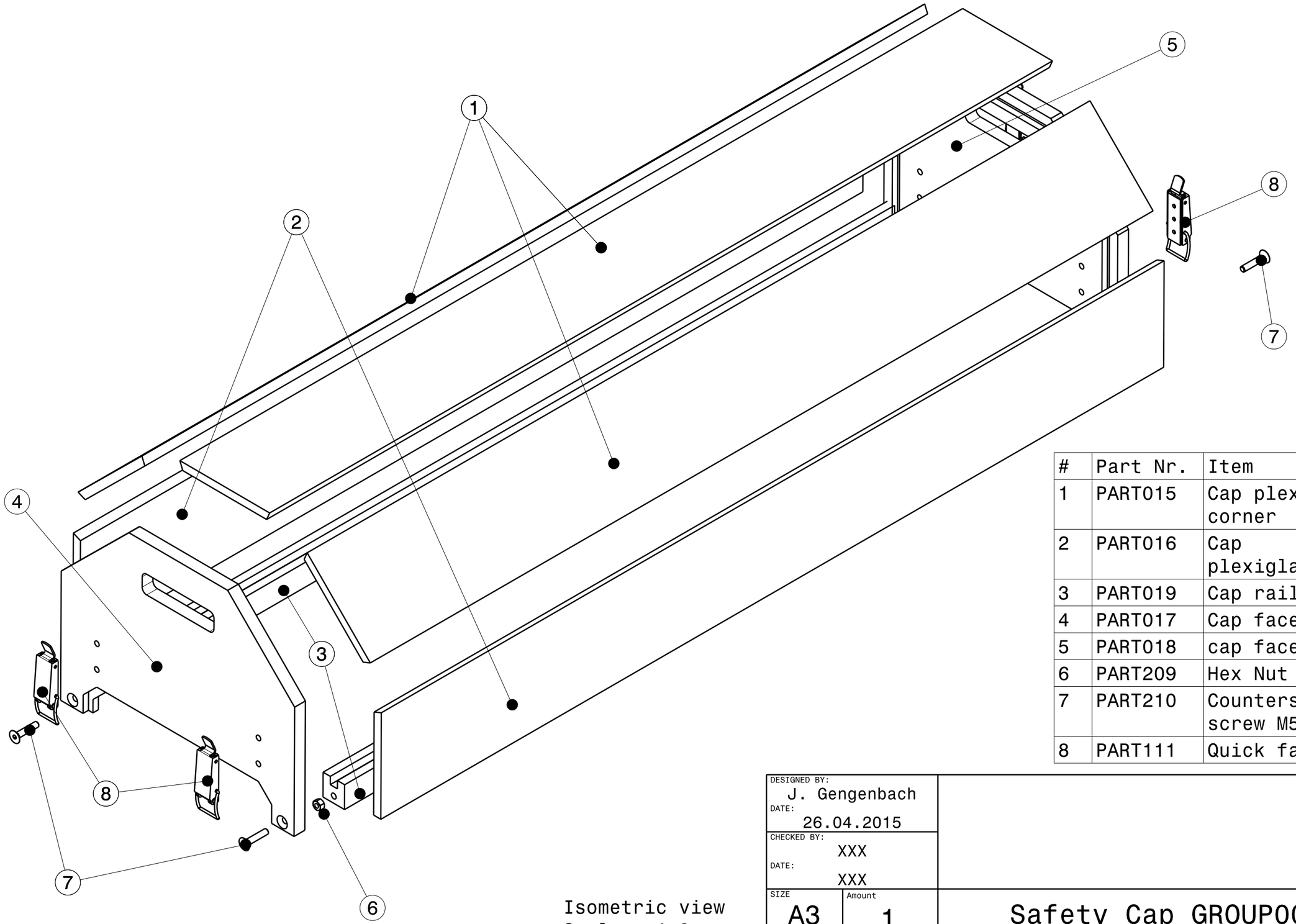

#	Part Nr.	Item	Amount
1	PART015	Cap plexiglass corner	3
2	PART016	Cap plexiglassside	2
3	PART019	Cap rail	2
4	PART017	Cap face	1
5	PART018	cap face motor	1
6	PART209	Hex Nut M5	4
7	PART210	Countersunk screw M5x25	4
8	PART111	Quick fastener	4

Isometric view
Scale: 1:3

DESIGNED BY: J. Gengenbach
DATE: 26.04.2015
CHECKED BY: XXX
DATE: XXX

SIZE: A3 | Amount: 1

Safety Cap GROUP001

SCALE | WEIGHT (kg): 6,1 | DRAWING NUMBER: DWR021 | SHEET: 1/1

I	_
H	_
G	_
F	_
E	_
D	_
C	_
B	_
A	_

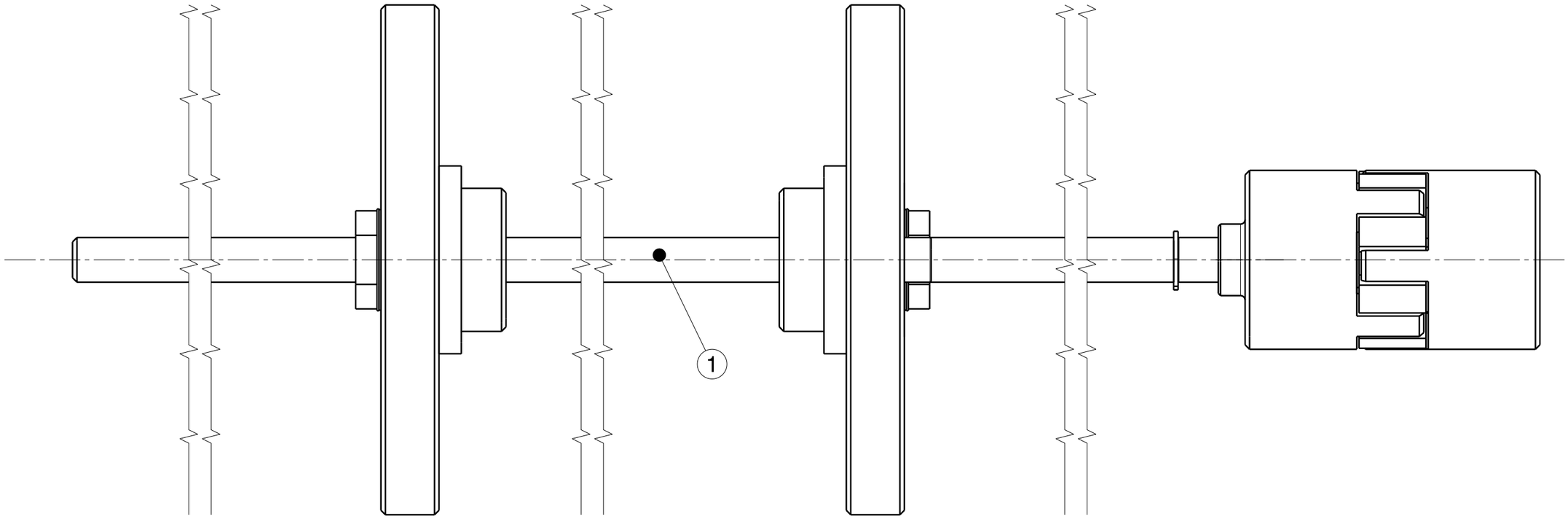

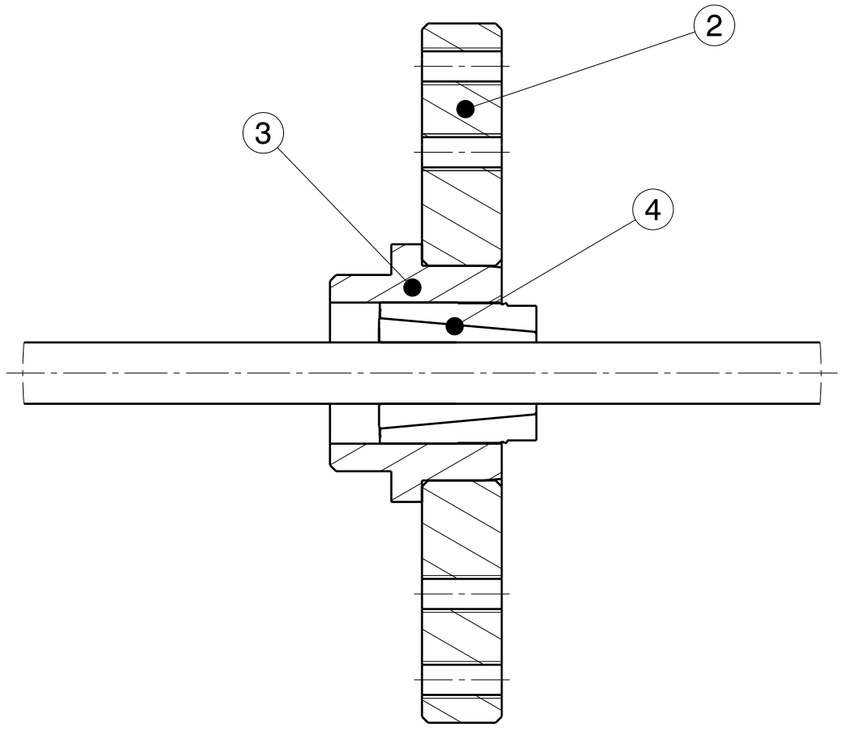

Detail B
Scale: 1:1

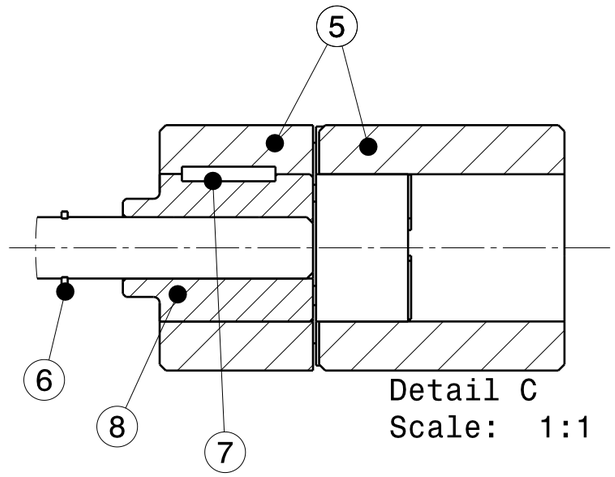

Detail C
Scale: 1:1

#	Part Nr.	Item	Amount
1	PART004	Shaft	1
2	PART002	Rotor outer	2
3	PART003	Rotor inner	2
4	PART105	Ringspann	2
5	PART106	Rotex coupling	1
6	PART212	Retaining ring	1
7	PART211	Feather key	1
8	PART005	Hull	1

DESIGNED BY: Jonathan Gengenbach
DATE: 26.04.2015
CHECKED BY: XXX
DATE: XXX

SIZE	Amount		
A3	1	Rotor GROUP002	
SCALE	WEIGHT (kg)	DRAWING NUMBER	SHEET
	3,1	DWR022	1/1

I	_
H	_
G	_
F	_
E	_
D	_
C	_
B	_
A	_

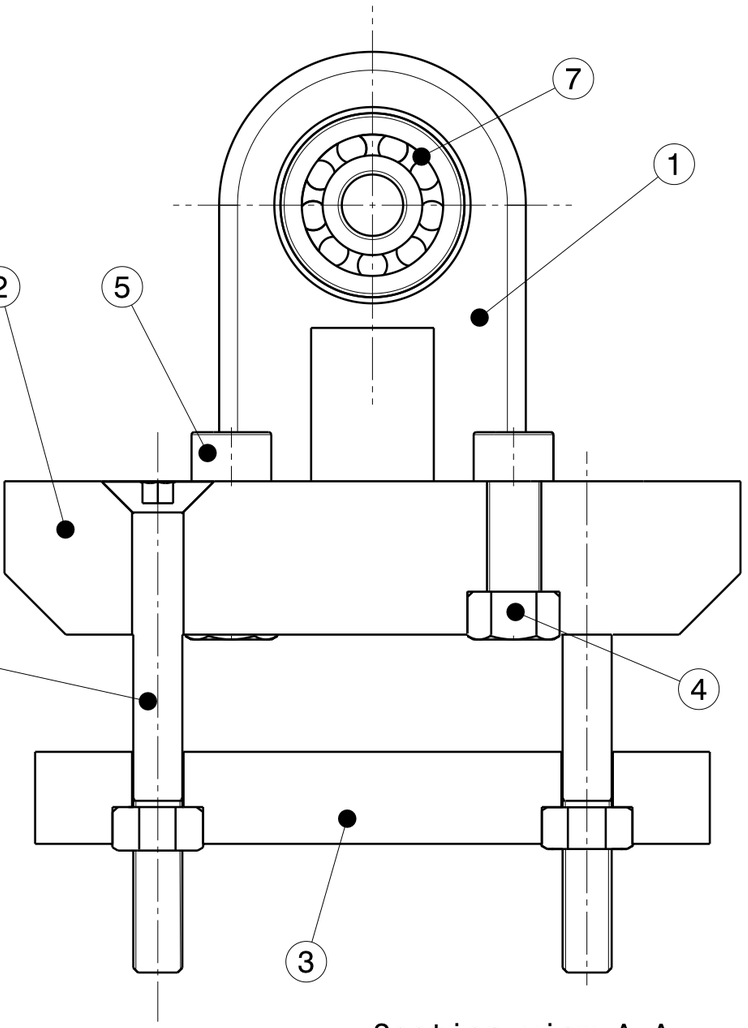

Section view A-A
Scale: 1:1

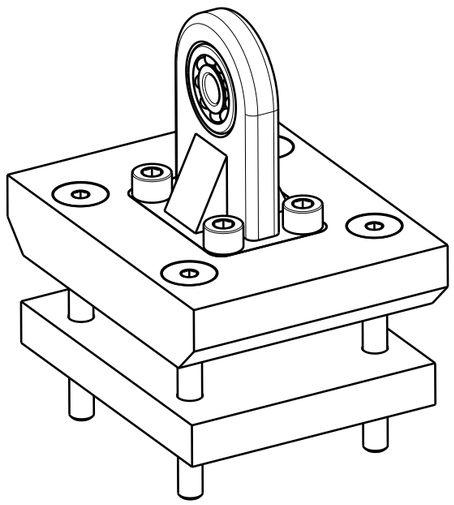

Isometric view
Scale: 1:2

#	Part Nr.	Item	Amount
1	PART001	Bearing housing	1
2	PART006	Supporting plate	2
3	PART003	Supporting strainplate	1
4	PART205	Hex Nut M8	8
5	PART204	Cylindric screw M8	4
6	PART209	Countersunk screw M8x80	4
7	PART107	Bearing	1

DESIGNED BY: J. Gengenbach DATE: 04.05.2015			
CHECKED BY: XXX DATE: XXX			
SIZE: A3	Amount: 2	Supporting GROUP003	
SCALE: 1:1	WEIGHT (kg): 0,7	DRAWING NUMBER: DWR023	SHEET: 1/1

I	_
H	_
G	_
F	_
E	_
D	_
C	_
B	_
A	_

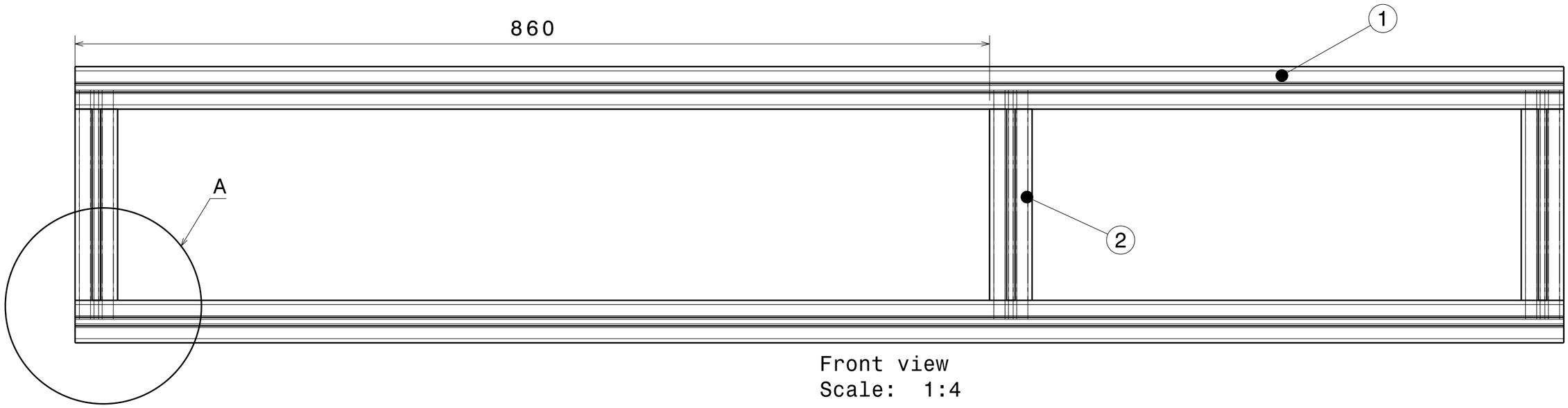

Front view
Scale: 1:4

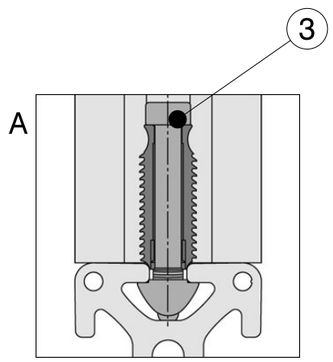

#	Part Nr.	Item	Amount
1	PART103	ITEM 40x40x1400	2
2	PART102	ITEM 40x40x180	3
3	PART110	Automatic Fastening set	6

DESIGNED BY: J. Gengenbach DATE: 04.05.2015			
CHECKED BY: XXX DATE: XXX			
SIZE: A3	Amount: 1	Frame GROUP004	
SCALE	WEIGHT (kg): 8,3	DRAWING NUMBER: DWR024	SHEET: 1/1

I	_
H	_
G	_
F	_
E	_
D	_
C	_
B	_
A	_

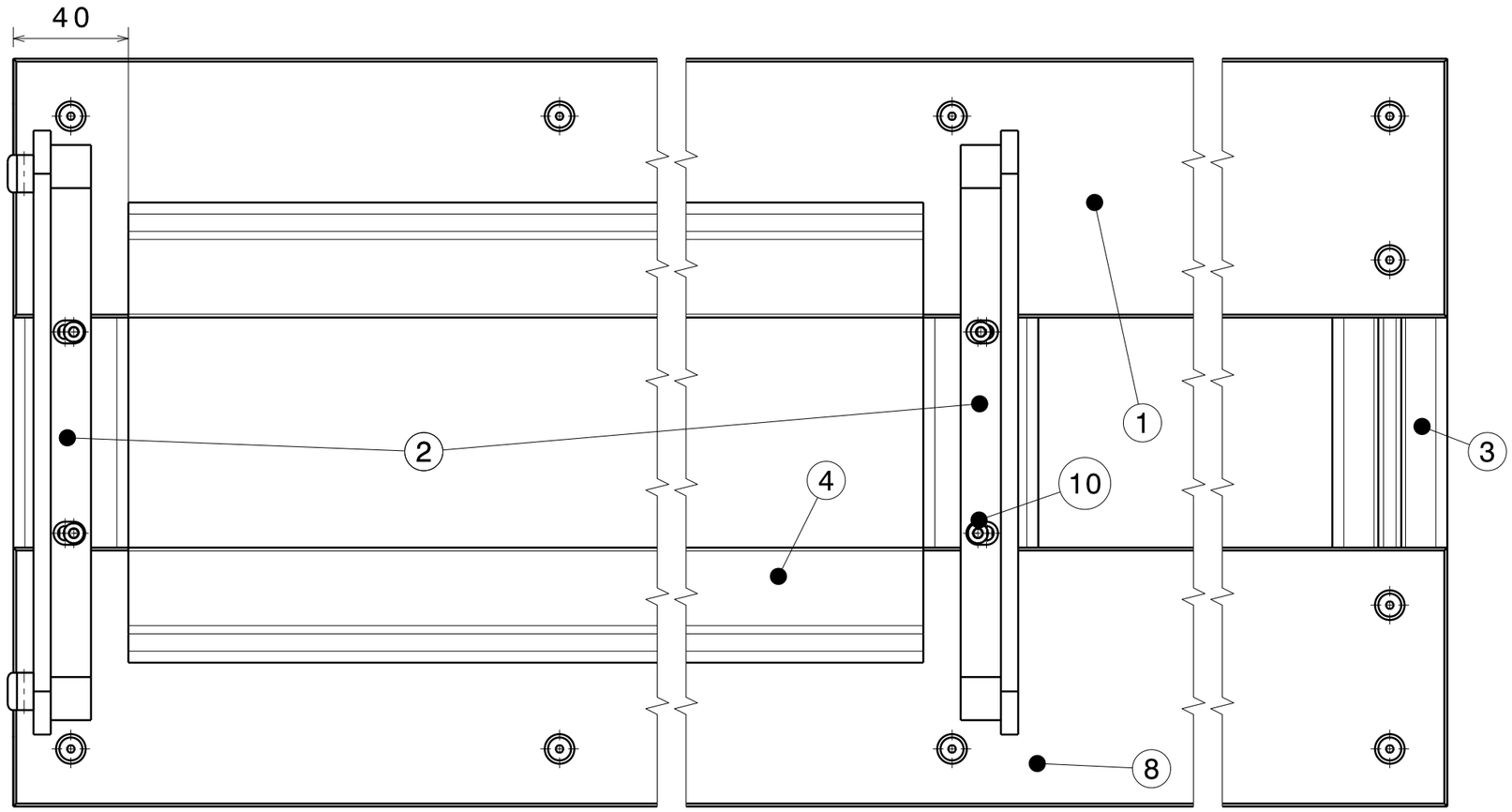

Top View
Scale: 1:2

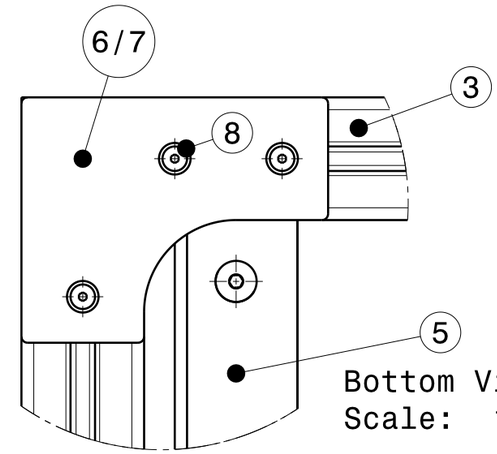

Bottom View
Scale: 1:2

#	Part Nr.	Item	Amount
1	PART012	Groundplate	2
2	PART020	Cap Shoulder	2
3	GROUP004	Frame	1
4	PART101	ITEM 40x40 45°	2
5	PART104	ITEM L-profile	2
6	PART013	Corner 1	2
7	PART014	Corner 2	2
8	PART201	Countersunk screw M4x22	40
9	PART202	Countersunk screw M6x25	12
10	PART213	Cylinder screw M4x40	4
11	PART108	ITEM Nut M4	44
12	PART109	ITEM Nut M6	12

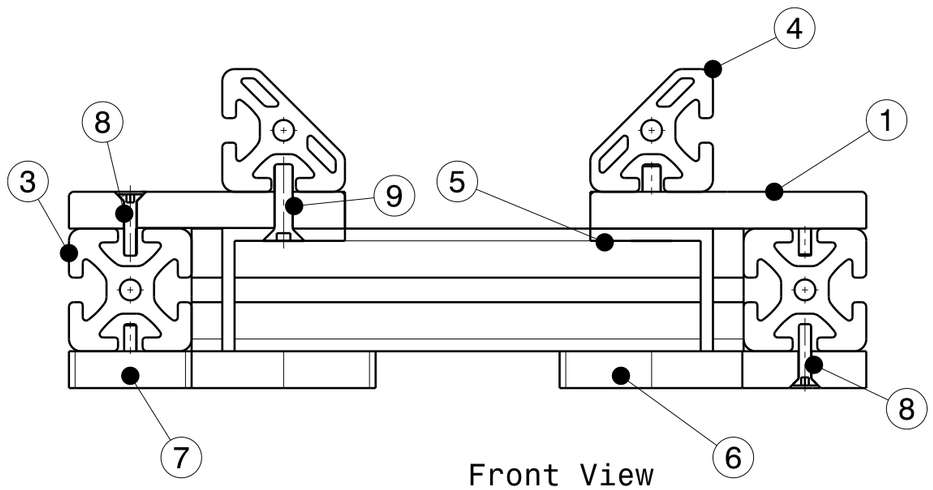

Front View
Scale: 1:2

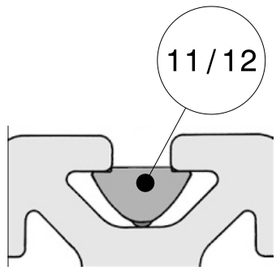

DESIGNED BY: J. Gengenbach
DATE: 05.05.2015
CHECKED BY: XXX
DATE: XXX
SIZE: A3
Amount: 1
SCALE:
WEIGHT (kg): 14
DRAWING NUMBER: DWR025
SHEET: 1/1

Housing GROUP005

I	_
H	_
G	_
F	_
E	_
D	_
C	_
B	_
A	_

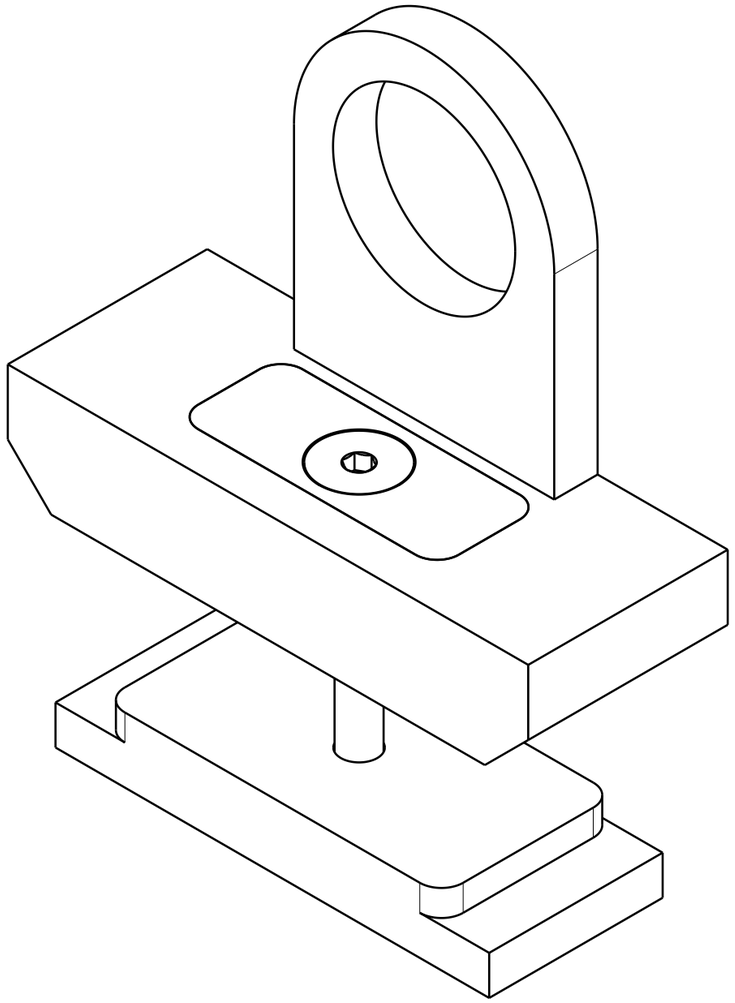

Isometric view
Scale: 1:1

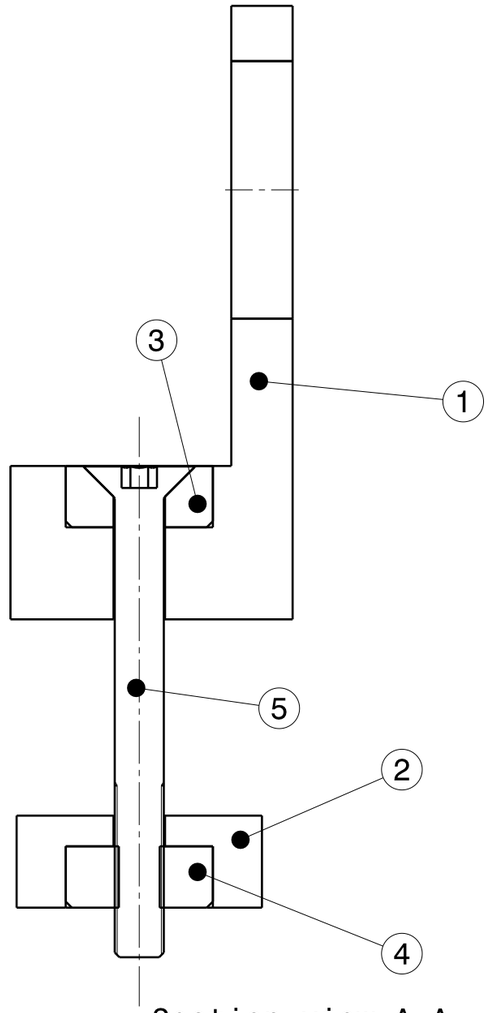

Section view A-A
Scale: 1:1

#	Part Nr.	Item	Amount
1	PART008	Safetybearing	1
2	PART009	Safetybearing strainplate	1
3	PART010	Mountingplate safetybearing	1
4	PART011	Mountingplate strainplate	1
5	PART203	Countersunk screw M8x80	1

DESIGNED BY: J. Gengenbach DATE: 05.05.2015			
CHECKED BY: XXX DATE: XXX			
SIZE: A3	Amount: 2	Safetybearing unit GROUP006	
SCALE: 1:1	WEIGHT (kg): 1,2	DRAWING NUMBER: DWR026	SHEET: 1/1

I	_
H	_
G	_
F	_
E	_
D	_
C	_
B	_
A	_

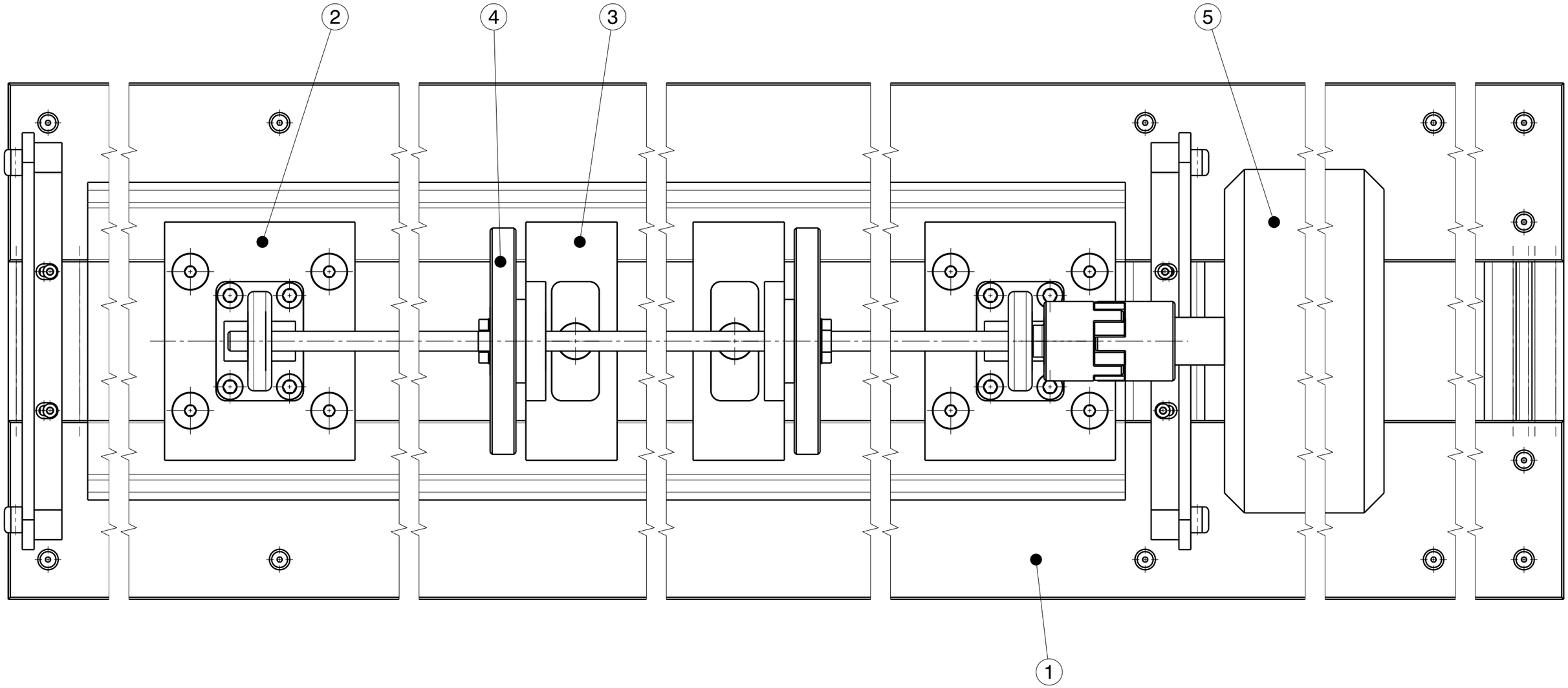

#	Part Nr.	Item	Amount
1	GROUP004	Frame	1
2	GROUP003	Supporting	2
3	GROUP006	Safetybearing unit	2
4	GROUP002	Rotor	1
5	PART112	Motor	1

DESIGNED BY: J. Gengenbach
DATE: 05.05.2015
CHECKED BY: XXX
DATE: XXX

SIZE	Amount	
A3	1	Complete device GROUP007

SCALE	WEIGHT (kg)	DRAWING NUMBER	SHEET
1:2	44	DWR027	1/1

I	_
H	_
G	_
F	_
E	_
D	_
C	_
B	_
A	_

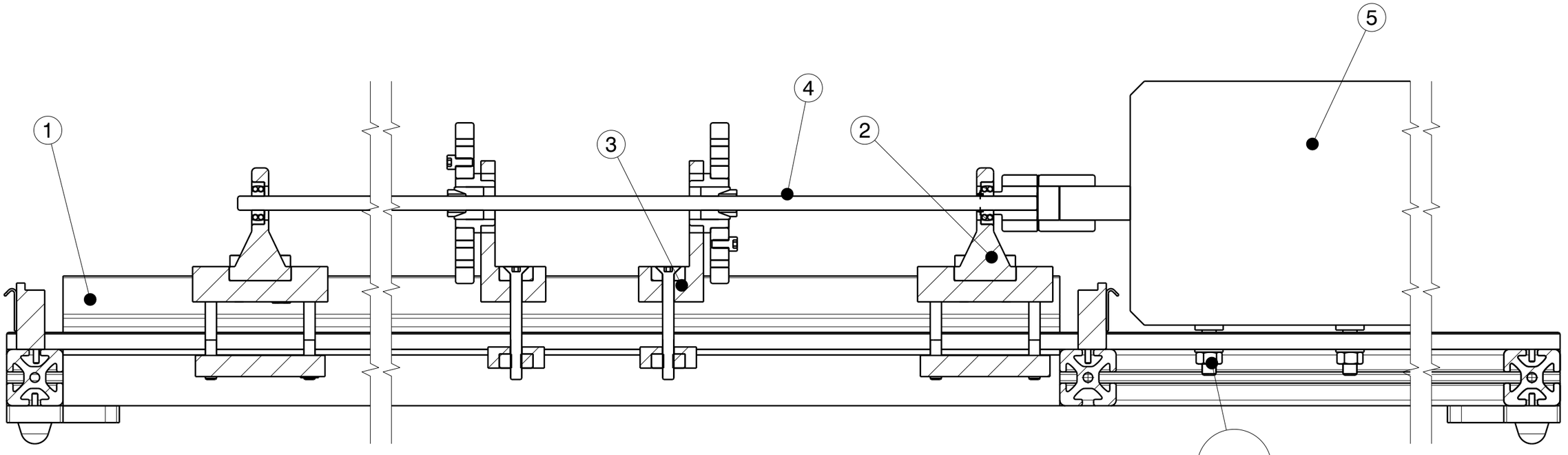

Section view A-A
Scale: 1:3

#	Part Nr.	Item	Amount
1	GROUP004	Frame	1
2	GROUP003	Supporting	2
3	GROUP006	Safetybearing unit	2
4	GROUP002	Rotor	1
5	PART112	Motor	1
6	PART206	Hex Screw M10x40	4
7	PART214	Washer M10	8
8		Hex Nut M10	4

DESIGNED BY: J. Gengenbach
DATE: 05.05.2015
CHECKED BY: XXX
DATE: XXX

SIZE: A3
Amount: 1

Complete device GROUP007

SCALE: 1:3
WEIGHT (kg): 44
DRAWING NUMBER: DWR028
SHEET: 1/1

I	–
H	–
G	–
F	–
E	–
D	–
C	–
B	–
A	–

1)

The ITEM profiles (①,②) are connected on each link with two ITEM fastening sets (③) according the ITEM instructions.

2)

The groundplates (①) are mounted on the frame (②)with M4x22(③) countersunk screws and ITEM M4 T-Slot nuts (④). Therefor the ITEM nuts have to be positioned into frame beforehand.

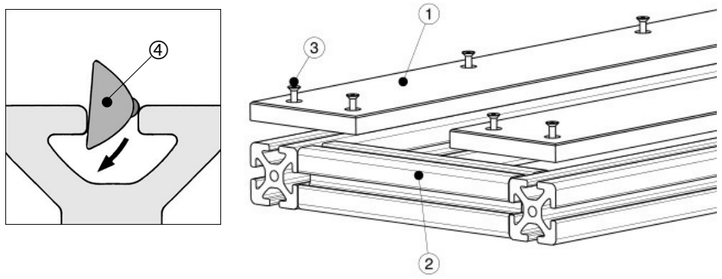

3)

The L-profiles(①) have to be aligned with the flank of the groundplates and placed up to contact with the cross profile. Next, the positions for the boreholes in the groundplates should be marked and drilled with 6,4 mm diameter.

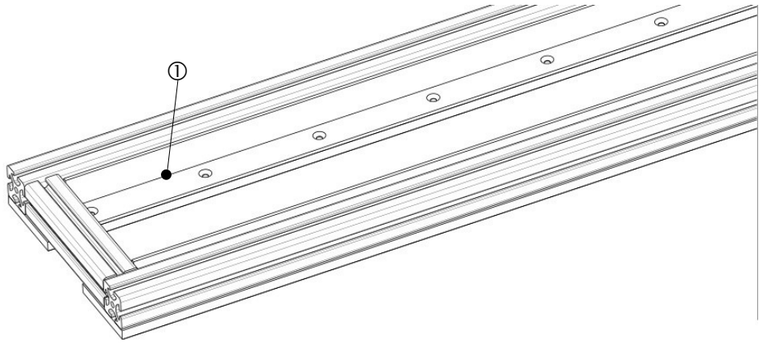

4)

Now, the triangular ITEM profiles (①) can be mounted with M6x25 countersunk screws and ITEM M6 T-Slot nuts as well as the corner parts (②) with M4x22 countersunk screws IM4 slot nuts. The safety-cap shoulder (③) have to be fixed with M4x40 cylinder screws and M4 slot nuts.

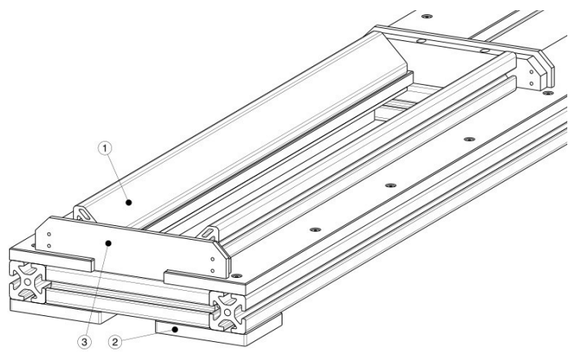

5)

The assembly of the shaft has to be done in a certain order. Firstly, the feather key (①) has to be inserted into the adapter (②) and the retaining key (⑤)´put onto the shaft (④). Next, the bearing (③) can be put onto the shaft with contact to the retaining ring. Afterwards, the adapter has to be glued onto the shaft. Therefor Loctite 638 or a similar glue has to be used. The adapter should be put with contact to the bearing so that the bearing does not have an axial play. The glue must be used according the instructions.

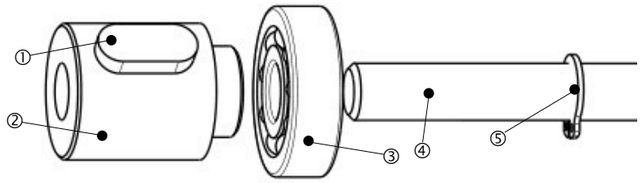

6)

Now, the bearings and housings can be joined. To join the bearings (②) and their housings (①) forceless the housings have to be heated on about 80°C. The heating can be either done with a hot air gun or with an oven.

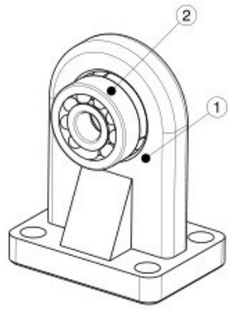

7)

The bearing housings (①) should now be mounted on the mounting plates (②). Therefor M8x25 cylinder screws and M8 nuts are used.

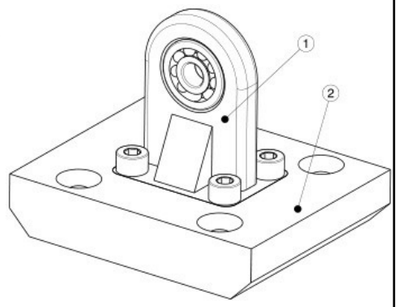

8)

The second bearing can now also be put onto the shaft. Next, the shaft-supporting unit has to be placed on the triangular profiles.

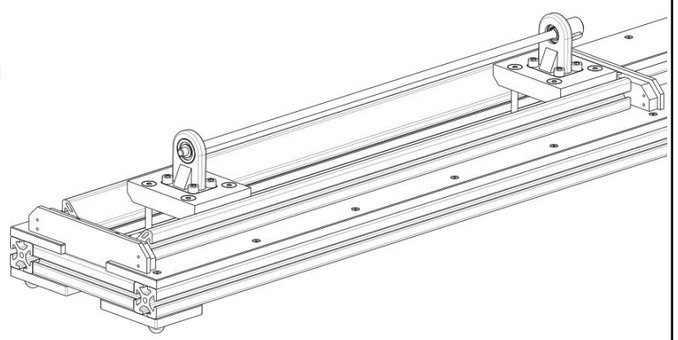

9)

The supporting plates are fixed together with their strainplates (①). Therefor M8x80 countersunk screw and M8 nuts are used.

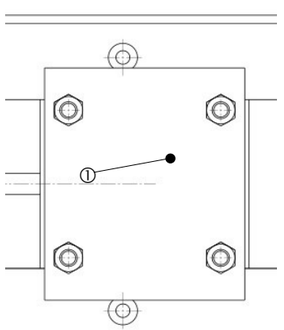

10)

To join the inner rotor (①) and the outer rotor (②) forceless, they need a temperature difference of about 300 °C. The shoulder's face of the inner rotor and the outer rotor should be in contact after joining.

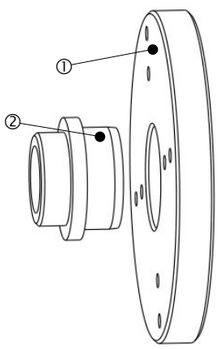

11)

Now, the rotors (①) and safety-bearings (②) can be mounted. Therefor the free supporting has to be slide of the shaft. The shaft must be keep horizontally. The rotors are clamped with the Ringspann coupling onto the shaft. The required torque is 31 Nm and should not be exceed. The safety-bearings are mounted with their metal plates and a M8x80 counter-sunk screw each.

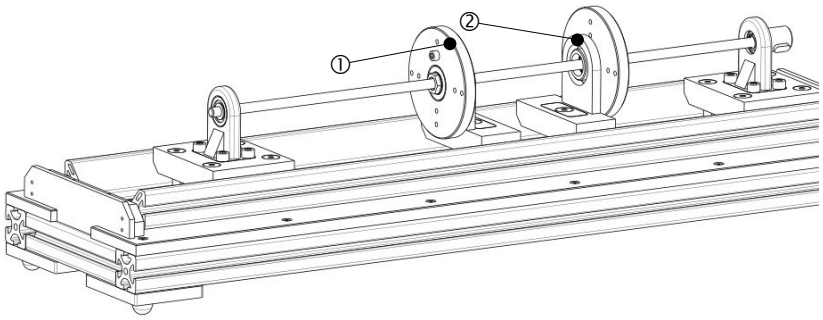

12)

The second feather key has to be put onto the motor's shaft. Next, the Rotex coupling (①) can be put onto the rotor's shaft. The motor with the Rotex coupling must be put gently on the shaft. The motor's vertically position should be set with thin spacer discs. If the motor's final position is found, the holes for the clamping bolts can be marked and 12 mm holes drilled. The motor is fixed with four M10x40 bolts and nuts.

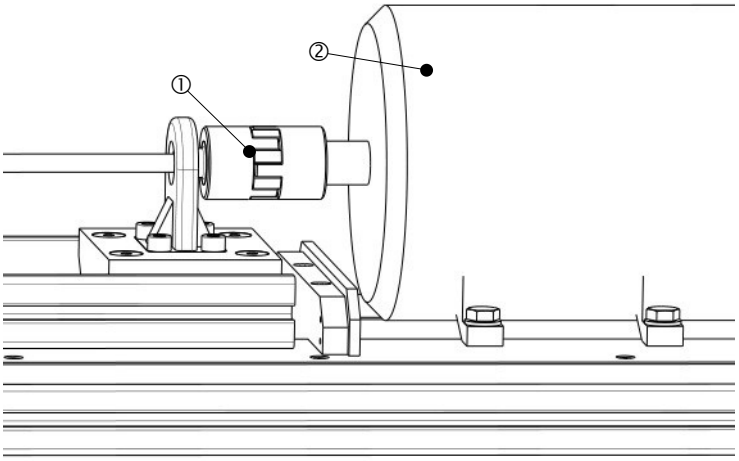

13)

The Plexiglas plates of the cap have to be glued into one of the cap-ends. If the plates do not fit into the slot, the slot should be widen with sandpaper. The applied glue should be a suitable glue for plastic materials.

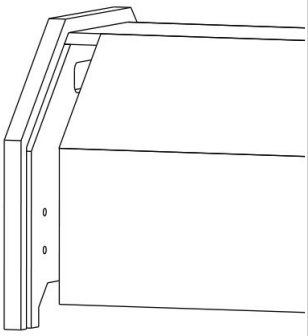

14)

Now, the cap-rails (②) should be mounted on the cap-end (①) with a M5x25 counter-sunk screws and M5 nut each. Afterwards, the second cap-end can be glued on Plexiglas plates and strained with the cap-rails.

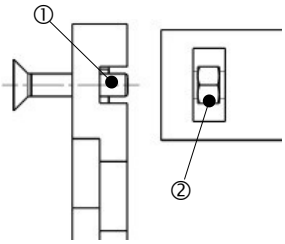

15)

The quick fasteners (①) should be mounted in that way that there is a slight tension between the cap and the cap shoulders.

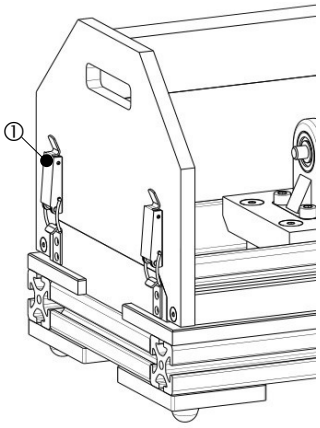

Operation manual:

Read operation manual before using the device!

While shaft rotating, the safety-cap must not be removed!

While shaft rotating, the safety-bearings must always be at the disks!

To change the rotor's layout, open the quick fasteners and remove the safety-cap.

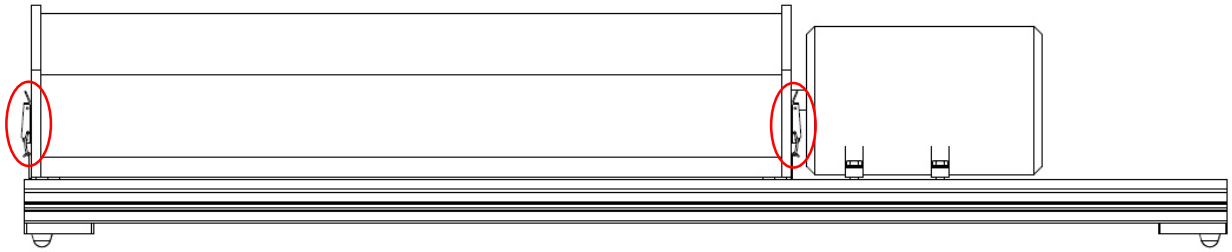

The oscillating system consists of the shaft (1), the free supporting (2), the fixed supporting (3), two disks (4), two safety-bearings (5) and imbalance-screws (6). The free support, the disks with their safety-bearings and the imbalance-screws can be adjusted.

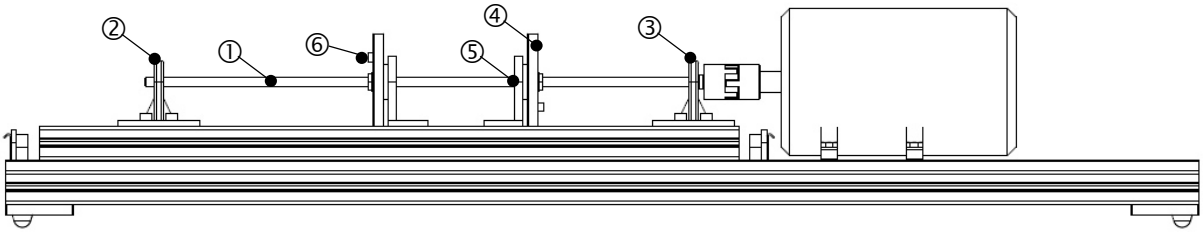

To adjust the position of the free supporting, loose the four straining bolts (internal hexagon 5 mm). The fixed supporting must not be shifted.

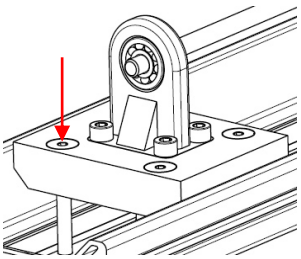

To shift the disk, the nut of the shaft hub connection has to be loosen. Therefore, one person holds the disk and another person carefully loose the nut with an open-ended wrench (19 mm). The tightening torque must not exceed 31 Nm.

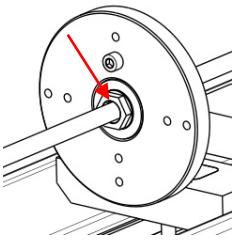

Before starting the device, the safety-bearing always have to be shifted on the disk's rim (1). The safety-bearing restricts the maximal deflexion of the shaft. The safety-bearing should be in position, that it barely not clamps the disk's shoulder (2). The safety-bearing is strained with 5 mm internal hexagon 5 wrench.

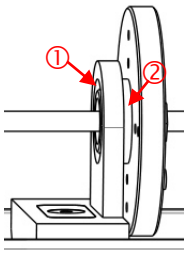

Before removing the free supporting from the shaft, the safety-bearing must be put onto the disk's shoulder. Now, the safety-bearing serves as an additional supporting of the shaft and keeps the shaft horizontally if the free supporting is removed.

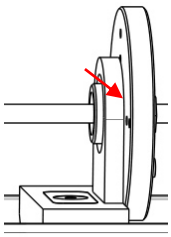

To remove or attach a disk and safety-bearing, the free supporting has to be shifted to the end of the rails.

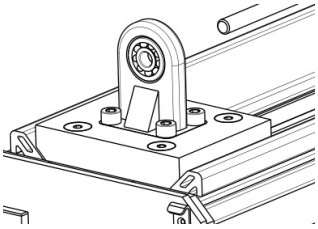

To remove the safety-bearing its strainplate has to be 90° rotated. Therefor its bolt has to be loosen as far as required to turn the strainplate. Now, the safety-bearing can be taken.

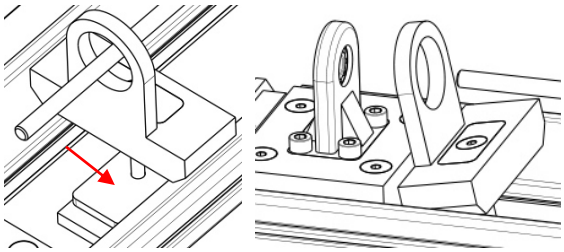

The layout can be put in every desired way. Before starting the device make sure that each screw and the disks are nuts are tightened. Check if the safety-bearings are properly positioned to the disks.